Stony Brook University

OFFICIAL COPY

The official electronic file of this thesis or dissertation is maintained by the University Libraries on behalf of The Graduate School at Stony Brook University.

© All Rights Reserved by Author.

Primary cilia modulate functionality of dentate granule cells in the adult brain

A Dissertation Presented

by

Soyoung Rhee

to

The Graduate School

in Partial Fulfillment of the

Requirements

for the Degree of

Doctor of Philosophy

in

Molecular and Cellular Pharmacology

Stony Brook University

August 2015

Stony Brook University

The Graduate School

Soyoung Rhee

We, the dissertation committee for the above candidate for the

Doctor of Philosophy degree, hereby recommend

acceptance of this dissertation.

Shaoyu Ge – Ph.D., Associate Professor
Department of Neurobiology and Behavior

David Talmage – Ph.D., Professor
Department of Pharmacological Science

Ken-Ichi Takemaru – Ph.D., Associate Professor
Department of Pharmacological Science

Amar Sahay – Ph.D., Assistant Professor
Department of Psychiatry
Harvard Medical School
Center for Regenerative Medicine

This dissertation is accepted by the Graduate School

Charles Taber
Dean of the Graduate School

Abstract of the Dissertation

Primary cilia modulate functionality of dentate granule cells in the adult brain

by

Soyoung Rhee

Doctor of Philosophy

in

Molecular and Cellular Pharmacology

Stony Brook University

2015

Adult born neurons in the hippocampal dentate gyrus start to assemble primary cilia at 14 days after their birth. At 21 days, all newborn neurons show a typical primary cilium. Although this small microtubule-based structure has been shown to be important for early neuronal development, its physiological/behavioral roles remain elusive. Therefore, I set out to investigate both behavioral and physiological functions of primary cilia in immature and mature dentate granule cells (DGCs) of the adult brain.

After selectively knocking out *IFT20* to ablate primary cilia from mature DGCs, I found defects of hippocampal spatial and cognitive memory, suggesting a crucial role of primary ciliary in mature neurons. I further observed that ablation of primary cilia in mature DGCs increased long-term potentiation in mossy fiber pathway. The decrease of synaptic plasticity after primary cilia depletion in mature DGCs may consequently increase the portion of synaptic activity of young adult born DGCs. Furthermore, my research indicated that primary cilia modulate early tangential dispersion and radial

migration of adult born DGCs. Taken together, my thesis work suggests that primary cilia of DGCs play critical roles in regulating neuronal migration of newborn neurons and physiological/behavioral activities of mature neurons. These findings will facilitate us in understanding the role of primary cilia in neuronal development and function, as well as molecular mechanisms for ciliopathies.

Table of Contents

List of Figures vii

List of Abbreviation x

Chapter 1 General Introduction

1.1 General introduction about cilium 1

1.2 Signaling pathway of primary cilia 2

1.3 Hippocampus associated behaviors 6

1.4 Adult neurogenesis and development 7

1.5 Specific aims and Rationale 9

Chapter 2 Materials and Methods 13

Chapter 3 Primary cilia and hippocampal associated behaviors

3.1 Introduction - primary cilia and memory and other AC3 related behaviors 22

3.2 Results

3.2.1 Deletion of primary cilia in mature dentate granule cells 24

3.2.2 Primary cilia in mature dentate granule cells regulate contextual memory 25

3.2.3 Primary cilia in mature dentate granule cells regulate spatial novelty recognition but not novel object recognition 25

3.2.4 Absence of primary cilia in mature dentate granule cells impairs patter completion 27

3.2.5 Absence of primary cilia in mature dentate granule cells enhances contextual fear discrimination 27

3.2.6 Absence of primary cilia in mature dentate granule cells shows no effects on anxiety related behaviors 28

3.3 Discussion 29

Chapter 4 Primary cilia and synaptic plasticity in DG-CA3 circuit

4.1 Introduction – tri-synaptic circuit and plasticity 52

4.2 Results

4.2.1 Enhanced mossy fiber synaptic plasticity after removal of primary cilia in mature DGCs 54

4.2.2 Ablation of adult neurogenesis decreases DG-CA3 synaptic plasticity 55

4.2.3 Ablation of adult neurogenesis diminishes the enhanced DG-CA3 LTP by primary cilia depletion of mature DGCs 56

4.3 Discussion 57

Chapter 5 Primary cilia and neuronal migration in dentate gyrus

5.1 Introduction - primary cilia and migration 71

5.2 Results

5.2.1 Adult born neurons without primary cilia expression localize near to ML 73

5.2.2 Ablation of primary cilia alters dendritic refinement in adult born neurons 74

5.2.3 Direction of early neuronal migration of adult born neurons in GCL is regulated by primary cilia 75

5.2.4 Ablation of primary cilia do not alter early migration of adult born neurons 76

5.2.5 Defects in primary cilia assembly alters early dendritic development of adult born neurons 77

5.3 Discussion 78

Chapter 6 Conclusion and perspective 98

Chapter 7 Reference 101

List of Figures

Figure 1.1 Markers for staging adult neurogenesis in the hippocampus 12

Figure 3.1 Ablation of primary cilia in mature dentate granule cells in *IFT20* fl/fl mice 34

Figure 3.2 Adult neurogenesis was not altered by removal of primary cilia 35

Figure 3.3 Experiment design for contextual memory test 36

Figure 3.4 Ablation of primary cilia in mature dentate granule cells impairs contextual memory 37

Figure 3.5 Experimental design for spatial novelty recognition test 38

Figure 3.6 Ablation of primary cilia in mature dentate granule cells impairs spatial memory 39

Figure 3.7 Experimental design for novel object recognition test 40

Figure 3.8 Ablation of primary cilia in mature dentate granule cells do not alter novel object recognition memory 41

Figure 3.9 Experimental design for pre-exposure dependent context fear test 42

Figure 3.10 Ablation of primary cilia in mature dentate granule cells decreases pattern completion 43

Figure 3.11 Experimental design for contextual fear discrimination test 44

Figure 3.12 Ablation of primary cilia in mature dentate granule cells increases contextual fear discrimination 45

Figure 3.13 Ablation of primary cilia in mature dentate granule cells increases contextual fear discrimination – discrimination ratio 46

Figure 3.14 Ablation of primary cilia in mature dentate granule cells increases contextual fear discrimination on day 8 47

Figure 3.15 Apparatus for elevated plus maze 48

Figure 3.16 Ablation of primary cilia in mature dentate granule cells do not alter anxiety like behavior 49

Figure 3.17 Apparatus for light and dark transition test 50

Figure 3.18 Ablation of primary cilia in mature dentate granule cells do not alter anxiety like behavior 51

Figure 4.1 Tri-synaptic circuit 60

Figure 4.2 I-O curve for CTRL and IFT20 (-/-) $^{\text{mature DGCs}}$ 61

Figure 4.3 Removal of primary cilia from mature GCs increases DG-CA3 synaptic plasticity 62

Figure 4.4 Experimental design for Ablation of adult neurogenesis in Nestin-Cre ^{ERT2}; iDTR mice 63

Figure 4.5 Ablation of adult neurogenesis in Nestin-Cre ^{ERT2}; iDTR mice 64

Figure 4.6 I-O curve – Nestin-Cre ^{ERT2}; iDTR 65

Figure 4.7 Ablation of adult neurogenesis diminishes the increased DG-CA3 synaptic plasticity caused by removal of primary cilia from mature DGCs 66

Figure 4.8 Ablation of adult neurogenesis and primary cilia in Nestin-Cre ^{ERT2}; iDTR mice 67

Figure 4.9 Ablation of adult neurogenesis and primary cilia in Nestin-Cre ^{ERT2}; iDTR mice 68

Figure 4.10 I-O curve – Nestin-Cre ^{ERT2}; iDTR-dnKif3A 69

Figure 4.11 Ablation of adult neurogenesis diminishes the increased DG-CA3 synaptic plasticity caused by removal of primary cilia from mature DGCs 70

Figure 5.1 Analysis of final position of adult born DGCs 82

Figure 5.2 Experimental design to ablate primary cilia by IFT20 removal from 21dpi 83

Figure 5.3 Distribution curves of final neuronal positioning of adult born neurons in GCL at 35 and 42 dpi in IFT20 mice 84

Figure 5.4 Experimental design to ablate primary cilia by dnKif3A expression from 21dpi 85

Figure 5.5 Distribution curves of final neuronal positioning of adult born neurons in GCL at 35 and 42 dpi 86

Figure 5.6 Experimental design to ablate primary cilia by IFT20 removal from 28dpi 87

Figure 5.7 Distribution curves of final neuronal positioning of adult born neurons in GCL at 42 dpi 88

Figure 5.8 Ablation of primary cilia in adult-born neurons alters dendritic refinement 89

Figure 5.9 Analysis of dendritic angle in adult born neurons 90

Figure 5.10 Experimental design to test effect of primary cilia ablation on dendritic angle of adult born neurons in IFT20 mice 91

Figure 5.11 Display of dendritic angle at 7 and 14dpi in adult born neurons of IFT20 mice 92

Figure 5.12 Experimental design to test effect of primary cilia ablation on dendritic angle of adult born neurons 93

Figure 5.13 Display of dendritic angle at 7 and 14dpi in dnKif3A expressing adult born neurons 94

Figure 5.14 Clonal analysis 95

Figure 5.15 Ablation of primary cilia assembly does not alter tangential migration distance of adult born neurons 96

Figure 5.16 Primary cilia regulate early dendrite development of adult born neurons 97

List of Abbreviations

Adeno-associated viruses (AAV)

Contextual fear conditioning (CFC)

Cyclin-dependent kinase 5 (CDK5)

Dentate granule cells (DGCs)

Dentate gyrus (DG)

Diphtheria toxin receptor (DTR)

Dishevelled (Dvl)

Doublecortin (DCX)

Elevated plus maze (EPM)

Entorhinal cortex (EC)

Field excitatory postsynaptic potentials (fEPSPs)

G protein-coupled receptors (GPCRs)

Glial fibrillary acidic protein (GFAP)

Glioma (Gli)

Granule cell layer (GCL)

Green fluorescent protein (GFP)

High frequency stimulation (HFS)

Intraflagellar transport (IFT)

Inversin (Inv)

Long-term depression (LTD)

Long-term potentiation (LTP)

Melanin concentrating hormone receptor1 (MCH1)

Molecular layer (ML)

Mossy fiber (MF)

Paraformaldehyde (PFA)

Patched (Ptc)

Phosphate buffered saline (PBS)

Pre exposure dependent contextual fear conditioning (PECFC)

Serotonin selective reuptake inhibitors (SSRIs)

Serotonin subtype 6 receptor (5-HT6)

Smoothened (Smo)

Somatostatin receptor3 (SSTR3)

Sonic Hedgehog (Shh)

Subgranular zone (SGZ)

Subventricular zone (SVZ)

Acknowledgments

First, I would like to thank my advisor, Dr.Shaoyu Ge. He was a great mentor who always provided the guidance, motivation and support throughout four and half years as a student in his lab. His scientific knowledge and scientific enthusiasm always encouraged me and guided me to become an individual scientist. I would also like to thank to my committee, Drs.David Talmage, Ken-Ichi Takemaru and Amar Sahay for their insightful advice and support through out my PhD study.

Many thanks to Dr.Yan Gu, who taught me how to arrange behavior and electrophysiology experiments. I also thanks to other Ge lab members: Adrian DiAntonio, Greg Kirshen, Jia Shen, Dr.Jia Wang, Dr. Natsuko Kumamoto and Steve Janoschka and Dr. Maya Shelly and her lab members, who were all good lab mates as well as a good collaborator. This thesis dissertation would not been possible without their consideration and encouragement during the last year of my graduate school.

I acknowledge all staffs from department of pharmacological science and department of neurobiology and behaviors in Stony Brook University. I would also like to thank my 2010 entering class, Dex-Ann, Jason, Ken and Luisa, and other co-students in molecular and cellular pharmacology program. I thank my friends in Stony Brook and old friends back in Korea, providing friendship and encouragement.

Lastly, I would like to deeply thank to my family. My mom, dad and brother show unconditional trust, love and patience in all my pursuits and always are there for me. Also thanks to my parents in law who have provided encouragement and support. And most of all, I especially thank with love to my husband, Jinwoo. He was the one who provided an incredible support and friendship, raised me up when I was in a slump, encouraged, and helped me during my graduate studies. With out him, this thesis would never have been written. Thank you.

Chapter 1 General Introduction

1.1 General introduction about the cilium

Cilia are hair-like organelles projecting out from the cell membrane. From vertebrates to invertebrates such as *C. elegans* and *D. melanogaster*, cilia are widely expressed among species and in a variety of cell types (Gerdes et al., 2009). During development of cells, cilia regulate cell proliferation and development by sensing growth factors, hormones, and other development related signals (Berbari et al., 2008b, Corbit et al., 2005, Schneider et al., 2005, Singla and Reiter, 2006).

A cilium consists of microtubule cytoskeleton axoneme, which is projected from the ciliary basal body, and the ciliary membrane that is surrounding the axoneme. To assemble a cilium, first, centrioles dock onto the plasma membrane of a cell. Basal body derived from the mother centriole associates with membrane vesicles and set up the membrane compartment. Triplet axonemal microtubules are nucleated from the basal body to the transition zone, the distal region of the basal body. Doublet microtubules are formed to elongate cilium from the transition zone, by associating with vesicular transport and intraflagellar transport (IFT) proteins (Sorokin, 1962, Sorokin, 1968).

During cilium assembly, ciliary proteins are transported from the cytoplasm to the ciliary tip through the IFT machinery. Active kinesin-2, an anterograde IFT motor, transports IFT complex B and A, axonemal proteins and inactive cytoplasmic dynein-2 to the tip of the cilium. At the tip of cilium, IFT complex A and B, axonemal proteins and cytoplasmic dynein-2 are released, disassociate and rearrange into retrograde

conformation. Active cytoplasmic dynein-2 binds to IFT complex A and B, inactive kinesin-2 and axonemal turnover protein, and delivers them back towards the cell body (Ishikawa and Marshall, 2011, Pedersen and Rosenbaum, 2008).

The axoneme is showing two structural pattern; nine doublet microtubules surrounding a central pair (9+2) and nine doublet microtubules missing a central pair (9+0). Based on the motility, cilia can be classified into two categories: motile cilia and non-motile primary cilia. Motile cilia have 9+2 axoneme structure including dynein arms. Unlike in primary cilia, axonemal dynein arms in motile cilia are anchored to doublet microtubules and allow microtubules to slide along each other, which give force to bending motion. It is known that motile cilia are expressed in the oviduct, ependymal cell surfaces of the trachea and in the ventricle lining in the brain, and are required for fluid flow, mucus clearance and sperm motility (May-Simera and Kelley, 2012).

On the other hand, primary cilia do not have the central pair, but consist of only 9+0 axoneme structure. Unlike motile cilia, which are multiple in each cell, only one primary cilium is present in an individual cell. Primary cilia are present in most human cells including most brain cells; neural stem cells, neurons and astrocytes, and sense signaling transduction (Lee and Gleeson, 2011).

1.2 Signaling pathways of primary cilia

Structural and functional abnormalities in cilia lead to ciliopathies in human. Neurological defects are commonly found in ciliopathies such as mental retardation and structural deficits (Badano et al., 2006). Many studies have provided evidence that

these pathological phenotypes of ciliopathies are due to defects in downstream signaling pathways of primary cilia (Goetz and Anderson, 2010, Valente et al., 2014). For the following section, I will discuss about signaling pathways of primary cilia, which are essential during development.

Sonic Hedgehog (Shh)

Shh signaling is one of the most well studied signaling pathways of primary cilia. During development, Shh is required for neural patterning (Huangfu et al., 2003, Wilson et al., 2012) and maintenance of neural progenitors (Han et al., 2008, Machold et al., 2003). In the absence of the Shh ligand, Patched (Ptc) protein localizes to the cilium and represses the activity of Smoothened (Smo) by preventing trans-localization to the cilium. Also Glioma (Gli) transcription factors are processed into inactive repressor forms, which inhibit transcription of Shh target genes. In the presence of the Shh ligand, Ptc is removed whereas Smo translocates to the ciliary membrane. Gli transcription factors are activated (GliA) and promote expression of Shh target genes.

Mutations in IFT- B genes, *IFT 172* and *IFT 88*, result in the absence of primary cilia and disruption of Shh signaling leading to mis-patterning of the neural tube (Huangfu and Anderson, 2006, Huangfu et al., 2003). Furthermore, both *Kif3A* mutants and *Smo* mutants have a disrupted the dentate gyrus structure (Han et al., 2008). These researches demonstrate that the Shh signaling pathway is regulating both embryonic and postnatal development through primary cilia, and loss of primary cilia results in defects in neural patterning and morphology.

Wnt

Primary cilia have been suggested to regulate another development pathway, the Wnt signaling pathway. Wnt signaling can be divided into two signal transduction pathways, the canonical and non-canonical Wnt pathways. In the absence of the Wnt ligand, β-catenin is phosphorylated and degraded by the ubiquitin-proteasome. When canonical Wnt signaling is activated, β-catenin in the cytoplasm is stabilized by the dishevelled (Dvl) protein, and translocates into the nucleus to initiate the transcription of Wnt target genes (Moon et al., 2002, Wharton, 2003). In contrast to the canonical Wnt signaling pathway, the non-canonical Wnt pathway is independent of the β-catenin stability; depending on the Dvl-mediated Rho/JNK or CAMKII/PKC signaling pathways. Activation of non-canonical Wnt pathway, rather than target gene transcription, regulates cell polarity, actin dynamics and cell morphology (May-Simera and Kelley, 2012).

Several studies have implied primary cilium is acting as a switch between the canonical and non-canonical Wnt pathways. Inversin (Inv), which is responsible for left–right determination during embryonic development, is localized to the basal body of the cilium (Watanabe et al., 2003). Inv levels can be increased by the non-canonical pathway and inhibit the canonical Wnt signaling pathway by degrading cytoplasmic Dvl (Corbit et al., 2008, Simons et al., 2005). In addition, inhibition of retrograde IFT in primary cilia dampens canonical Wnt activity by sequestering β-catenin from nucleus translocation (Lancaster et al., 2011). However, there are some controversial studies that contradict the role of primary cilia in inhibiting the canonical Wnt pathway. The loss

of *IFT 88,IFT 172 or Kif3A* genes prevents cilia assembly and express dampened Shh signaling but normal Wnt mediated development (Huang and Schier, 2009, Ocbina et al., 2009). Together, still the role of cilia in the canonical Wnt pathway is imprecise and insignificant compared to Shh signaling. Nevertheless, it is sure that primary cilia regulate cell morphology during embryonic development via Wnt signaling pathways.

Other signaling pathways

Primary cilia in neurons express several G protein-coupled receptors (GPCRs) including Somatostatin receptor3 (SSTR3), Melanin concentrating hormone receptor1 (MCH1) and Serotonin subtype6 receptor (5-HT6) (Berbari et al., 2008a, Brailov et al., 2000b, Hamon et al., 1999, Handel et al., 1999). Somatostatin has been shown to regulate behavior effects; learning and memory, locomotor behavior, and abnormal somatostatin levels in CNS lead to cognitive impairment. Furthermore, somatostatin also regulates the release of neurotransmitters such as GABA and 5-HT (Viollet et al., 2000). MCH-expressing neurons are mostly located in the lateral hypothalamus in brain. Injection of MCH into the lateral ventricles increases food consumption, and MCH overexpressing transgenic mice were found to be obese (Ludwig et al., 2001, Qu et al., 1996). On the other hand, transgenic mice lacking MCH expression exhibit hypoplasia and a lean phenotype (Shimada et al., 1998), suggesting that MCH regulates feeding behavior and energy balance. Based on these previous studies, it seems that expression of neuronal cilia in the CNS is important for behavioral development.

1.3 Adult neurogenesis in the hippocampus

After birth, postnatal neurogenesis occurs in restricted regions in the brain: in the subgranular zone (SGZ) of the dentate gyrus (DG) in the hippocampus, and in the subventricular zone (SVZ) of the lateral ventricle (Eriksson et al., 1998, Kuhn et al., 1996). Postnatal neurogenesis in these areas occurs throughout life, and is modulated by physiological and pathological environments. For instance, the level of neurogenesis declines with age, but has been shown in rodents to increase following exercise or pathological conditions such as seizure (Kempermann et al., 1997, Kuhn et al., 1996, Parent et al., 1997, van Praag et al., 2005).

Adult born neurons are generated in the SGZ in the hippocampus and undergo 5 step of developmental process as shown in Figure 1.1 (Kempermann et al., 2004, Ming and Song, 2005). During the proliferation stage, Nestin and glial fibrillary acidic protein (GFAP) positive radial glial stem cells undergo self-renewal and generate transient amplifying progenitor cells (Seri et al., 2001). During differentiation stage, within 4 days after birth, transient amplifying progenitor cells start to differentiate into immature neurons. At this stage, immature neurons start to express immature neuronal markers such as doublecortin (DCX) (Brown et al., 2003). Next, immature neurons migrate into the granule cell layer (GCL) of the DG. After a short migration to the GCL, adult born immature neurons migrate tangentially within GCL at 4 to 10 days after birth and start to elongate axons and dendrites to their target areas. Axon fibers project toward CA3 pyramidal cells and dendrites arborize their trees toward to the molecular layer (ML) of the DG (Hastings and Gould, 1999). In the synaptic integration stage, immature granule neurons integrate into the neural circuits receiving inputs from entorhinal cortex and

sending outputs to the hilar and CA3 regions (Gu et al., 2012, van Praag et al., 2002). At this stage, adult born dentate granule cells (DGCs) display similar physiological and functional properties to that of mature DGCs such as dendritic spine expression and synaptic plasticity.

1.4 Adult neurogenesis and hippocampus-associated behaviors

The hippocampus is a critical structure in brain, regulating certain behaviors such as learning, memory, spatial navigation and emotional behaviors (Sahay and Hen, 2007, Squire, 1992). Based on the anatomical region of hippocampus, the hippocampus has distinct function along the septotemporal axis. The dorsal hippocampus regulates cognitive behaviors, whereas the ventral hippocampus regulates emotional behaviors such as anxiety and depression (Bannerman et al., 2004, Moser and Moser, 1998). The dorsal hippocampus receives inputs from lateral and caudomedial entorhinal cortex and sends outputs to lateral entorhinal cortex. On the other hand, the ventral hippocampus receives inputs from rostomedial entorhinal cortex and sends outputs to prefrontal cortex. This different connectivity and activity between the hippocampus and limbic system gives distinct and dissociative functions along the septotemporal axis (Kheirbek et al., 2013, Sahay and Hen, 2007).

As adult neurogenesis occurs throughout life in the DG, many studies have shown the function of adult born neurons in hippocampus associated behaviors. Here I will discuss adult neurogenesis, and the relationship with hippocampus associated behaviors.

Learning and memory is a representative function of the hippocampus. Memory is the capability of an animal to store encoded information and retrieve previously stored information to drive a behavioral output. Learning is the process of encoding received information. In the hippocampal circuit, the DG receives inputs from the entorhinal cortex and sends outputs to the CA3 region. Synaptic transmission from this hippocampal circuit is regulating memory encoding, storage and retrieval (Deng et al., 2010).

Previous studies have shown that altering the level of adult neurogenesis affects hippocampus-dependent learning and memory. Ablation of adult neurogenesis impairs contextual fear memory (Saxe et al., 2006) and formation of long-term spatial memory (Snyder et al., 2005). Furthermore, mice lacking adult neurogenesis fail to discriminate similar spatial patterns (Clelland et al., 2009) whereas mice with increased adult neurogenesis show enhanced contextual fear discrimination (Sahay et al., 2011a). Together, these studies suggest that newly generated neurons facilitate the encoding and storage of new information.

Another function of the hippocampus is its contribution to emotional behaviors such as anxiety and depression. Anxiety is an excessive and unregulated fear response to either an actual threat or an unthreatening stimulus. Adult neurogenesis has been demonstrated to increase following antidepressant treatment (Boldrini et al., 2009, Malberg et al., 2000). In addition, Santarelli et al. have shown that neurogenesis is required for the efficacy of antidepressants, which supports that the mechanism of antidepressants is via enhancing the level of neurogenesis (Santarelli et al., 2003).

However, a direct connection between increased adult neurogenesis and anxiety-like behaviors is still unclear. Inhibition of apoptosis in adult born neurons enhanced pattern separation but had no effect on anxiety-like behaviors (Sahay et al., 2011a). In contrast, other studies determined that deficits in adult neurogenesis lead to increased anxiety and depression (Revest et al., 2009, Snyder et al., 2011). Although the link between neurogenesis and anxiety-like behaviors is still elusive, one promising hypothesis is that reduced adult neurogenesis leads to high anxiety level, whereas increased neurogenesis results in low anxiety level due to reduced fear and stress response.

1.5 Specific aims and rationale

My research elucidates the function of primary cilia of dentate granule neurons in the hippocampus. Previous studies have focused on the role of primary cilia during embryonic or early postnatal neurogenesis. In my studies, I determined the physiological and behavioral functions of primary cilia in DGCs both in early neuronal development and after maturation. This study, it will give us new insights into functionality of primary cilia through out the development of dentate granule neurons.

Aim 1. Determine whether ablation of primary cilia in mature dentate granule neurons affects hippocampus-associated behaviors.

Although adult neurogenesis occurs throughout life, the number of newly generated neurons is small compared to the total population of dentate granule cells. The population of newly generated DGCs per month is only 6% of the total size of

DGCs in the GCL (Cameron and McKay, 2001). Our lab has verified that primary cilia are essential for glutamatergic synapse formation and dendritic refinement of adult born neurons in the DG (Kumamoto et al., 2012). However, the role of primary cilia in mature DGCs after synaptic integration has yet to be defined. As the hippocampus neural circuit is mainly composed of mature DGCs, I specifically ablated primary cilia in mature DGCs to determine the functionality of primary cilia in hippocampus-associated behaviors. In chapter 3, I will test whether the absence of primary cilia in mature DGCs alters memory encoding and emotional behaviors.

Aim 2. Determine whether ablation of primary cilia in mature dentate granule neurons affects neuronal electrophysiological properties.

Synaptic transmission from the DG to CA3 region regulates memory encoding and its retrieval. The absence of primary cilia formation disrupts excitatory glutamatergic synapse formation in adult born DGCs (Kumamoto et al., 2012). It is therefore possible that the ablation of primary cilia in DGCs may alter synaptic activity and output of these neurons in the hippocampal circuit, which leads to abnormal behavioral activity. In chapter 4, I will test whether the removal of primary cilia in mature DGCs alters mossy fiber output from the DG to CA3. Moreover, I will examine whether the absence of primary cilia in mature DGCs affects the activity balance between adult-born immature DGCs and mature DGCs in the DG.

Aim 3. Determine whether primary cilia regulate migration and final positioning of newly generated DGCs in the GCL.

Aim 3.1. Determine whether defects in primary cilia expression alter final positioning and dendritic development of adult born dentate granule neurons.

Adult born neurons in the DG finalize their position in the GCL at around day 21 when most of the newborn DGCs express primary cilia after day 21 (Kumamoto et al., 2012). This suggests the possibility that primary cilia might function as an anchor in radially migrating neurons. Thus in the following chapter 5, I will examine whether the failure to express primary cilia alters the final position of adult born DGCs in the GCL. Furthermore, I will test whether dendritic refinement is altered following primary cilia removal.

Aim 3.2. Determine whether inhibition of primary cilia assembly alters early migration and dendritic development of adult born dentate granule neurons.

Primary cilia are associated with the centriole, which is also involved in cell migration (Dawe et al., 2007). Newly generated dentate granule neurons undergo tangential dispersion and radial migration from their birthplace. So I asked whether primary cilia play essential roles for the migration of adult born neurons in the DG. Here in chapter 5, I will determine whether defects in primary cilia assembly alter the early migration and the dendritic development of adult born DGCs.

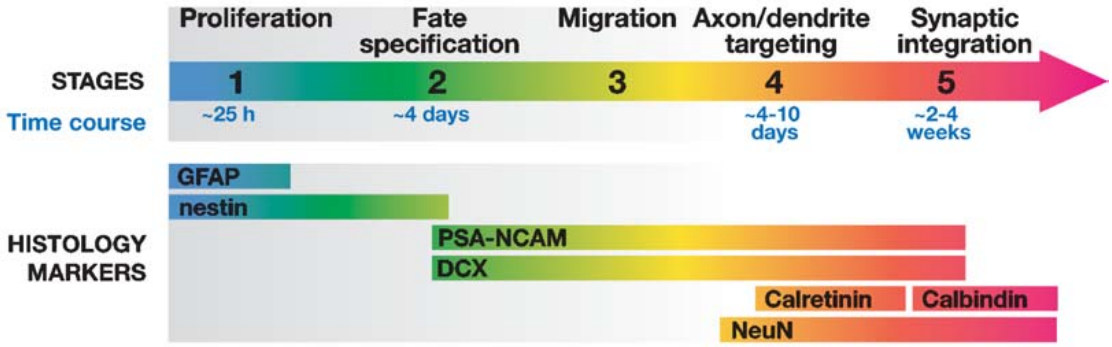

Figure 1.1. Markers for staging adult neurogenesis in the hippocampus
This illustration was obtained from a review from Ming and Song (Ming and Song, 2005). Newly generated granule neurons undergo 5 developmental processes - Proliferation, Fate specification, Migration, Axon and dendrite targeting and Synaptic integration in dentate gyrus. In each stage developing cells express specific proteins, which can be used as a marker for development stage.

Chapter 2 Materials and Methods

Transgenic mice

***IFT20* fl/fl:** Conditional *IFT20* mutant mice were kindly provided from Dr. Gregory J Pazour (University of Massachusetts Medical School). Generation of *IFT20* fl/fl transgenic mice was described previously (Jonassen et al., 2008). Briefly, LoxP sites were inserted into *IFT20* intronic region1 and 3 to generate chimeric mice that carry the *IFT20* ^{neo} allele. *IFT20* ^{neo} mice were crossed with FLPe mice to create mice carrying *IFT20*^{floxed} allele.

Nestin-Cre ^{ERT2}; iDTR: Inducible DT receptor mice were purchased from Jackson lab. Generation of Nestin-Cre ^{ERT2}; iDTR mice was followed as previously (Arruda-Carvalho et al., 2011). Nestin-Cre ^{ERT2}+ mice were crossed with iDTR+/+ mice resulting Nestin-Cre ^{ERT2}+/iDTR+ or Nestin-Cre ^{ERT2}-/iDTR+ offspring. Mice were genotyped by PCR with generic Cre primers (5'-5'- GCG GTC TGG CAG TAA AAA CTA TC – 3' and 5'- GTG AAA CAG CAT TGC TGT CAC TT- 3') and only Nestin-Cre ^{ERT2}+/iDTR+ mice were used in experiments.

All mice were housed under standard condition with 12-hour light/dark cycle. All animal procedures were in accordance with the institutional animal guidelines and were approved by the ethical committee. Prior to all behavior experiments, mice were handled twice a day for three constitutive days.

Viral production and stereotaxic injection

High titer of adeno-associated viruses, AAV-CAMKII-eGFP and AAV-CAMKII-eGFP-Cre, were purchased from the inventory of University of Pennsylvania viral vector core-facility. High titer AAV-DIO-*dnKif3A*-dTomato was produced and purified from University of North Carolina viral vector core facility. *dnKif3A* sequence, described previously (Kumamoto et al., 2012), was packed as AAV9 virus.

Purified engineered retroviruses were produced by transfection of retroviral vectors with retroviral packaging vectors into HEK 293 cells. Each *eGFP*, inducible *Cre* ^{ERT2} and *dnKif3A* sequences were inserted into retroviral vectors.

High titer of engineered viruses were streotaxically injected into 4~6 week old C57BL/6 mice (Charles River), *IFT20* fl/fl mice and Nestin-Cre ^{ERT2};iDTR mice. For the efficient viral transduction, viruses were injected into the dentate gyrus along the anterior-posterior axis, bilaterally (0.5μl per each injection, titer of 4~6 × 10^{13}). Coordinates were followed as previously described (Ge et al., 2006) : -2.0 a/p, ±1.6 m/l, -2.5 d/v and -3.0 a/p, ±2.6 m/l, -3.2 d/v from bregma in mm.

Immunohistology

Mice were transcardially perfused with 4% of paraformaldehyde (PFA) in phosphate buffered saline (PBS). After overnight post fixation, fixed brains were transferred into 30% sucrose solution. Fixed brains were sliced by a sliding microtome, creating coronal brain sections (40μm). The sections were blocked with 10% donkey

serum in 0.25% Triton-PBS for 1 hour. Next, the sections were incubated at 4 °C with primary antibodies diluted in 10% donkey serum in 0.25% Triton-PBS for overnight. On the next day, the sections were rinsed with PBS three times for 5 minutes each. After rinsing off primary antibodies, the sections were incubated with secondary antibodies diluted in the same solution used for primary antibody incubation for 2 hours. The sections were rinsed with PBS, and mounted on a glass slide. During the mounting, DAPI containing mounting media was used to stain the nucleus. Images were acquired on Olympus FV1000 confocal system.

Behavior Tests

Contextual Fear Conditioning (CFC): CFC procedure was described previously (Gu et al., 2012). On day 1, mice were placed into the fear-conditioning chamber, which consists with stainless steel walls with transparent front and back, and a stainless steel shock grid floor (18×18×30 cm). 70% ethanol was used to provide background odor on context A. During the training, mice were able to explore the context A (fear context) for 3 minutes. After 2 minutes of exploration, a tone (2800 Hz, 85dB) was given for 30 seconds following a 2 second foot shock (0.5 mA). Mice were removed from the context A and transferred back to home cages. 24 hours after the training, mice were re-exposed into the context A without any foot shock or tone, measured the freezing level during 5 minutes. 4 hours later, mice were placed into a novel context, which is consist with white plastic surrounding walls and covered floor. During 5 minutes of the probe

test, a tone was presented for 3 minutes after 2 minutes of delay and measured the freezing level during the test.

All mouse movements during the experiments were recorded through FreezeFrame software and percentage of freezing was analyzed by FreezeView software with 1 second of minimum bout duration.

Spatial novelty recognition test: Spatial novelty recognition test probes spatial memory whether mice can recognize the new location of the object. After 3 days of habituation, I placed two identical objects in the box (50cm×50cm) and allowed mice to explore for 10 minutes. On the next day, one of the objects was re-located. Contact time and frequency on both objects were measured during 10 minutes probe test.

Novel object recognition test: Novel object recognition test probes cognitive memory whether mice can recognize the novel object. After 3 days of habituation, two identical objects were placed in the box (50cm×50cm) and let mice to explore for 10 minutes. On the next day, one of the objects was replaced into distinct object at same the location. Contact time and frequency on both objects were measured during 10 minutes.

Pre exposure dependent contextual fear conditioning (PECFC): PECFC paradigm probes a memory recall ability of mice based on completing the pattern of CFC. PECFC procedure was based on Nakashiba et al (Nakashiba et al., 2008). On day 1, mice were placed into the conditioning chamber and let them explore the chamber freely for 10 minutes, and transported back to their home cages. On day 2, mice were re-exposed to the conditioning chamber, received a 2 second 0.75mA single foot shock at 10 seconds after placement into the chamber. Mice were removed from the conditioning chamber

and back to home cages 30 seconds after the foot shock termination. On day 3, context fear was probed by placing mice back in to the conditioning chamber for 5 minutes.

All mouse movements during the experiments were recorded through FreezeFrame software and percentage of freezing was analyzed by FreezeView software with 1 second of minimum bout duration. Freezing levels during 5 minutes on day 3 were averaged over the each group for analysis.

Contextual fear discrimination test (Pattern Separation): Contextual fear discrimination test probes ability of mice distinguishing two similar contexts. Pattern separation procedure was based on previous research (Sahay et al., 2011a). To generate fear memory, mice were exposed to the shock-associated context A. This context contains stainless steel grid floor, transparent front and back walls with a mild alcohol scent for the olfactory cue. This context was cleaned with 70% ethanol before every mouse was placed in the context. For fear memory learning, mice received a 2 second single foot shock (0.5mA) at 185 seconds after placement into the chamber. Mice were removed from the chamber and back to home cages 15 seconds after the foot shock termination. Context B is the similar context without shock. It is consisted with stainless steel grid floor same as in context A, but black and white striped front and back walls without olfactory cue. This context was cleaned with odorless non-alcoholic antiseptic solution before every mouse was placed in the context. Mice were allowed to explore freely for 180 seconds without any shock.

On day 0, mice were exposed to the context A for fear memory learning. On days 1 through 7 mice were trained for discrimination by exposed to both context A and

context B. The order of exposure on each day was AB/AB/BA/BA/AB/BA/AB and there were 4 hours gap between exposures to each context.

All mouse movements were recorded through FreezeFrame software and percentage of freezing was analyzed by FreezeView software with 1 second of minimum bout duration. Freezing levels during first 180 seconds on each sessions were averaged over the each group and used to calculate the discrimination ratio; Discrimination Ratio = (Freezing Context A – Freezing Context B) / (Freezing Context A + Freezing Context B). Discrimination ratio scoring 1 indicates perfect discrimination; on the other hand score close to 0 indicates failure of discrimination.

Elevated Plus Maze (EPM): EPM is a paradigm, which can test anxiety level of rodents (Komada et al., 2008).The apparatus used for EPM has two open arms and two closed arms surrounded with transparent plastic walls. The entire apparatus is 50 cm above from the floor and placed in a large circular tank. To test anxiety level, mice were placed at the center of the apparatus and allowed to explore freely for 5 minutes. The time spent in each arms and the center was measured and analyzed.

Light and Dark transition test: Light and dark transition test measures innate anxiety level using light avoidance of rodents. The apparatus has two compartments- light compartment covered with transparent plastic walls and dark compartment covered with black and opaque plastic walls, connected with each other. At the beginning mice were placed at the dark compartment. Latency to enter the light compartment and time spent in each compartments are measured.

Electrophysiology: Mice for the electrophysiology tests were processed at least14 days after AAV injection into the DG. Electrophysiology procedure was followed as previously described (Ge et al., 2006). To examine synaptic output from DG to CA3, the stimulating electrode was placed at mossy fibers near DG. High Frequency Stimulation (HFS) delivers 100 stimuli at 100 Hz frequency, was given to evoke synaptic plasticity at the CA3. Recording electrode located at the CA3. Slope of field excitatory postsynaptic potentials (fEPSPs) in each traces were measured and averaged in every 4 sweeps for plotting synaptic plasticity. Synaptic plasticity was analyzed by comparing the averaged slope of the baseline and the last 10 minutes field EPSPs.

Relative position and dendritic angle: For neuronal final positioning analysis, single scanned confocal images of eGFP expressing adult born neurons were used. The process to measure relative position was previously described (Kumamoto et al., 2012). A perpendicular distance from the inner GCL was measured.

Similarly dendritic angle was analyzed by measuring the angle between apical dendrite and the inner GCL.

Clonal analysis: For tracing neurons from the same lineage, lenti-virus expressing Cre under GFAP promoter and retrovirus expressing eGFP was co-injected into *IFT20* fl/fl mice. Mice were processed after 7 days post injection. Averaged distance between neurons in same lineage was analyzed using Imaris software.

Sholl analysis: For dendritic development analysis, dendritic trees were reconstructed into 3D from z-series stacked confocal images using Imaris software. Total dendritic length, number of dendrites and number of crossings from the soma were analyzed to examine dendritic refinement.

Antibodies

The following antibodies were used: rabbit anti-adenylyl cyclase III (1:300, Santa Cruz Biotechnology; sc-588), goat anti-GFP (1:500, Rockland; 600-101-215), goat anti-DCX (1:500, Santa Cruz Biotechnology; sc-8066), mouse anti-goat AlexaFluoro 488 (1:1000, Jackson Labs), Donkey anti-rabbit Cy-3 (1:1000, Jackson Labs), donkey anti-rabbit AlexaFluoro 647 (1:1000, Jackson Labs).

Drugs

Tamoxifen: Tamoxifen (Sigma) was dissolved in ethanol, and suspended in corn oil. Tamoxifen was administrated by oral gavage (160mg/Kg). Mice received three rounds of administration, once a day for three constitutive days.

Diphtheria Toxin: DT toxin preparation and administration was followed as described (Arruda-Carvalho et al., 2011). DT (Sigma) was dissolved in BSA containing PBS. To ablate DTR expressing cells, mice received daily injections of DT (i.p 16μg/Kg) for two constitutive days after the tamoxifen administration.

Doxycycline: Doxycycline (Sigma) was dissolved into the water with 5% sucrose (wt/vol) to mask the taste of the drug. Doxycycline was administrated daily by replacing drinking water into doxycycline dissolved water.

Statistical analysis

Most of data were analyzed using two-tailed unpaired student t-test. Neuronal distribution was analyzed by Kolmogorov-Smirnov (KS) test and proportion of the dendritic angle was analyzed by chi-square test. Statistically significance was considered only p value is smaller than 0.05. All data were presented as mean ± SEM.

Chapter 3 Primary cilia and hippocampus-associated behaviors

3.1 Introduction

Syndromes characterized with functional and genetic defects in cilia are called ciliopathies. In human ciliopathies, neurological abnormalities such as mental retardation, cognitive defects and development delay are commonly found (Badano et al., 2006), suggesting the role of neuronal primary cilia in cognition.

Neuronal primary cilia express several GPCRs and act as a sensor of extracellular stimuli such as SSTR3 (Handel et al., 1999), 5-HT6 (Hamon et al., 1999) and MCH1 (Ludwig et al., 2001). Furthermore, type III adenylyl cyclase (ACIII) is localized in neuronal primary cilia throughout the adult brain (Bishop et al., 2007). ACIII, coupled with GPCRs, converts ATP to cyclic AMP (cAMP) and pyrophosphate. The cAMP activates downstream molecules, and function as a second messenger (Defer et al., 2000).

Several recent studies revealed that ACIII associated with primary cilia plays an essential role in hippocampal learning and memory. In 2010, Einstein at al. found that constitutive and global SST3 KO animals showed abnormality in novel object discrimination but normal spatial memory. They further demonstrated that SST3 KO showed reduced cAMP mediated long-term potentiation (LTP) in CA1 (Einstein et al., 2010). Another research group by using ACIII KO animals showed ACIII mutants exhibited impaired learning and memory in temporally dissociative passive avoidance test, novel object memory and extinction of the contextual fear memory (Wang et al., 2011). These studies suggest some roles of neuronal primary cilia in regulating

cognitive memory. Since the researchers depleted ACIII or SST globally and constitutively, it remains unknown whether these defects resulted from ciliary dysfunction or developmental abnormality. It also remains elusive whether behavioral defects directly resulted from hippocampal dysfunction. However, these tests indeed suggest that primary cilia are likely important for cognitive memory.

There is another study that supports that the functionality of primary cilia in learning and memory. When assembly of primary cilia was ablated in adult stem/progenitor cells, mutant mice displayed impaired spatial memory and enhanced cued fear responses. The authors mentioned that there was no difference in anxiety related and depression like behaviors in *IFT20* mutant mice (Amador-Arjona et al., 2011). However, the level of adult neurogenesis was altered by primary cilia ablation in adult stem/progenitor cells in this research. As anxiety and depression like behaviors are highly related to adult neurogenesis level, sole effect of primary cilia on emotional behaviors need to be confirmed. More importantly, primary cilia express 5-HT6 receptors, which is a potential target for psychotropic drugs (Brailov et al., 2000a, Svenningsson et al., 2007).

Ablation of primary cilia expression in brain cells causes cognitive learning and memory impairment. However, behavioral effect of primary cilia selectively in mature DGCs is unknown. In chapter 3, I found that ablation of primary cilia in mature DGCs impaired spatial discrimination and learning. Additionally, by using *IFT20* fl/fl transgenic mice together with inducible Cre viral transduction, I dissected the function of primary cilia by neuronal development.

3.2 Results

3.2.1 Deletion of primary cilia in mature dentate granule cells

To examine the role of primary cilia in mature DGCs, I targeted IFT20, which is an anterograde motor protein essential for cilium assembly (Follit et al., 2006). In order to remove *IFT20* alleles in mature DGCs, I injected high titer adeno- associated virus (AAV) expressing Cre recombinase under CAMKII promoter into the DG of 6-week old *IFT20* fl/fl mice (Jonassen et al., 2008). At 28 days post injection (dpi), over 95% of DGCs in the DG were transduced by the AAV confirmed by the number of GFP positive cells (Figure 3.1 A-B). To verify whether Cre recombinase expression through this viral transduction indeed removed primary cilia in mature DGCs of *IFT20* fl/fl mice, I stained the brain sections for ACIII, a marker for primary cilium (Bishop et al., 2007). I found that all Cre-expressing DGCs lacked visible primary cilia in IFT20 (-/-) $^{\text{mature DGCs}}$ mice (Figure 3.1 D), whereas control DGCs injected with AAV-CAMKII-eGFP still expressed primary cilia (Figure 3.1 C). To verify whether Cre recombinase is only expressed in mature GCs, I co-stained the brain sections with ACIII and doublecortin (DCX), a marker for immature neuron, and found that virus infected GCs, which express eGFP, did not co-localize with DCX positive cells in both groups, and furthermore primary cilia were still present in DCX+ DGCs (Figure 3.1 C-D). To test whether the number of adult born neurons was affected by removal of primary cilia from mature DGCs, I randomly selected fields (320μm × 320μm × 993.35μm) from dorsal to ventral the DG and counted the number of DCX positive cells. I found that the number of DCX positive cells per field was similar between control and IFT20 (-/-) $^{\text{mature DGCs}}$ group (Figure 3.2, two tailed unpaired t-test: p=0.94). Together, these results indicate that AAV-CAMKII-eGFP-

Cre transduction in IFT20 (-/-) $^{\text{mature DGCs}}$ mice selectively ablated primary cilia in mature DGCs without affecting adult neurogenesis.

3.2.2 Primary cilia in mature dentate granule cells regulate contextual memory

In early developmental stage, primary cilia modulate hippocampus-associated learning and memory by regulating proliferation of progenitor cells (Amador-Arjona et al., 2011). However, whether primary cilia in mature DGCs can modulate hippocampus-associated behaviors remained unknown. To test the role of primary cilia in mature DGCs during hippocampus-associated learning and memory, I performed contextual fear conditioning (CFC) test (Nakashiba et al., 2008) with *IFT20* fl/fl mice 28 days after AAV injection. Twenty-four hours after the training session, the animals were placed back in the same context, and a 5-minute probe test was performed (Figure 3.3). IFT20 (-/-) $^{\text{mature DGCs}}$ mice showed significantly less freezing than CTRL mice, which were injected with AAV-CAMKII-eGFP (Figure 3.4 A, 41.42±2.36% for CTRL and 31.43±2.07% for IFT20 (-/-) $^{\text{mature DGCs}}$, p=0.0017). IFT20 (-/-) $^{\text{mature DGCs}}$ mice did not show difference in freezing with CTRL mice in a toned fear test in a different context B (Figure 3.4 B, 41.27±2.33% for CTRL and 34.75±2.85% for IFT20 (-/-) $^{\text{mature DGCs}}$ at post-tone, p=0.08), indicating that only hippocampus-associated contextual fear memory is altered by removing primary cilia from mature DGCs (Figure 3.4 B). This suggests that primary cilia in mature DGC are required for contextual learning and memory.

3.2.3 Primary cilia in mature dentate granule cells regulate spatial novelty recognition but not novel object recognition

Next, to examine whether hippocampus-associated cognitive and spatial memory are also altered due to the ablation of primary cilia in mature GCs, I performed novel location and novel object recognition test During the training following three days habituation sessions, mice were allowed to explore two identical objects in the chamber for 10 minutes. In the probe test 24 hours after the training session, I re-located one of the objects and measured contacting time and frequency of the mice with objects at familiar and novel locations (Figure 3.5). I found CTRL mice spend significantly more time (Figure 3.6 left, 21.03±2.38 seconds at old and 28.39±2.45 seconds at novel location, two tailed unpaired t-test: p= 0.04) and higher frequency (Figure 3.6 right, 162±19.71 at old and 200±28.91 at novel location, two tailed unpaired t-test: p=0.1) contacting with the object at new location, whereas IFT20 (-/-) $^{\text{mature DGCs}}$ mice did not show preference between two locations on both time (Figure 3.6 left, 27.15±3.41 seconds at old and 26.59±2.50 seconds at novel location, two tailed unpaired t-test: p=0.89) and contacting frequency (Figure 3.6 right, 21.63±24.66 at old and 196.81±21.04 at novel location, two tailed unpaired t-test: p=0.93).

The novel object recognition test was performed similarly to novel location test. After training mice by exposing into two identical objects, one of the objects was replaced into distinct object and measured contacting time and frequency of the mice with two objects (Figure 3.7). Unlike novel location test CTRL and IFT20 (-/-) $^{\text{mature DGCs}}$ mice did not show difference in the behavior pattern, both mice spent more time (Figure 3.8 left, 26.25±5.87 seconds at old and 41.20±7.67 seconds at new object for CTRL and 21.86±4.34 seconds at old and 37.43±9.62 seconds at new object for IFT20 (-/-) $^{\text{mature DGCs mice}}$) and preference at the novel object (Figure 3.8 right, contact frequency for

CTRL180.92±39.54 at old and 293.46±50.17 at new object, and IFT20 (-/-) $^{\text{mature DGCs}}$ 156.63±28.19 at old and 253.36±55.40 at new object). These results suggest that primary cilia in mature DGCs are important for novel location recognition.

3.2.4 Absence of primary cilia in mature dentate granule cells impairs patter completion

In CFC experiment, IFT20 (-/-) $^{\text{mature DGCs}}$ mice exhibited less freezing in fear context but not in cued context (Figure 3.4 B). To find out whether the impaired contextual memory by removal of the primary cilia from mature DGCs is due to a defect in contextual completion, I performed a pre-exposure contextual fear-conditioning (PECFC) test (Nakashiba et al., 2008). After 10minutes of pre-exposure to a context, a fear was generalized by giving a foot shock to mice 10 seconds after they entered the context (Figure 3.9). This test probes whether mice can complete and retrieve a context fear memory in a short time. In the PECFC test, IFT20 (-/-) $^{\text{mature DGCs}}$ mice exhibited less freezing pattern during the probe test (Figure 3.10 A, p=0.002 at 2 minute), and average freezing level during 5 minutes probe test was significantly decreased (Figure 3.10 B, 35.23±2.06% for CTRL and 27.84±1.77% for IFT20 (-/-) $^{\text{mature DGCs}}$, two-tailed unpaired t-test: p=0.007), indicating IFT20 (-/-) $^{\text{mature DGCs}}$ mice showed impairment in completing context pattern based on the pre-exposed context.

3.2.5 Absence of primary cilia in mature dentate granule cells enhances contextual fear discrimination

Next, I examined whether primary cilia ablation from mature DGCs alters pattern separation, with which mice can discriminate distinct representations between similar

contexts/episodes. As described in Figure 3.11, on day 0 a fear context was generalized by a foot shock. For next 8 constitutive days mice were trained by exposing them to fear context (context A) and similar but safe context (context B). During 8 days of training, CTRL mice start to discriminate two similar contexts from day 6 (Figure 3.12 A, 66.92±4.37% for context A and 58.67±4. 05% for context B, two tailed unpaired t-test: p= 0.009) whereas IFT20 (-/-) $^{\text{mature DGCs}}$ mice start to discriminate from day3 (Figure3.12 B, 53.63±4.93% for context A and 41.33±4.72% for context B, two tailed unpaired t-test: p=0.002). Discrimination ratio in each group of mice over 8 days of training indicates that IFT20 (-/-) $^{\text{mature DGCs}}$ mice show significantly higher level of contextual fear discrimination on day 8 (Figure 3.13 and 3.14, 0.037±0.034 for CTRL and 0.172±0.045 for IFT20 (-/-) $^{\text{mature DGCs}}$ on day 8, two tailed unpaired t-test: p=0.03). Thus, these results suggest that mice with primary cilia ablated in mature granule cells exhibit better discrimination between similar contexts.

3.2.6 Absence of primary cilia in mature dentate granule cells shows no effects on anxiety related behaviors

Hippocampus also regulates emotional behaviors such as anxiety or depression. I examined whether primary cilia ablation from mature DGCs alters anxiety related behaviors in *IFT20* fl/fl mice. To test anxiety related behaviors, I performed elevated plus maze and light and dark transition test.

In elevated plus maze test, I placed mice at the center of the plus maze and measured time spent and number of crossings at open arms, closed arms and the

center during 5 minutes (Figure 3.15). Elevated plus maze examines mice anxiety level by utilizing conflict between exploration instinct and propensity to stay in safe place. IFT20 (-/-) $^{\text{mature DGCs}}$ mice were showing a tendency to stay longer in open arms compare to CTRL mice, however it was not statistically significant (Figure 3.16 left , 24.80±5.14% for CTRL and 32.87±5.86% for IFT20 (-/-) $^{\text{mature DGCs}}$ mice at the open arm, two tailed unpaired t-test: p=0.31). Number of entries to open arms did not differ between two groups (Figure 3.16 right, 16.56±1.89 for CTRL and 18.65±1.33 for IFT20 (-/-) $^{\text{mature DGCs}}$ at the open arm, two tailed unpaired t-test : p=0.37).

In addition, I also performed light and dark transition test to confirm phenotype in anxiety related behaviors in primary cilia removed mice. Based on the innate aversion of bright areas, the time spent at light and dark compartments and number of entries during 10 minutes were measured to analyze anxiety level (Figure 3.17). Both CTRL and IFT20 (-/-) $^{\text{mature DGCs}}$ mice spend more time in dark compartment, but no significant difference was observed between two groups (Figure 3.18 left, 80.48±2.39% for CTRL and 78.40±1.88 for IFT20 (-/-) $^{\text{mature DGCs}}$ at the dark compartment, two-tailed unpaired t-test: p=0.50). Together these results indicate that mice with primary cilia removed in mature DGCs exhibit normal anxiety level.

3.3 Discussion

Here, I determined the role of primary cilia in mature DGCs in hippocampus-associated behaviors. When I ablated primary cilia in mature DGCs, mice exhibited impairment in spatial memory, contextual fear memory and pattern completion, but enhancement in contextual fear discrimination. On the other hand, anxiety related

behaviors were not altered by primary cilia ablation. Overall, our results indicate that primary cilia in mature DGCs are playing a role in cognitive and spatial memory.

These results somewhat correspond to previous studies that ablation of ciliary protein or primary cilia associated signaling pathways, such as ACIII or SSTR3, in brain impairs cognitive memory but normal anxiety and depression like behaviors (Amador-Arjona et al., 2011, Berbari et al., 2014, Einstein et al., 2010, Wang et al., 2011). However, I provided a novel approach by selectively manipulating mature DGCs in the hippocampus by conditional deletion of IFT20 (Jonassen et al., 2008). This approach allows to reveal and dissect the role of primary cilia by neuronal developmental stage without affecting adult neurogenesis level (Figure 3.2) so that excludes the possibility of memory impairment is due to decreased number of adult born neurons (Amador-Arjona et al., 2011, Clelland et al., 2009, Sahay et al., 2011a).

Animals undergo three processes to memorize received information; encoding, consolidation and retrieval. In this study, I examined several types of memory and emotional behaviors to elucidate which memory process is altered by the consequences of a conditional ablation of primary cilia.

Interestingly, our data show impaired pattern completion memory but enhanced contextual fear discrimination. Pattern completion is a recall of previously encoded memories by using partial information as reactivation cues. Synaptic transmission and plasticity in the recurrent collateral of CA3 is involved in recall of memory in pattern completion (Gold and Kesner, 2005, Kesner, 2007, Nakazawa et al., 2002). When I removed primary cilia in mature DGCs, mice failed to recognize pre-exposed fear

context exhibiting less freezing level (Figure 3.9). This behavior phenotype was also observed in CFC, as IFT20 (-/-) $^{\text{mature DGCs}}$ mice freeze less in context A (Figure 3.4). There are two possibilities to explain the failure in pattern completion; failure in encoding the spatial representation during the training or disruption in recall from incomplete cues. Previous research revealed that memory encoding relies on DG to CA3 input (Lee and Kesner, 2004), which supports that the information encoding is altered rather than its retrieval under conditional removal of primary cilia in mature DGCs.

On the other hand, contextual fear discrimination is a memory that discriminates similar episodes based on previously formatted spatial and temporal representation. It relies on the synaptic transmission and plasticity in mossy fiber pathway from DG to CA3 area (Leutgeb et al., 2007, Rolls, 2013). Interestingly our result shows that IFT20 (-/-) $^{\text{mature DGCs}}$ mice have better discrimination ability than CTRL mice (Figure 3.13) even though other memories, such as spatial and pattern completion, have been impaired. A recent study suggests that pattern separation requires adult born young DGCs (Nakashiba et al., 2012). It is possible that ablation of primary cilia in mature DGCs alters the synaptic output from DG to CA3 by changing the activity balance between young and old DGCs. In chapter 4, I will discuss this part further.

As described previously, hippocampus is an important brain region, which regulates spatial, recognition and working memory (Bannerman et al., 2004, Moser and Moser, 1998). However, IFT20 (-/-) $^{\text{mature DGCs}}$ mice show normal recognition memory (Figure 3.8) where as the spatial memory was impaired (Figure 3.6). Previously Broadbent et al have shown that spatial memory is more sensitive on the integrity of the

hippocampus than recognition memory. They showed that over 75% of total hippocampal volume is required to show impairment in recognition memory where as only 30~50 % of hippocampal lesion leads to impairment in spatial memory (Broadbent et al., 2004). Behavioral pattern of IFT20 (-/-) $^{\text{mature DGCs}}$ mice observed from spatial novelty recognition test suggests that DG specific manipulation of primary cilia is sufficient for leading impairment in hippocampal dependent spatial memory.

Although neuronal primary cilia are highly expressing 5-HT6 receptor, IFT20 (-/-) $^{\text{mature DGCs}}$ mice did not show difference in anxiety level. In my preliminary research, when primary cilia were removed in POMC+ immature neurons (TJ et al., 2007), mice without primary cilia in immature neurons show a trend of increased anxiety level. Mice spent less time in the open arms of the elevated plus maze test (not significant, data not shown). Previous study also showed similar results, as mice with depletion of DCX + cells spend less time in open arms (Vukovic et al., 2013). Although these results are not showing statistically significance, still it suggests a possibility that immature neurons are more responsible for the regulation of anxiety like behaviors.

Previous studies show that treatment of serotonin selective reuptake inhibitors (SSRIs), increases neurogenesis and increase network activity, which is suggested as a potential mechanism of antidepressant drugs (Boldrini et al., 2009, Malberg et al., 2000, Santarelli et al., 2003). 5-HT6 receptors are mostly expressed in the CNS (Ruat et al., 1993) and it has been shown that administration of 5-HT6 receptor agonists exhibit antidepressant and anxiolytic effect in rat similar to SSRI treatment (Carr et al., 2011). As primary cilia ablation in mature DGCs alters activity balance between mature and

immature neurons in dentate gyrus, it will be interesting to test the efficacy of SSRIs or 5-HT6 agonists on IFT20 (-/-) $^{\text{mature DGCs}}$ mice.

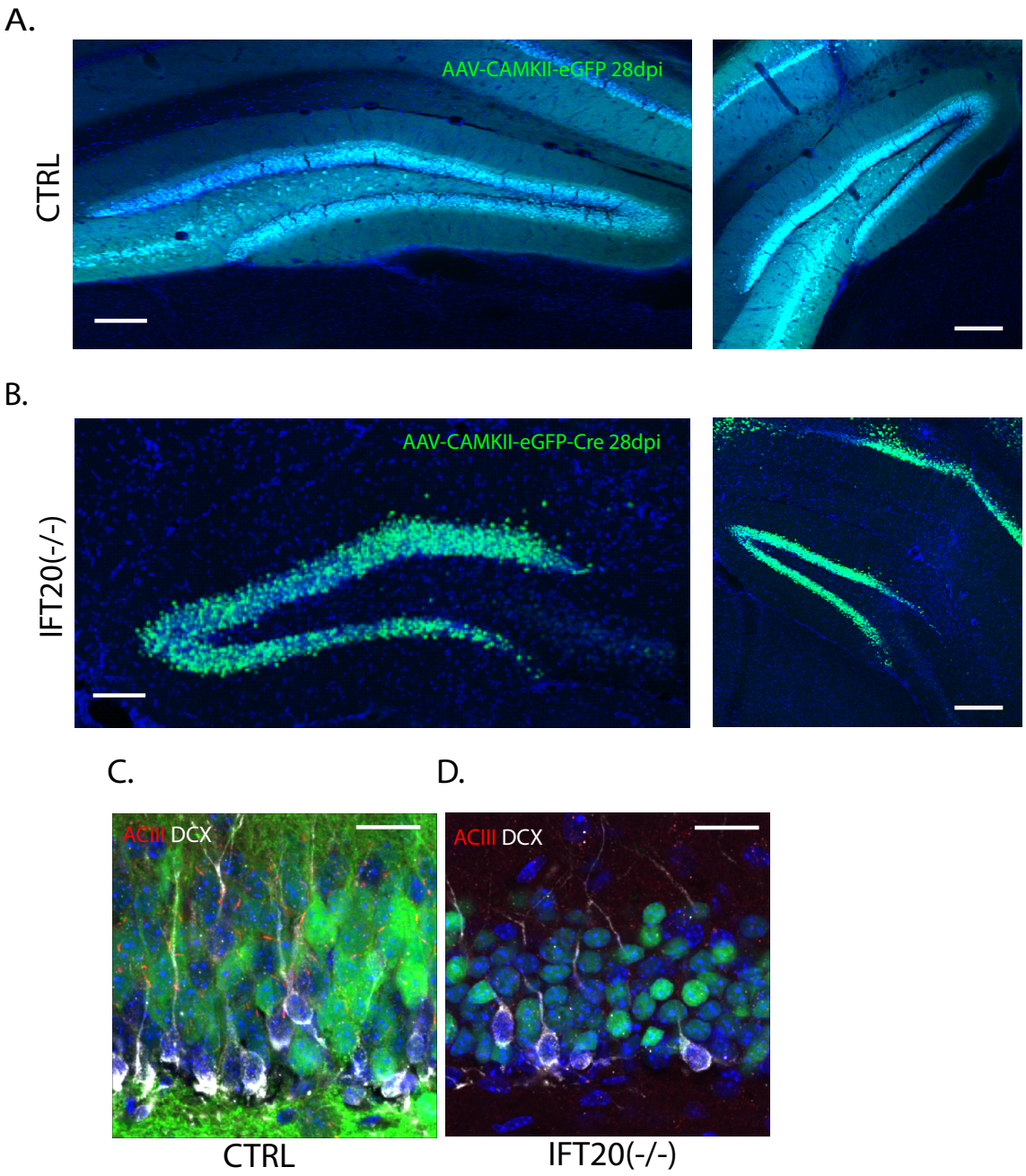

Figure 3.1. Ablation of primary cilia in mature dentate granule cells in *IFT20* fl/fl mice.

A-B. Most of dentate granule cells (>95%) in the DG (both dorsal and ventral) were transduced with AAV-CAMKII-eGFP (A, CTRL) or AAV-CAMKII-eGFP-Cre (B, IFT20 (-/-) $^{\text{mature DGCs}}$) at 28dpi. Scale bars : 100μm.

C-D. Immunofluorescence showing DCX+ young dentate granule cells (white) do not co-localize with eGFP+ mature granule cells in CTRL and IFT20 (-/-) $^{\text{mature DGCs}}$ mice. Primary cilia (ACIII, red) were present matured granule cells in CTRL mice (C), but not in IFT20 (-/-) $^{\text{mature DGCs}}$ mice (D). Scale bars : 20μm.

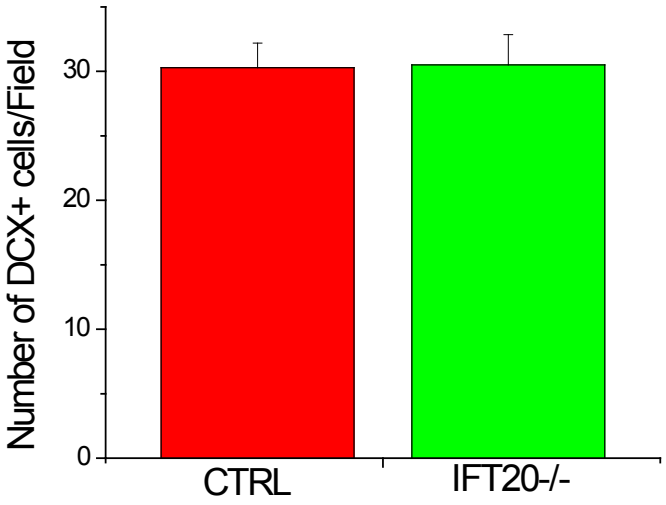

Figure 3.2. Adult neurogenesis was not altered by removal of primary cilia
Quantification of DCX+ cells per field in the DG. No significant difference was found between the number of DCX positive cells in CTRL and IFT20 (-/-) $^{\text{mature DGCs}}$ mice (CTRL n=3 mice , 60 fields, IFT20 (-/-)$^{\text{mature DGCs}}$ n=4 mice, 72 fields, p=0.94).
Field size : 320μm × 320μm× 993.35μm.
p>0.05, two-tailed unpaired t-test. Data are expressed as mean values ± SEM.

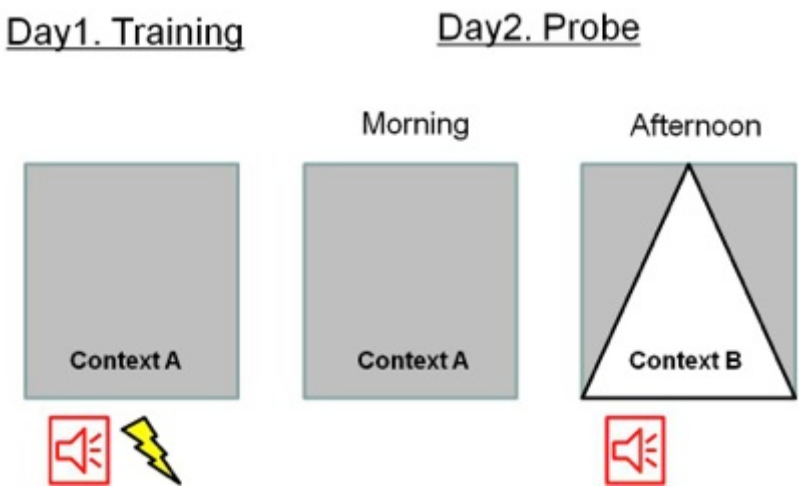

Figure 3.3. Experiment design for contextual memory test
On the training day, mice were placed in context A and receive a tone followed by a foot shock to generate fear context. Next morning, mice were re-exposed to context A without tone or shock. Same day afternoon, mice were placed in context B, a novel context, and received a tone without any shock. Freezing response was analyzed during 5 minutes of exposure to context A and B.

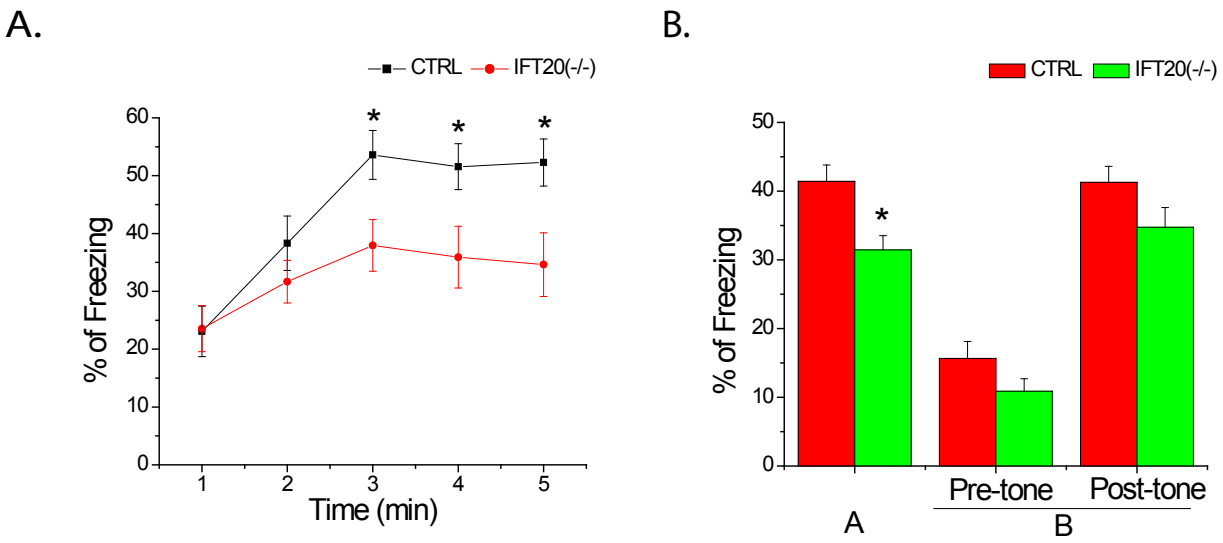

Figure 3.4. Ablation of primary cilia in mature dentate granule cells impairs contextual memory

A. IFT20 (-/-) $^{\text{mature DGCs}}$ mice showed smaller freezing response in context fear test (p=0.016, 0.027 and 0.016 at 3,4 and 5 minutes).

B. Average freezing behavior showing IFT20 (-/-) $^{\text{mature DGCs}}$ mice expressed significant less freezing response compare to CTRL mice in contextual fear memory test (CTRL red bar n=18, and IFT20 (-/-) $^{\text{mature DGCs}}$ green bar n=20, p=0.0017 in context A). Freezing response did not show significant difference between CTRL and IFT20 (-/-) $^{\text{mature DGCs}}$ mice in toned fear memory test in a novel safe context (CTRL red bar and IFT20 (-/-) $^{\text{mature DGCs}}$ green bar, p=0.084 in context B post tone).

*p<0.05, two-tailed unpaired t-test. Data are expressed as mean values ± SEM.

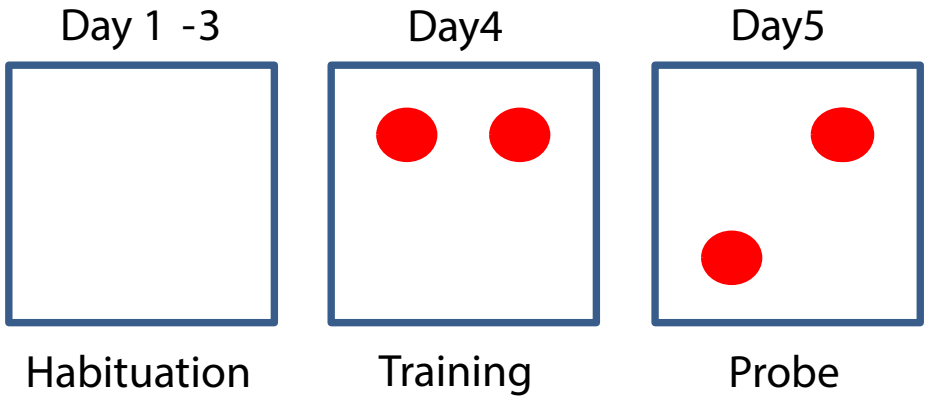

Figure 3.5. Experimental design for spatial novelty recognition test
Two same shaped objects were exposed to mice during training. After 24 hours, one of the objects was relocated and contact time and frequency were analyzed during the probe test.

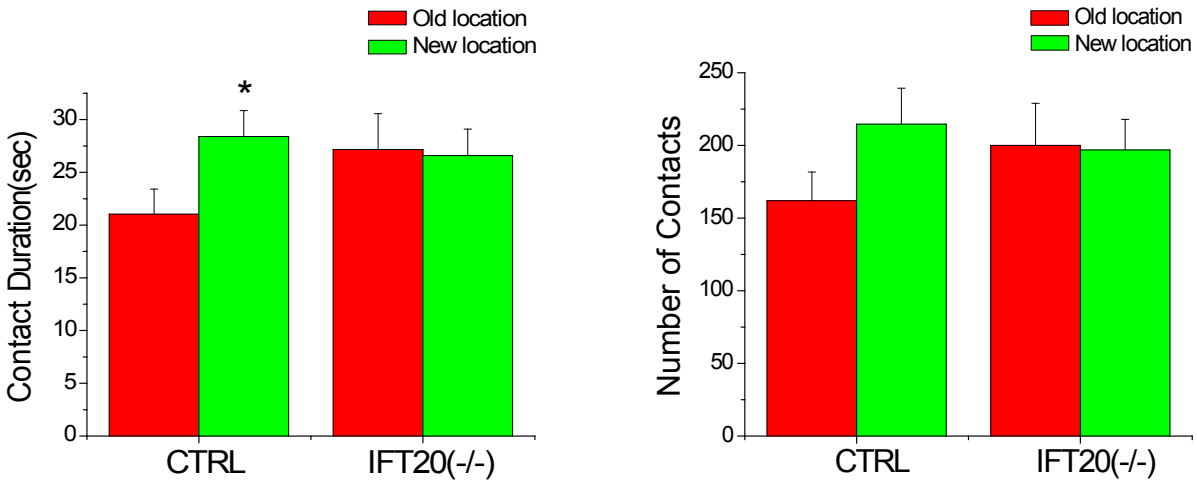

Figure 3.6. Ablation of primary cilia in mature dentate granule cells impairs spatial memory

In spatial novelty recognition test, CTRL mice prefer object in novel location (CTRL n=11, p= 0.04), while IFT20 (-/-) $^{\text{mature DGCs}}$ mice did not show preference in both total contacting time (left, IFT20 (-/-) $^{\text{mature DGCs}}$ n=11, p=0.89) and number of contacts (right, p=0.93).

*p<0.05, two-tailed unpaired t-test. Data are expressed as mean values ± SEM.

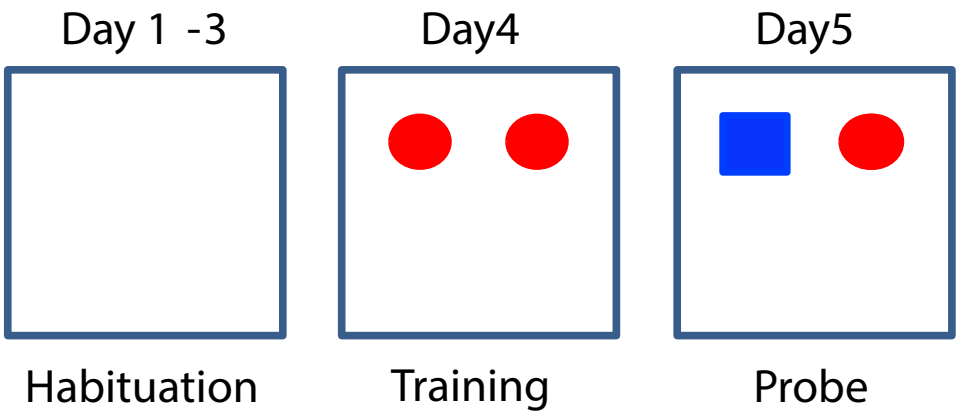

Figure 3.7. Experimental design for novel object recognition test
Two same shaped objects were exposed to mice during training. After 24 hours, one of the objects was replaced and contact time and frequency were analyzed during the probe test.

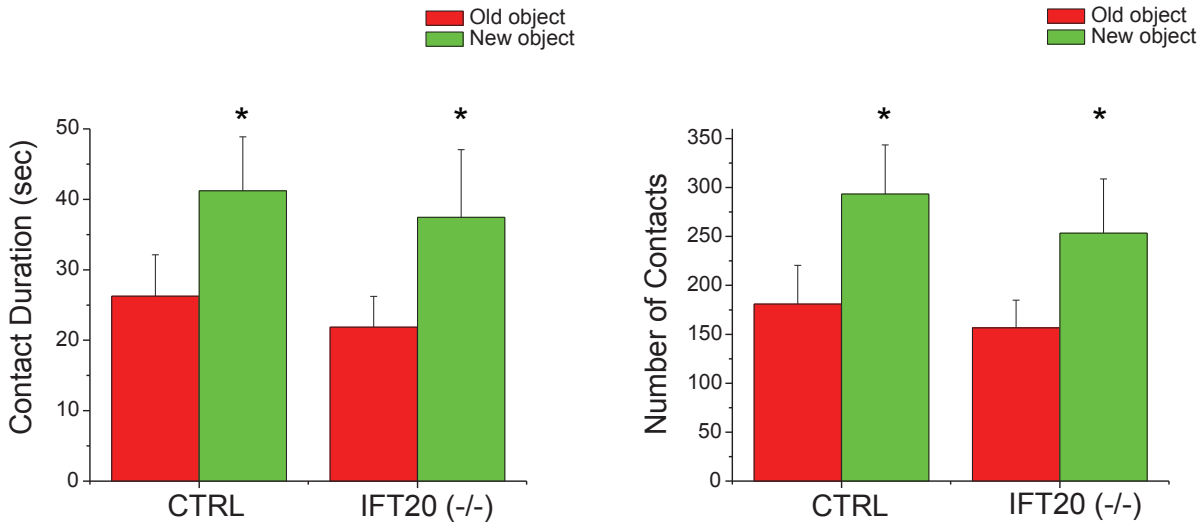

Figure 3.8. Ablation of primary cilia in mature dentate granule cells do not alter recognition memory

In novel object recognition test, both CTRL and IFT20 (-/-) $^{\text{mature DGCs}}$ mice prefer new object in total contacting time (left, CTRL n=13, p= 0.02 and IFT20 (-/-) $^{\text{mature DGCs}}$ n=11, p=0.04) and number of contacts (right, CTRL p= 0.01 and IFT20 (-/-) $^{\text{mature DGCs}}$ n=0.02). *p<0.05, two-tailed unpaired t-test. Data are expressed as mean values ± SEM.

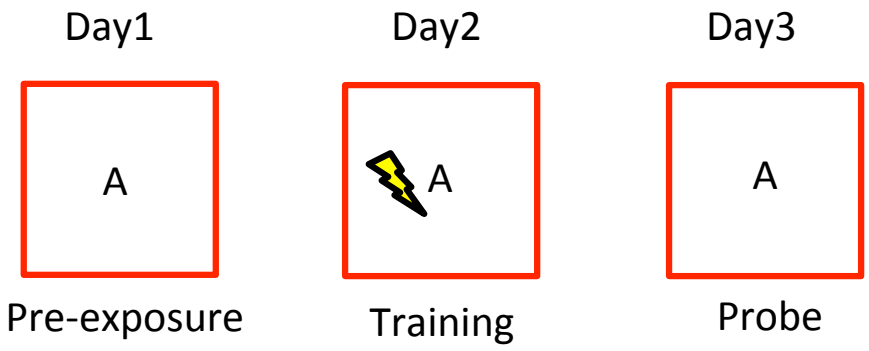

Figure 3.9. Experimental design for pre-exposure dependent context fear test
Mice were exposed to context A for 10 minutes on day1. On training day fear was generated by a foot shock 10 seconds after mice entered the pre-exposed context. After 24 hours, freezing response was analyzed during 5 minute of re-exposure to context A.

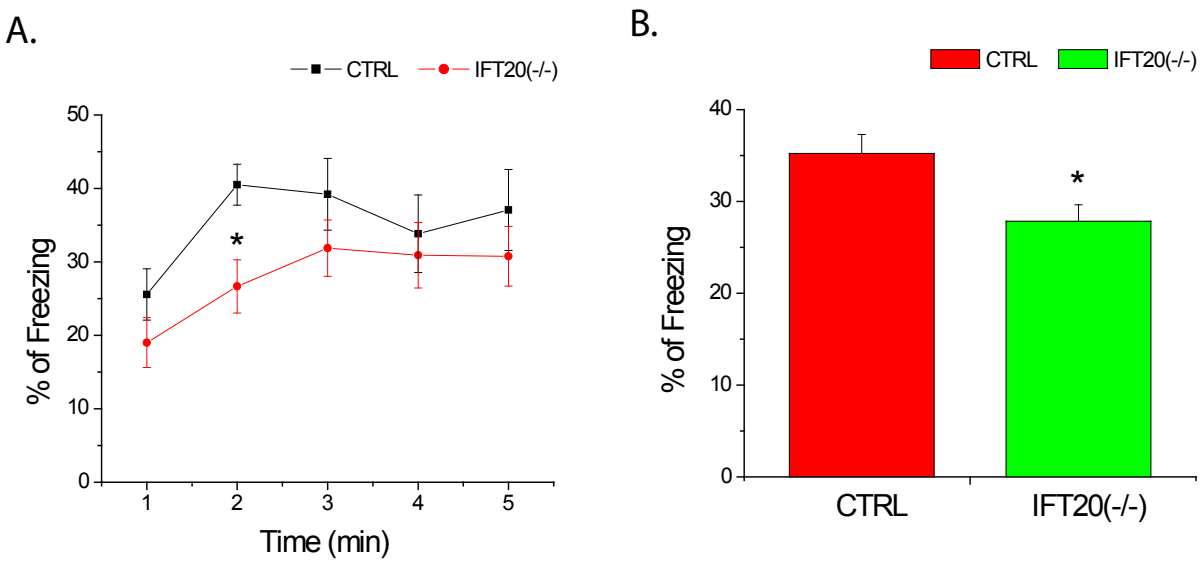

Figure 3.10. Ablation of primary cilia in mature dentate granule cells decreases pattern completion

A. IFT20 (-/-) $^{\text{mature DGCs}}$ mice showed decreased freezing response compared to CTRL when re-exposed to fear context in pattern completion test (p=0.002 at 2 minute).

B. Average freezing data showing significant decreased freezing response in IFT20 (-/-) $^{\text{mature DGCs}}$ mice. IFT20 (-/-) $^{\text{mature DGCs}}$ fail to complete context pattern based on pre-exposed cues compare to CTRL mice (CTRL red bar n=15 and IFT20 (-/-) $^{\text{mature DGCs}}$ green bar n=15, p=0.007).

*p<0.05, two-tailed unpaired t-test. Data are expressed as mean values ± SEM.

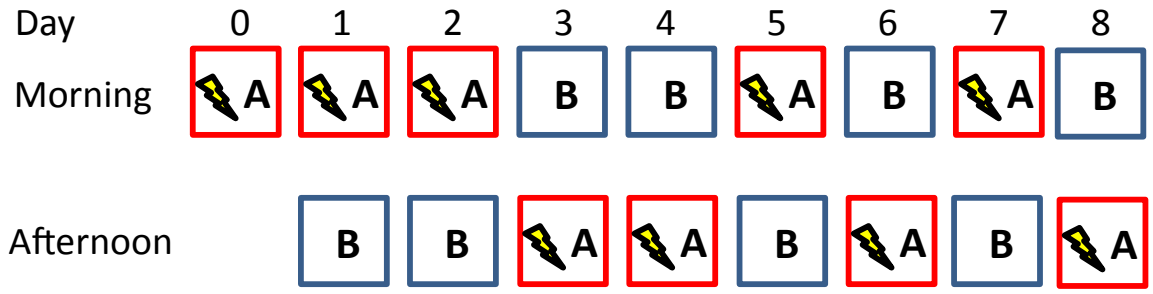

Figure 3.11. Experimental design for contextual fear discrimination test
On day 0, mice receive a foot shock at context A to generate a fear context. Everyday mice were exposed to context A (fear context) and similar context B (safe context) until they start to discriminate two similar contexts.

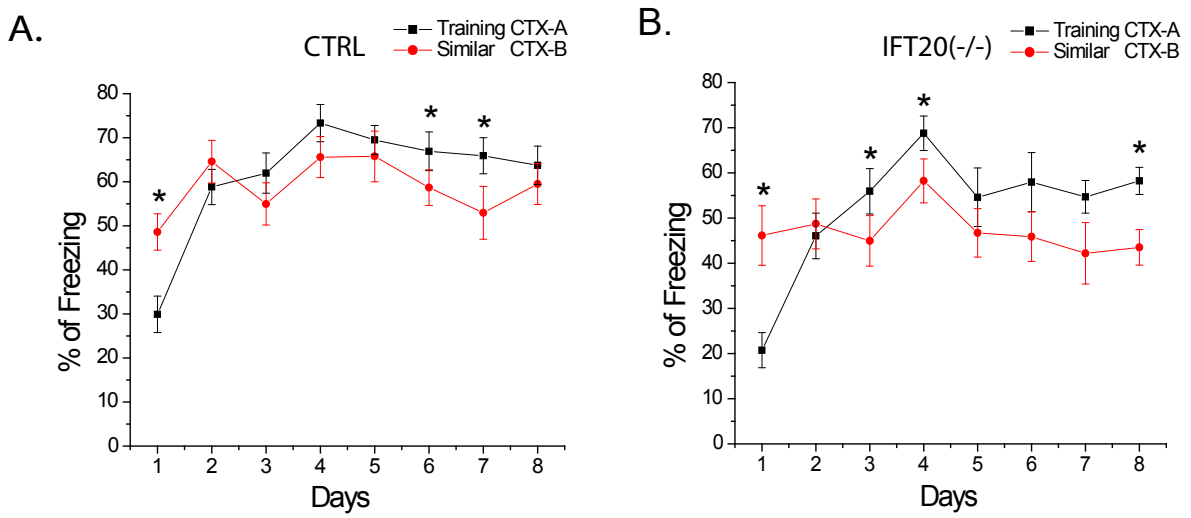

Figure 3.12. Ablation of primary cilia in mature dentate granule cells increases contextual fear discrimination

A. Freezing response of CTRL mice over the duration of training (p=0.009 and 0.015 at day 6 and 7, n=13).

B. Freezing response of IFT20 (-/-) $^{\text{mature DGCs}}$ mice over the duration of training (p=0.003, 0.008 and 0,003 at day 3,4 and 8, n=11).

*p<0.05, two-tailed unpaired t-test. Data are expressed as mean values ± SEM.

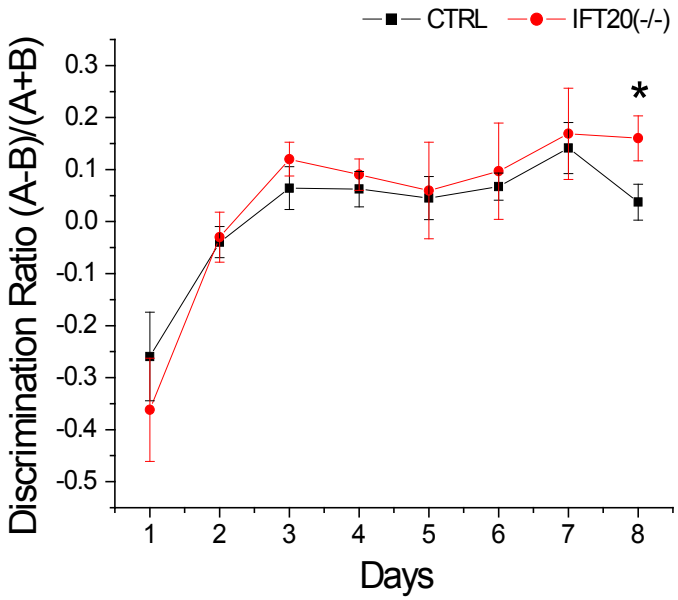

Figure 3.13. Ablation of primary cilia in mature dentate granule cells increases contextual fear discrimination

Analysis of discrimination ratios. IFT20 (-/-) $^{\text{mature DGCs}}$ mice start to show significantly better discrimination compare to CTRL mice on training day 8 (CTRL black line n=13 and IFT20 (-/-) $^{\text{mature DGCs}}$ red line n=11, p=0.03 on day 8).

*p<0.05, two-tailed unpaired t-test. Data are expressed as mean values ± SEM.

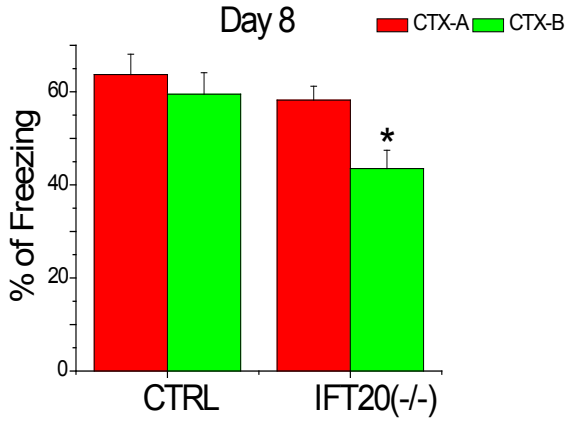

Figure 3.14. Ablation of primary cilia in mature dentate granule cells increases contextual fear discrimination

Average freezing response on training day 8. IFT20 (-/-) $^{\text{mature DGCs}}$ mice discriminates two similar contexts better that CTRL mice on day 8 (red and green bar of CTRL and IFT20 (-/-) $^{\text{mature DGCs}}$, p=0.32 and p=0.03).

*p<0.05, two-tailed unpaired t-test. Data are expressed as mean values ± SEM

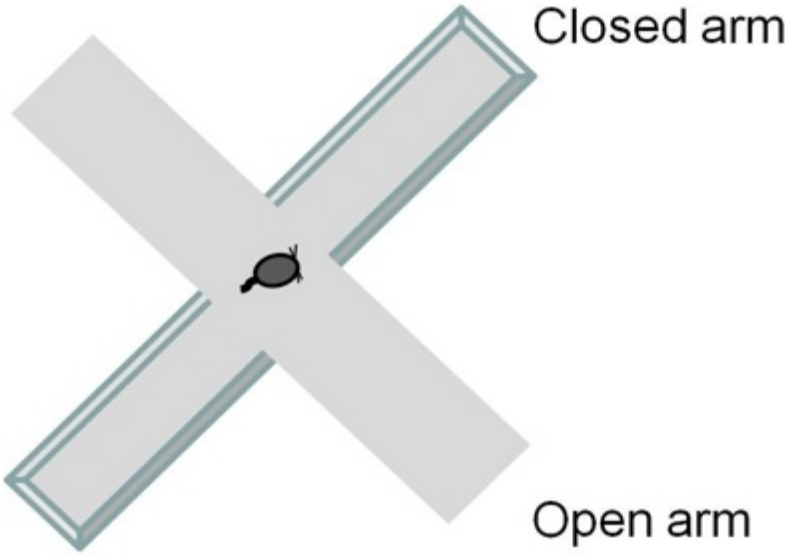

Figure 3.15. Apparatus for elevated plus maze
The apparatus used for elevated plus maze has two closed arms perpendicular to two open arms. Mice were placed in the center of the apparatus and allowed to explore freely for 5 minutes.

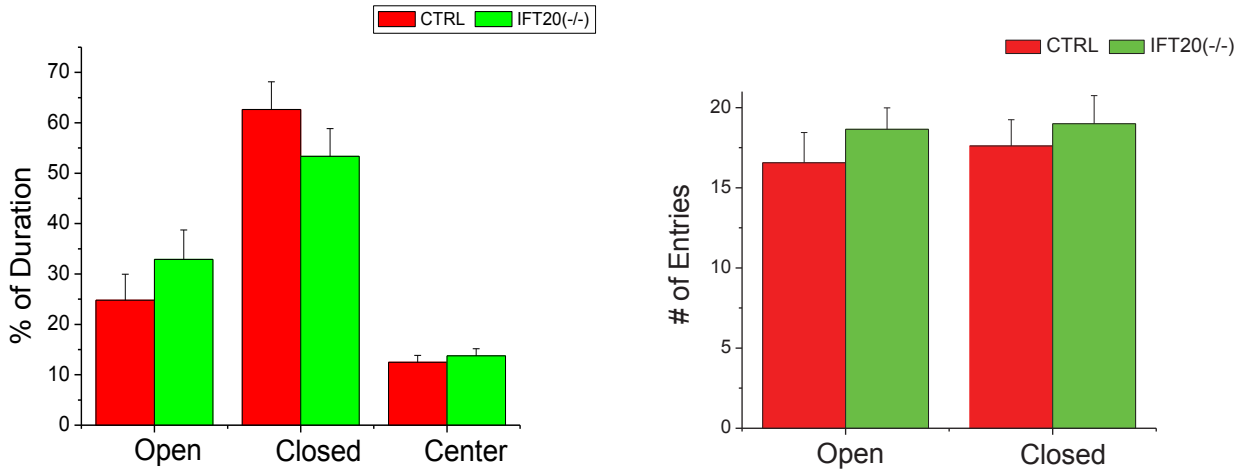

Figure 3.16. Ablation of primary cilia in mature dentate granule cells do not alter anxiety like behavior

Average time spent at center, open and closed arms during the experiment. No significant difference between CTRL and IFT20 (-/-) $^{\text{mature DGCs}}$ mice (CTRL red bar n=18, and IFT20 (-/-) $^{\text{mature DGCs}}$ green bar n=20, p=0.31 at the open arm). p>0.05, two-tailed unpaired t-test. Data are expressed as mean values ± SEM.

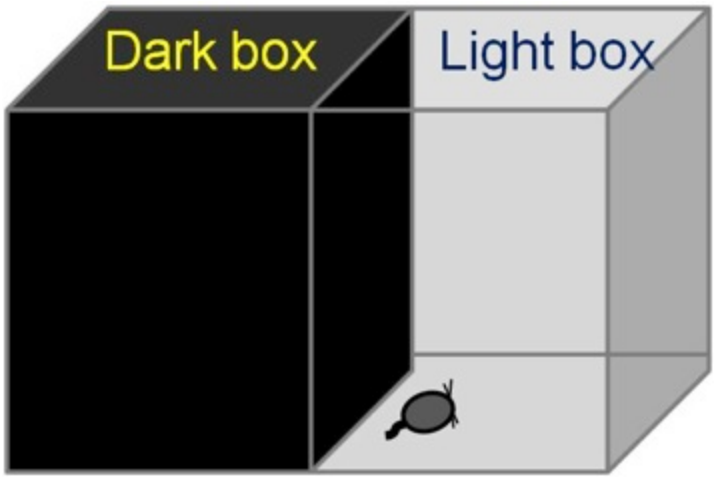

Figure 3.17. Apparatus for light and dark transition test
The apparatus has two compartments, a black compartment (dark) and a transparent compartment (light) under 400 lx light. Mice were placed in dark compartment and allowed to explore freely between two compartments during 10 minutes.

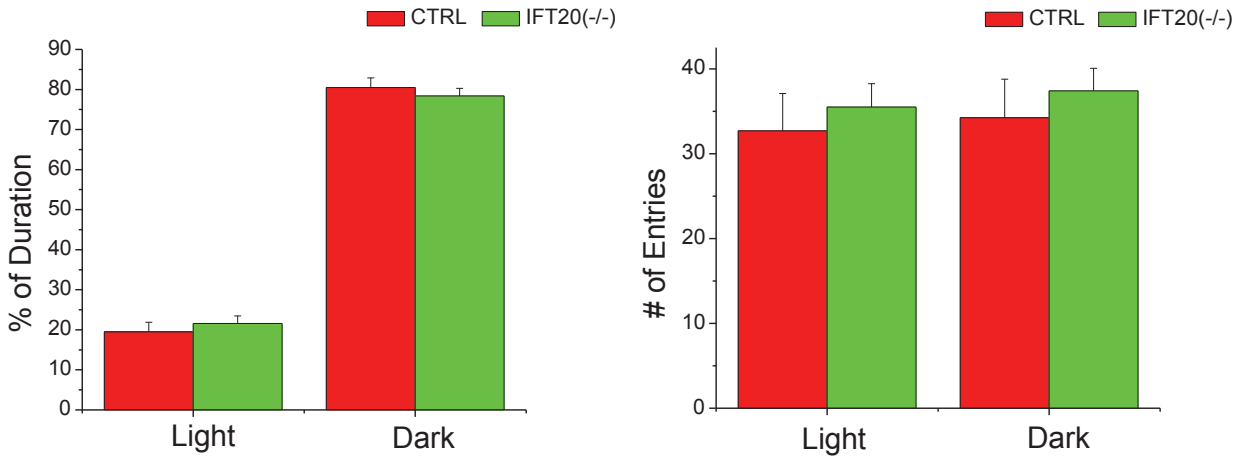

Figure 3.18. Ablation of primary cilia in mature dentate granule cells do not alter anxiety like behavior

Average time spent on light or dark compartment during 10 minutes. Both CTRL and IFT20 (-/-) $^{\text{mature DGCs}}$ mice spent mostly on dark box. No significant difference between two groups in both time (left, CTRL red bar n=16, and IFT20 (-/-) $^{\text{mature DGCs}}$ green bar n=20, p=0.50 at the dark compartment) and number of crossings (right, CTRL red bar and IFT20 (-/-) $^{\text{mature DGCs}}$ green bar p=0.55).

p>0.05, two-tailed unpaired t-test. Data are expressed as mean values ± SEM.

Chapter 4 Primary cilia and synaptic plasticity in DG-CA3 circuit

4.1 Introduction

Hippocampus receives sensory information from entorhinal cortex (EC) via axons of the perforant path. Perforant path axons connect to dendrites of DGCs and form excitatory synapse and DGCs transmit signals to CA3 pyramidal neurons through mossy fiber, axon projections of DGCs. In CA3 region, pyramidal neurons project to CA1 pyramidal neurons through Schaffer collateral pathway or to themselves via recurrent collaterals. CA1 pyramidal neurons send projections back to EC. This relay of synaptic transmission is called trisynaptic circuit (Rolls, 2007, Yassa and Stark, 2011) illustrated in Figure 4.1.

Excitatory synaptic transmission along the trisynaptic circuit is essential for two distinct hippocampus dependent learning and memory. As mentioned in chapter 3, pattern separation, discriminating similar representation, relies on mossy fiber inputs to CA3 (Leutgeb and Leutgeb, 2007, Rolls, 2013). When system receives similar input patterns it separates into distinct representation, where as unique inputs do not overlap with these memories. On the other hand, pattern completion, associated memory recall based on incomplete cues, is associated with monosynaptic pathway in recurrent collateral to CA3 (Nakashiba et al., 2008). In hippocampus, pattern separation and pattern completion balance each other, imbalance of these processes leads to diseases such as autism or schizophrenia (Hunsaker and Kesner, 2013).

Synaptic plasticity is known as a cellular mechanism of learning and memory. Change in neural activity leads to the change in neural excitability, which ends up with

long lasting synaptic plasticity. This change in synaptic efficacy modulates neurotransmitter release from the pre-synapse, post synaptic glutamatergic receptor modulation and activation of signal transduction for RNA or protein synthesis (Ho et al., 2011). The two most studied forms of synaptic plasticity are long-term potentiation (LTP) and long-term depression (LTD). LTP is a long lasting synaptic potentiation where as LTD is a stabilized decrease in synaptic efficacy. In memory processing, LTP is playing a critical role in memory encoding and storage process (Malenka and Bear, 2004, Malenka and Nicoll, 1999, Martin et al., 2000, Takeuchi et al., 2014).

What is the role of neurogenesis in synaptic plasticity? Leutgeb et al. showed that firing location of DGCs was correlated when animals exposed to similar pattern, however exposure to distinct pattern recruited new cell populations in CA3 (Leutgeb et al., 2007). During animal lifetime, old DGCs participate in encoding information and formatting the numerous memory engrams. As the amount of information encoded is large, engrams as well as synapse connections between EC and DG overlap with each other. On the other hand, adult born young DGCs likely integrate with existing neural circuits but less likely overlap with engrams from old DGCs.

Recently, a study showed that adult born DGCs switch their function from pattern separation to pattern completion as they development. They claimed old GCs regulate pattern completion whereas young GCs are responsible for pattern separation (Nakashiba et al., 2012). This somehow explains the reason why mice with depleted adult neurogenesis exhibit a deficit in pattern separation whereas mice have increased adult born neurons show enhanced pattern separation (Clelland et al., 2009, Sahay et al., 2011a).

In chapter 3, I observed mice without primary cilia in mature DGCs exhibit impaired contextual fear memory, spatial memory and pattern completion whereas enhanced contextual fear discrimination. Here, I will determine the physiological mechanism of these behavioral changes in IFT20 (-/-) $^{\text{mature DGCs}}$ mice. In addition I selectively depleted adult born neurons by using inducible DT receptor in Nestin-Cre $^{\text{ERT2}}$ transgenic mice and dissected the function of adult born neurons and mature DGCs in synaptic plasticity.

4.2 Results

4.2.1 Mossy fiber synaptic plasticity was enhanced after removal of primary cilia in mature DGCs

Synaptic plasticity is believed to be an important cellular mechanism of learning and memory. To find the mechanisms underlying the behavioral changes I observed in chapter 3, I examined LTP at CA3 region by stimulating mossy fibers, axon projections from DGCs (Figure 4.1). Synaptic transmission was not altered in IFT20 (-/-) $^{\text{mature DGCs}}$ mice compared to CTRL mice as both mice show similar I-O curve (Figure 4.2) at an increase in the amplitude from 10 to 35 mA. For the following experiments, baseline was recorded for 10 minutes with the amplitude of the half maximum response. LTP was induced by high frequency stimulation (HFS) that delivers 100 stimuli at 100 Hz frequency. Synaptic potentiation was determined by normalizing field EPSP slope from last 10 minutes of recording with average of the baseline to analyze stable synaptic plasticity after HFS stimulation.

Both CTRL and IFT20 (-/-) $^{\text{mature DGCs}}$ mice show increased postsynaptic potentials after HFS (Figure 4.3 A). However, IFT20 (-/-) $^{\text{mature DGCs}}$ mice show significantly increased LTP (163.69±18.59% of baseline) comparing to CTRL (117.75±8.25% of baseline) (Figure 4.3 B). Thus, although the baseline synaptic transmission was decreased in IFT20 (-/-) $^{\text{mature DGCs}}$ mice, they exhibited significantly enhanced synaptic plasticity after HFS at the mossy fiber (MF)-CA3 synapses.

4.2.2 Ablation of adult neurogenesis decreases DG-CA3 synaptic plasticity

Previously, Nakashiba et al. have showed that young and old DGCs have different contributions to pattern completion and pattern separation. They showed young GCs mediate pattern separation, whereas old GCs are involved in pattern completion (Nakashiba et al., 2012). To test whether the changes in learning behaviors and synaptic plasticity that occur after the primary cilia ablation from mature DGCs is the contribution of young GCs, I utilize Nestin-Cre $^{\text{ERT2}}$; iDTR mice (Arruda-Carvalho et al., 2011) to ablate adult neurogenesis transiently. Tamoxifen administration leads to diphtheria toxin receptor (DTR) expression in Nestin positive neural progenitor cells, which could be selectively ablated by DT administration, causing ablation in adult neurogenesis (Figure 4.4). Figure 4.5 is showing that DCX positive immature neurons are significantly removed in Nestin-Cre $^{\text{ERT2}}$; iDTR mice following tamoxifen and DT administration, whereas adult neurogenesis was not affected in Control; iDTR, which showed normal DCX positive cells in the SGZ of DG.

After ablation of adult neurogenesis, MF-CA3 post synaptic potentials of Nestin-Cre $^{\text{ERT2}}$; iDTR mice were 94.35±9.94% of the base line after HFS, while increased

to138±13.09% in Control; iDTR mice (Figure 4.7 A-B). Average potentiation during 50-60 minutes was significantly decreased in Nestin-Cre ^{ERT2}; iDTR mice (Figure 4.7 B, 134.12±8.82% for Control; iDTR and 94.51±9.51% for Nestin-Cre ^{ERT2}; iDTR, two tailed unpaired t-test: p=0.024), which suggests that young GCs in the DG contributed largely to MF-CA3 synaptic plasticity.

4.2.3 Ablation of adult neurogenesis diminishes the enhanced DG-CA3 LTP by primary cilia depletion of mature DGCs

Next, I ablated primary cilia in Nestin-Cre ^{ERT2}; iDTR mice to see whether synaptic plasticity is altered as in IFT20 (-/-) $^{mature\ DGCs}$ mice. To ablate primary cilia in mature DGCs, I co-injected AAV-CAMKII-Cre and AAV-DIO-*dnKif3A-dTomato* into Nestin-Cre ^{ERT2}; iDTR mice after tamoxifen and DT administration, while I injected AAV-CAMKII-eGFP into Control;iDTR mice (Figure 4.8). Through ACIII immunofluorescence staining, the expression of dnKif3A in mature GCs significantly ablates primary cilia in Nestin-Cre ^{ERT2}; iDTR mice, whereas primary cilia are expressed in Control; iDTR – eGFP mice (Figure 4.9).

Unlike IFT20 (-/-) $^{mature\ DGCs}$ (Figure 4.7 A-B), Nestin-Cre ^{ERT2}; iDTR- dnKif3A mice did not show synaptic plasticity after HFS (Figure4.11 A, 101.41±8.32%, two tailed paired t-test: p=0.31), while Control;iDTR-eGFP mice showed LTP after HFS (Figure 4.11 A, 135.04±13.89%, two tailed paired t-test: p=9.12×E-07).

The average potentiation level during 50 to 60 minutes after HFS shows that LTP was achieved in Control; iDTR-eGFP mice but not in Nestin-Cre ^{ERT2}; iDTR mice (Figure 4.11 B, 135.04±13.17% for Control; iDTR-eGFP and 101.41±7.38% for Nestin-Cre^{ERT2};

iDTR-dnKif3A, two tailed unpaired t-test: p=0.050). Expression of eGFP in Control; iDTR mice did not affect synaptic plasticity by comparing with Control; iDTR mice (134.12±8.82% for Control; iDTR and 135.04±13.17% for Control; iDTR-eGFP, two tailed unpaired t-test: p=0.69). Moreover, dnKif3A expression did not change synaptic plasticity when compared with Nestin-Cre ^{ERT2}; iDTR mice (94.51±9.51% for Nestin-Cre ^{ERT2}; iDTR and 101.41±7.38% for Nestin-Cre ^{ERT2}; iDTR-dnKif3A. two tailed unpaired t-test: p=0.57). These findings suggest increased MF-CA3 synaptic plasticity by removing primary cilia from mature DGCs is largely dependent on adult born young neurons.

4.3 Discussion

In this chapter, I determined the physiological mechanism of behavior changes obtained from IFT20 (-/-) $^{\text{mature DGCs}}$ mice as shown in chapter 3. Synaptic output from DG to CA3 was measured after HFS on mossy fibers since memory encoding and storage occurs through EC-DG-CA3 trisynaptic synaptic transmission (Rolls, 2007, Yassa and Stark, 2011). I observed that LTP was enhanced in brain slices with primary cilia ablated in mature DGCs (Figure 4.3). Interestingly, synaptic potentiation was only observed with the presence of immature neurons in brain regardless of the expression of primary cilia in mature DGCs (Figure 4.11).

Previously, Nakashiba and his colleagues suggested young GCs are involved in pattern separation and switch their function to pattern completion as they age (Nakashiba et al., 2012). They specifically inhibited output of old DGCs by tetanus toxin (DG-TeTX), which inhibits mossy fiber transmission without affecting perforant pathway

or recurrent collateral input in CA3. DG-TeTX mice exhibited enhanced contextual fear discrimination but impaired pattern completion, which correspond to my results observed from IFT20 (-/-) $^{\text{mature DGCs}}$ mice shown in chapter 3. This suggests a possibility that mossy fiber synaptic transmission is inhibited by primary cilia ablation in mature DGCs in IFT20 (-/-) $^{\text{mature DGCs}}$ mice.

Interestingly, LTP in CA3 pyramidal cells was enhanced in IFT20 (-/-) $^{\text{mature DGCs}}$ mice. Increased mossy fiber synaptic output in IFT20 (-/-) $^{\text{mature DGCs}}$ mice implies two possibilities. One possible reason is increase synaptic input from EC. In trisynaptic circuit in hippocampus, DG receives synaptic inputs from projections of perforant pathway (Witter, 2007). Previously, our lab showed dnKif3A expression in adult born DGCs results defects in excitatory glutamatergic synapse formation between projections from EC. Even mature DGCs expressing dnKif3A have normal dendritic synaptic activity (Kumamoto et al., 2012). Based on these previous findings, we expect synaptic input from EC is not altered in IFT20 (-/-) $^{\text{mature DGCs}}$ mice, which may not be the reason for the increase in synaptic plasticity.

The other possible reason is increased synaptic output from DG to CA3 in the hippocampus. Although majority of projections in neural circuit are from mature DGCs, still adult born young DGCs integrate and form synapses within existing circuits. These young DGCs exhibit unique properties during initial development stage. Young neurons are more efficient transducing synaptic activity since young neurons have higher excitability and synaptic plasticity, as well as enhanced susceptibility compare to developmentally born and mature neurons. This physiological properties last up to 6 weeks of neuronal age and become less active (Ge et al., 2007, Mongiat et al., 2009,

Schmidt-Hieber et al., 2004). In this study, IFT20 (-/-) $^{\text{mature DGCs}}$ mice exhibit increased LTP in CA3. Furthermore, increased LTP was diminished when DT conditionally depleted Nestin positive cells regardless of the expression of primary cilia in mature DGCs, which implies increased LTP is referring to immature DGCs rather than mature DGCs. As I-O relationship of MF input to CA3 from CTRL and IFT20 (-/-) $^{\text{mature DGCs}}$ mice do not differ, I can speculate that absence of primary cilia in mature DGCs do not alter functional release of DG to CA3 synapse. This suggests that ablation of primary cilia in mature DGCs inhibits neuronal activity through inefficient excitability in mature DGCs, consequently increase activity proportion of immature DGCs on synaptic output from DG.

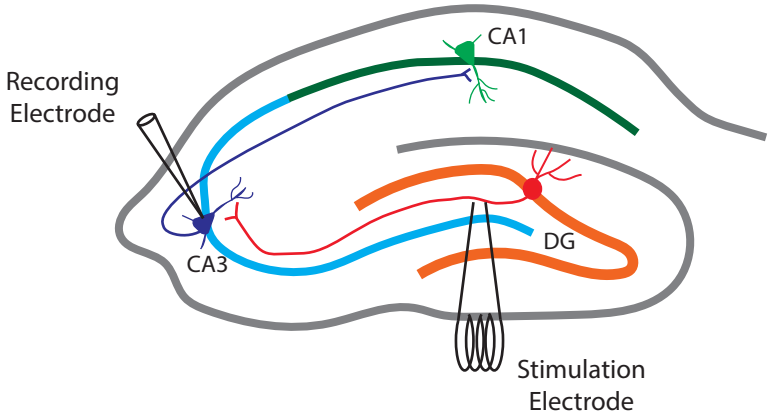

Figure 4.1. Tri-synaptic circuit
Schematic representation of tri-synaptic circuit and position of the stimulating and recording electrodes. High frequency stimulation protocol was used to stimulate mossy fiber. Recording electrode was placed at CA3 region.

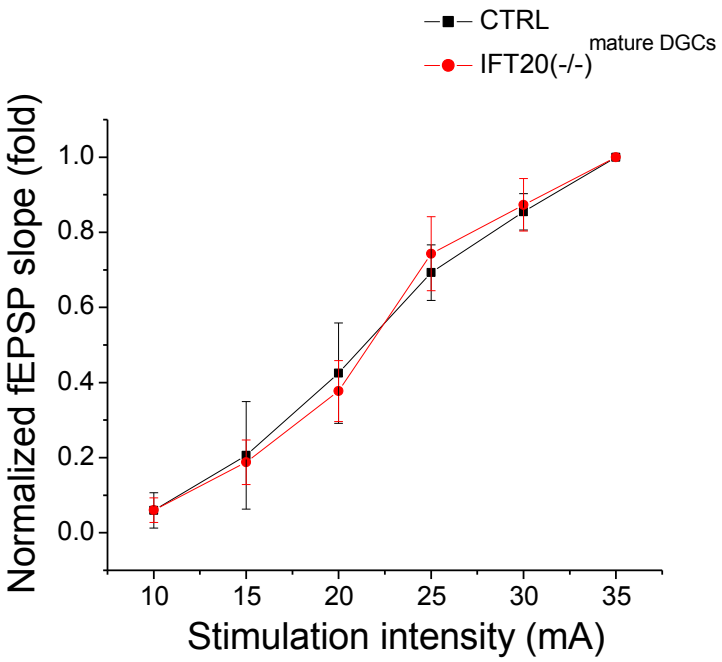

Figure 4.2. I-O curve
Input and output curve obtained from CTRL (n=5) and IFT20 (-/-) $^{\text{mature DGCs}}$ (n=6) mice. Synaptic transmission was not altered in IFT20 (-/-) $^{\text{mature DGCs}}$ compare to CTRL from 10 to 35 mA of stimulation intensity.
$p>0.05$, two-tailed unpaired t-test, Data are expressed as mean values ± SEM.

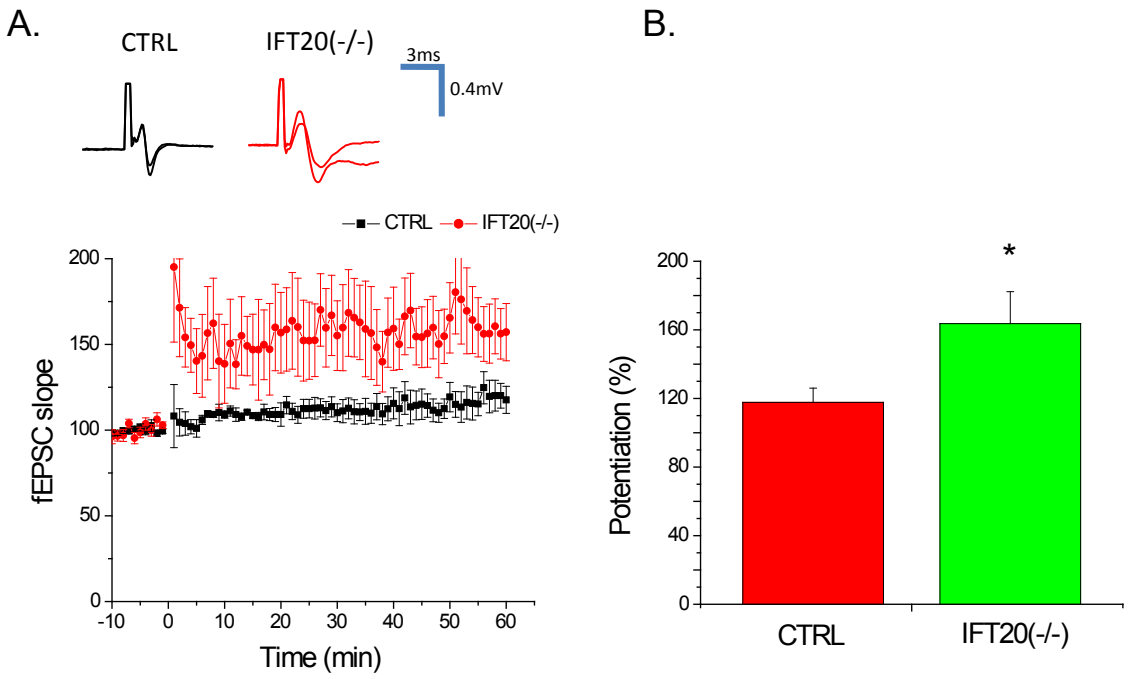

Figure 4.3. Removal of primary cilia from mature GCs increases DG-CA3 synaptic plasticity

A. (Upper) Representative traces of both CTRL and IFT20 (-/-) $^{\text{mature DGCs}}$ mice recorded before and after high frequency stimulation.
(Lower) IFT20 (-/-) $^{\text{mature DGCs}}$ mice (red round, n=8) show increased DG – CA3 LTP compare to CTRL mice (black square, n=7).
B. Average potentiation during 50-60 minute, showing significantly enhanced LTP in IFT20 (-/-) $^{\text{mature DGCs}}$ mice comparing to CTRL mice (p=0.048).
*p<0.05, two-tailed unpaired t-test. Data are expressed as mean values ± SEM.

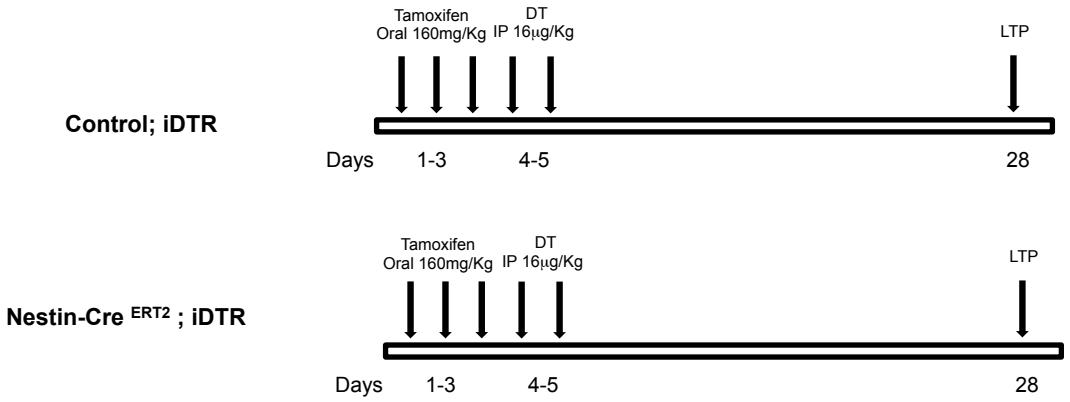

Figure 4.4. Experimental design for Ablation of adult neurogenesis in Nestin-Cre ^{ERT2}; iDTR mice

Schematic procedure illustrating adult neurogenesis ablation Nestin-Cre ^{ERT2}; iDTR mice. Tamoxifen followed by diphtheria toxin administration ablates Nestin positive cells in Nestin-Cre ^{ERT2};iDTR mice.

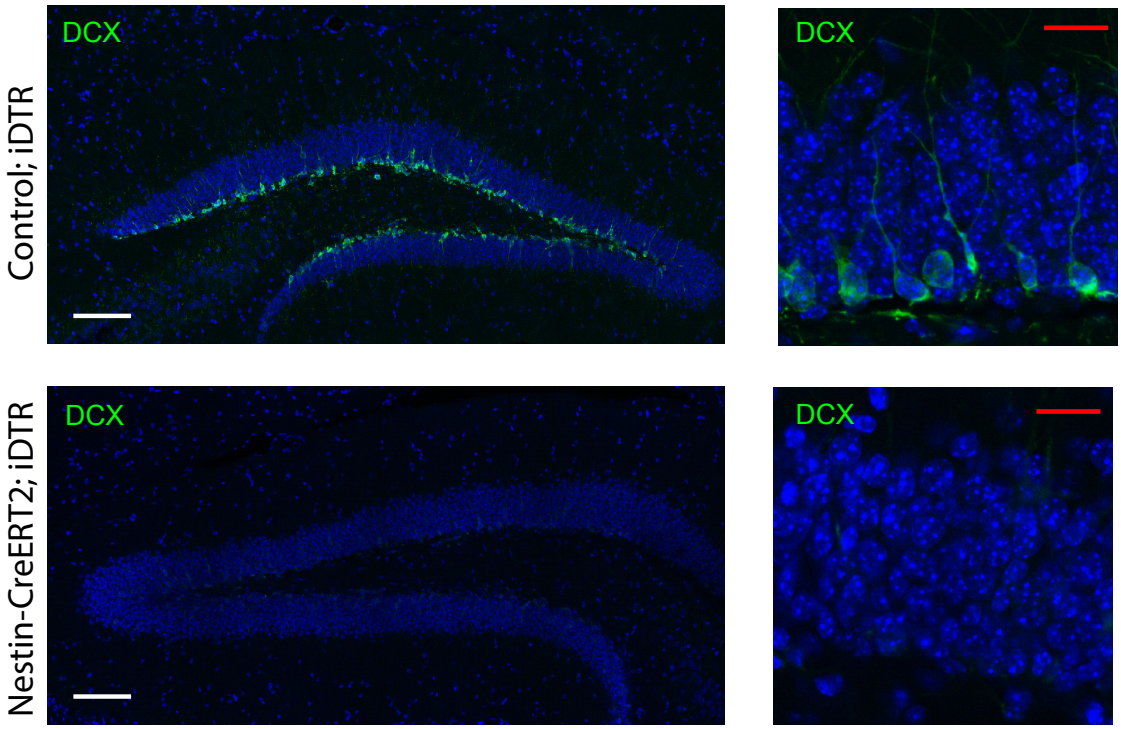

Figure 4.5. Ablation of adult neurogenesis in Nestin-Cre ^{ERT2}; iDTR mice
Diphtheria toxin induced ablation of adult neurogenesis. Immunofluorescence showing DCX + cells (Green) were reduced in DG of Nestin-Cre ^{ERT2}; iDTR mice compare to Control; iDTR mice.
Scale bars : 100μm(white) and 20μm(red).

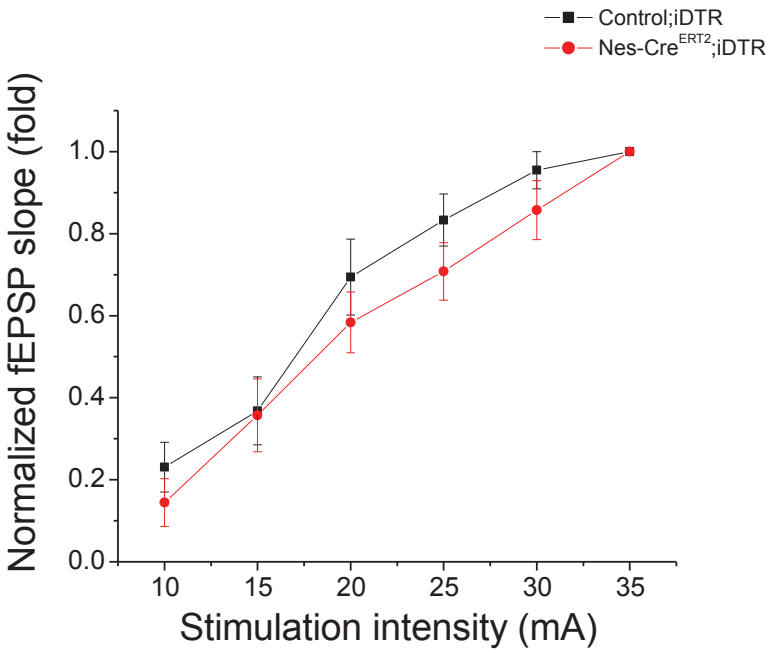

Figure 4.6. I-O curve – Nestin-Cre ^{ERT2}; iDTR
Input and output curve obtained from Control;iDTR (n=5) and Nestin-Cre ^{ERT2};iDTR (n=5) mice. Synaptic transmission was not altered in Nestin-Cre ^{ERT2};iDTR compare to Control;iDTR from 10 to 35 mA of stimulation intensity.
$p>0.05$, two-tailed unpaired t-test, Data are expressed as mean values ± SEM.

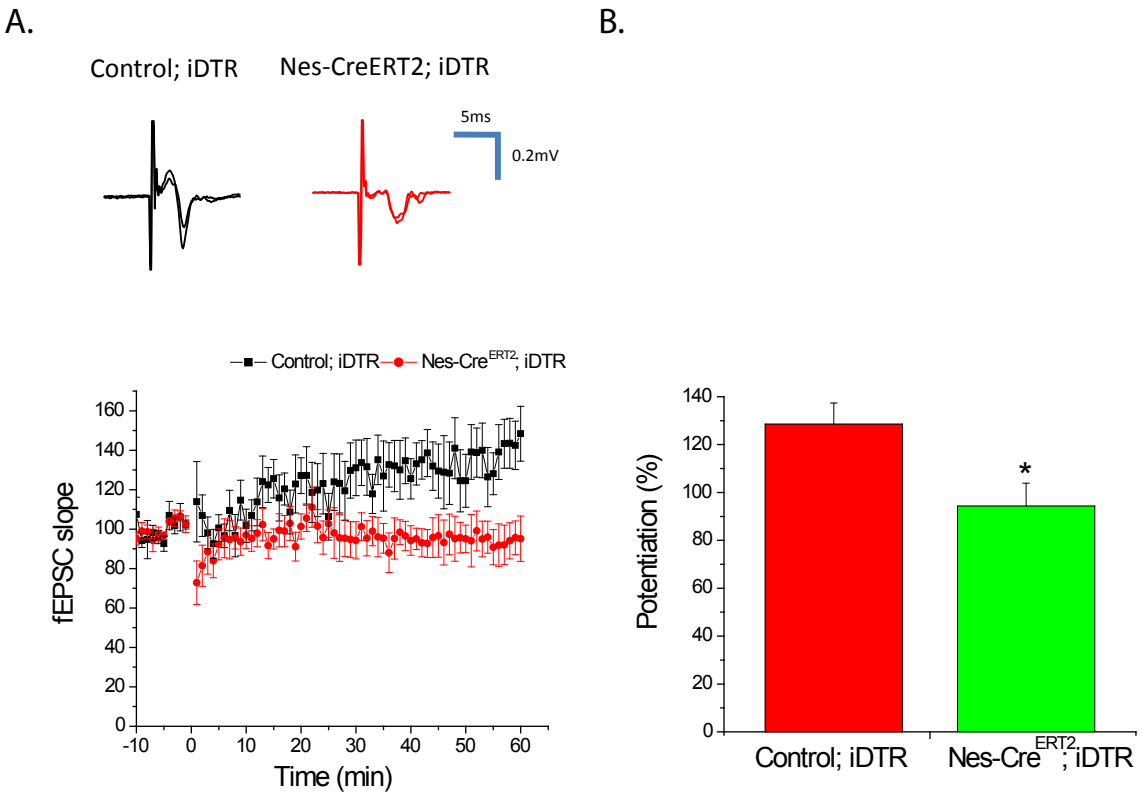

Figure 4.7. Ablation0.024 of adult neurogenesis diminishes the increased DG-CA3 synaptic plasticity caused by removal of primary cilia from mature DGCs

A. (Upper) Representative traces of both Control; iDTR and Nestin-Cre ^{ERT2}; iDTR mice recorded before and after high frequency stimulation.

(Lower) Nestin-Cre ^{ERT2}; iDTR mice (red round, n=6) show decreased DG -CA3 synaptic plasticity compare to Control; iDTR mice (black square, n=6).

B. Average potentiation of 50-60 minute, showing significantly decreased LTP in Nestin-Cre ^{ERT2}; iDTR mice com- paring to Control; iDTR mice (p= 0.024).

*p<0.05, two-tailed unpaired t-test. Data are expressed as mean values ± SEM.

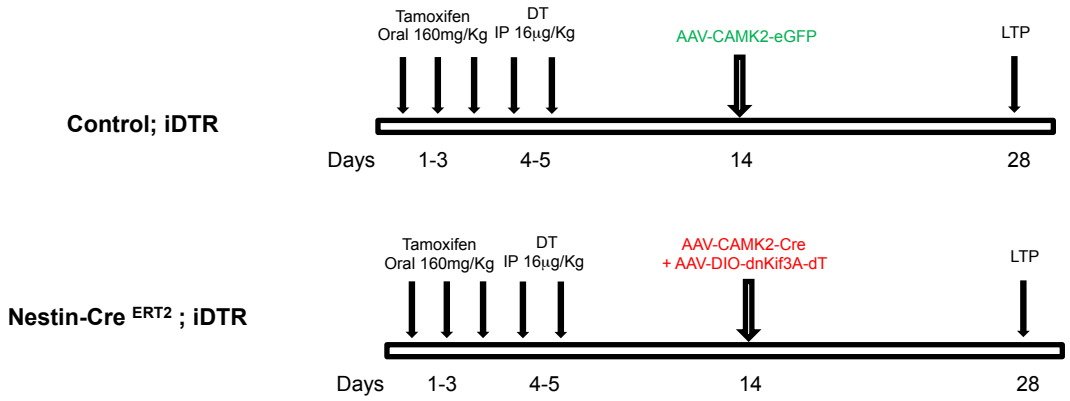

Figure 4.8. Ablation of adult neurogenesis and primary cilia in Nestin-Cre ^{ERT2}; iDTR mice

Schematic procedure of ablation of adult neurogenesis and primary cilia in Nestin-Cre ^{ERT2}; iDTR mice. AAV-CAMK2-eGFP were injected into Control; iDTR mice, since Nestin-Cre ^{ERT2}; iDTR mice were co-injected with AAV-CAMK2-Cre and AAV-DIO-*dnKif3A-dTomato* to ablate primary cilia in mature DGCs.

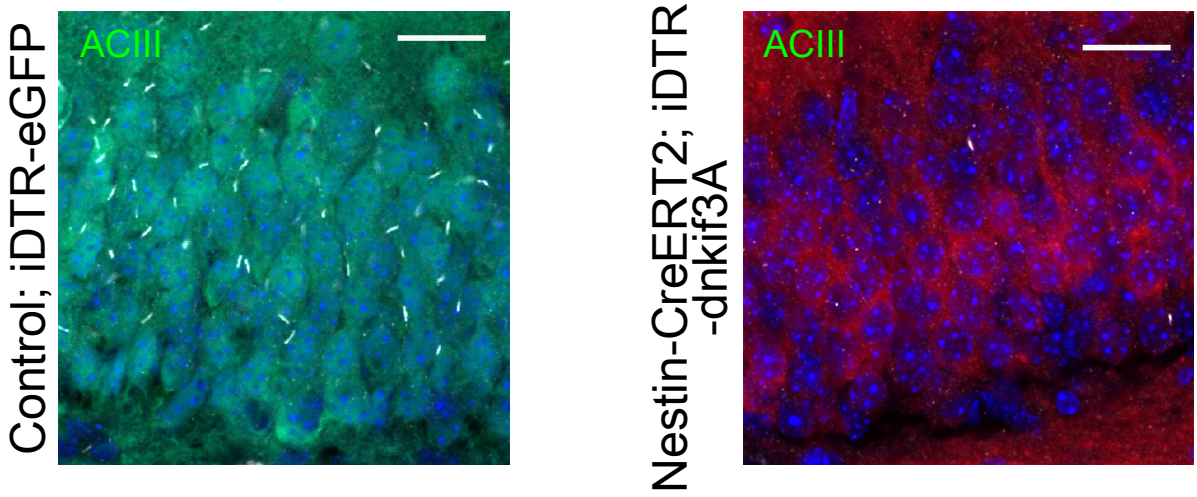

Figure 4.9. Ablation of adult neurogenesis and primary cilia in Nestin-Cre ^{ERT2}; iDTR mice

Ablation of adult neurogenesis and primary cilia under dnKif3A expression in Nestin-Cre ^{ERT2}; iDTR mice. Immunofluorescence images showing AAV-CAMKII-eGFP transduced Control; iDTR mice expresses primary cilia (ACIII, white) in DGCs, whereas co-injection of AAV-CAMKII-Cre and AAV-DIO-*dnKif3A-dTomato* into Nestin-Cre ^{ERT2}; iDTR mice do not express primary cilia in DGCs.

Scale bar : 20μm.

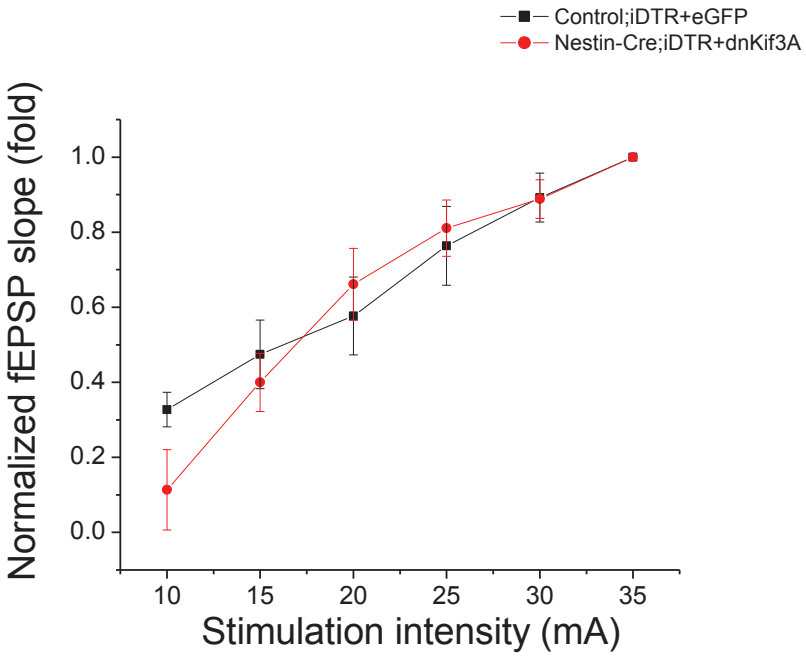

Figure 4.10. I-O curve – Nestin-Cre ^{ERT2};iDTR-dnKif3A
Input and output curve obtained from Control;iDTR-eGFP (n=5) and Nestin-Cre ^{ERT2};iDTR-dnKif3A (n=5) mice. Synaptic transmission was not altered in Nestin-Cre ^{ERT2};iDTR-dnKif3A compare to Control;iDTR-eGFP from 10 to 35 mA of stimulation intensity.
$p>0.05$, two-tailed unpaired t-test, Data are expressed as mean values ± SEM.

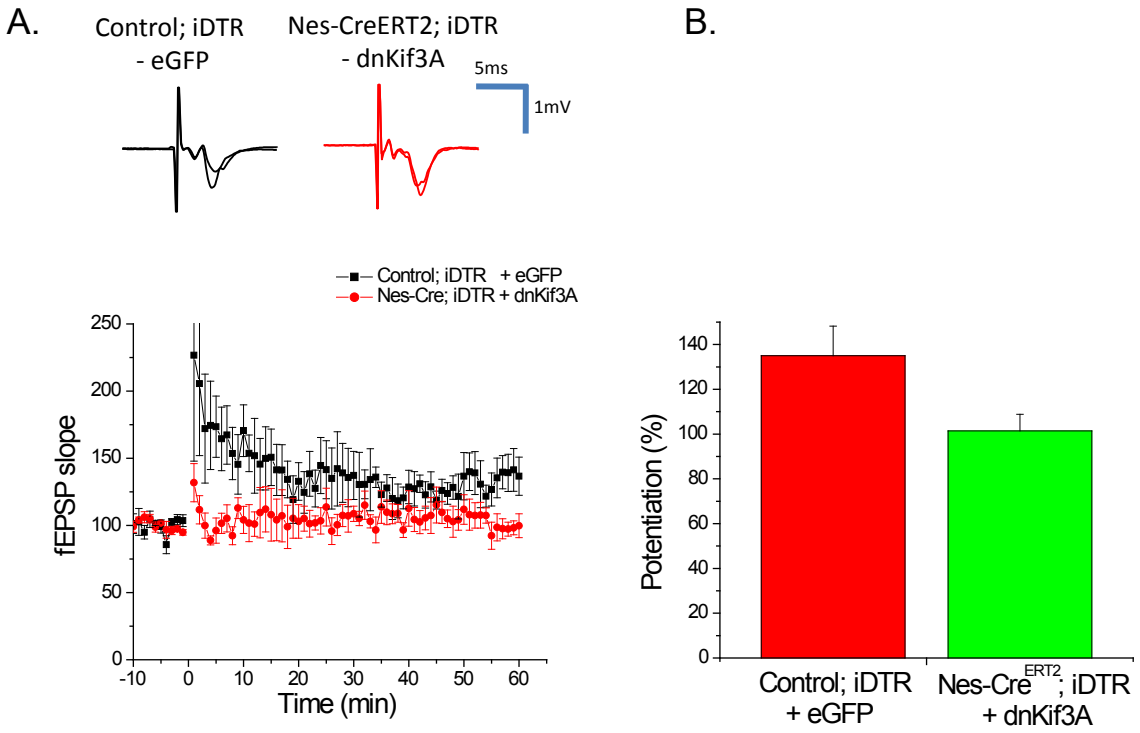

Figure 4.11. Ablation of adult neurogenesis diminishes the increased DG-CA3 synaptic plasticity caused by removal of primary cilia from mature DGCs
A. (Upper) Representative traces of both Control; iDTR – eGFP and Nestin-Cre ^{ERT2}; iDTR – dnKif3A mice recorded before and after high frequency stimulation.
(Lower) LTP was diminished in Nestin-Cre ^{ERT2}; iDTR – dnKif3A mice (red round, n=5) but not in Control; iDTR – eGFP mice (black square, n=5).
B. Average potentiation during 50-60 minutes, showing LTP was diminished in Nestin-Cre ^{ERT2}; iDTR- dnKif3A mice ($p=9.12 \times E-07$).
$p=0.05$, Data are expressed as mean values ± SEM.

Chapter 5 Primary cilia and neuronal migration in dentate gyrus

5.1 Introduction

Newly generated neurons undergo neuronal migration from their birth site. As adult neurogenesis only occurs at SGZ in DG and SVZ, neuronal migration is restricted to radial migration within the DG or rostral migratory stream from the SVZ to the olfactory bulb in adult brains (Ghashghaei et al., 2007).

The structure of DG is composed with SGZ, a narrow layer between GCL and hilus, GCL and ML. SGZ is the place where GFAP and Nestin positive radial glial cells generate new neurons throughout the lifetime (Kuhn et al., 1996, van Praag et al., 2002). After birth, adult born immature cells associating with proliferating progenitor cells, form clusters of cells in SGZ (Seki, 2002). Around 4days of neuronal age, most of immature neurons locate outside of clusters and migrate tangentially through the SGZ. In this stage, immature neurons also retract tangential processes and extend radial processes, which becomes apical dendrite (Seki et al., 2007). Next, immature neurons start radial migration towards ML around day14 and terminate and finalize their position around day 21 (Kumamoto et al., 2012).

Nucleokinesis is the mechanism how neurons migrate. There are two steps in nucleokinesis. First, centrosome and Golgi apparatus in the leading process move forward to the migration direction. Perinuclear microtubule cage pulls the nucleus forward which results in cytoplasmic swelling. Second step is the translocation of the nucleus. Forward pulling from perinuclear microtubule cage and pushing from myosin II

at the nucleus rear move the nucleus. These two steps are repeated during neuronal migration (Tsai and Gleeson, 2005).

The centrosome is composed with mother and daughter centrioles, and pericentriolar material. Near the plasma membrane, the mother centriole converts into basal body, where nucleates the primary cilium (Kobayashi and Dynlacht, 2011). In fact, primary cilia guide cells to the direction of migration, as they are oriented along the migration direction in fibroblasts (Albrecht-Buehler, 1977, Schneider et al., 2009).

Do neuronal primary cilia regulate neuronal migration in brain? In developing cerebral cortex primary cilia regulate the migration of interneurons from the ganglionic eminence to the dorsal cortex and the placement of interneurons (Higginbotham et al., 2012). Furthermore, primary cilia are required for the reorientation of GABAergic interneurons (Baudoin et al., 2012). They showed primary cilia help interneurons from medial ganglionic eminence to exit tangential migration and to enter cortical plate.

These previous studies gave me an idea that primary cilia in adult born DGCs play a role in the re-orientation from tangential dispersion to radial migration and termination of migration in the DG. Furthermore, as dendrite elongation and arborization occurs along with the early neuronal migration (Gu et al., 2013), dendrite development also can be regulated by primary cilia. Here in chapter 5, I will address the role of primary cilia in regulating neuronal migration and dendrite development in adult born DGCs.

5.2 Results

5.2.1 Adult born neurons without primary cilia expression localize near ML

After birth, adult born neurons start radial migration into GCL towards ML. Most adult born neurons locate their final position within the inner 1/3 of GCL at around day 21 and integrate into preexisting circuits (Kumamoto et al., 2012, van Praag et al., 2002). To determine whether the presence of primary cilia modulates the final position of adult born neurons, I ablated primary cilia at day 21 and 28, and analyzed the final position of adult born neurons in GCL, as shown in Figure 5.1. Briefly, I injected retrovirus carrying inducible Cre into DG of *IFT20* fl/fl mice, so that primary cilia were ablated by tamoxifen administration from day 21 in retrovirus labeled newborn neurons. Neuronal distribution of adult born neurons was analyzed at day 21, 35 and 42 (Figure 5.2).

Distribution of newborn neurons did not differ in CTRL neurons expressing EGFP between 21, 35 and 42 dpi. On the other hand, with expression of Cre ^{ERT2}, primary cilia ablation following tamoxifen administration from day 21, IFT20 (-/-) neurons showed distribution of location closer to ML compared to CTRLs at 35 and 42 dpi (Figure 5.3, KS test p=0.048 for 35dpi (red and green) and p=0.098 for 42dpi (blue and sky blue)). These data suggest that adult-born DGCs terminate their migration into the GCL before 21 days after birth, as adult born new neurons without primary cilia showed delayed termination of migration between day 21 and 35.

To confirm this phenotype is not due to non-ciliary function of IFT20, I ablated primary cilia with dnKif3A expression and analyzed the relative position of adult born

neurons in GCL (Figure 5.4). dnKif3A expressing neurons were also found closer to ML compared to CTRL neurons at 35 and 42dpi (Figure 5.5 green and blue curves), which confirms that presence of primary cilia in adult born neuron is required for the termination of radial migration into the GCL.

Next, to determine the critical time point for the regulation of final positioning of adult-born neurons by primary cilia, I ablated primary cilia at day 28 and analyzed relative position of newborn DGCs in GCL at 42dpi (Figure 5.6). The distribution curve of IFT20 (-/-) neurons shifted to the right compared to that of the CTRLs at 42dpi (Figure 5.7, KS-test: p=0.004), suggesting closer location of newborn neurons to the ML when primary cilia were ablated at 28 dpi. In addition, when I removed primary cilia starting from day 21, neuronal distribution of IFT20 (-/-) neurons showed similar distribution compare to distribution curve of neurons without IFT20 expression from day 28 (Figure 5.7, comparing red and blue curves, KS-test: p=0.004) which suggests that in adult born neurons, primary cilia are essential at day 28 for termination of radial migration and final positioning in GCL.

5.2.2 Ablation of primary cilia alters dendritic refinement in adult born neurons

Previous study has shown that blockage of primary cilia assembly at 14dpi leads to defects in dendritic refinement; shorter dendrites but similar dendritic branch numbers and crossings (Kumamoto et al., 2012). Here I examined whether ablation of primary cilia in later neuronal development alters dendritic refinement in adult born neurons. I analyzed dendritic arborization of IFT20 (-/-) neurons at 42dpi, in which primary cilia

were ablated from day 28. Total dendritic length, dendritic branch numbers, and number of dendritic crossings were measured in both CTRL and IFT20 (-/-) neurons.

At 42dpi, total dendritic length was not significantly different between CTRL and IFT20 (-/-) neurons (Figure 5.8 A, 612.47±37.51mm for CTRL and 707.59±48.24 mm for IFT20 (-/-), unpaired t-test: p=0.123). However, IFT20 (-/-) neurons have significantly higher number of dendritic branches compare to CTRL neurons (Figure 5.8 B, 5.07±0.32 for CTRL and 6.58±0.36 for IFT20 (-/-), unpaired t-test: p=0.003). In addition, sholl analysis of dendritic tree shows that IFT20 (-/-) neurons have higher numbers of shorter dendrite branches than CTRL neurons. Dendritic branches of IFT20 (-/-) neurons were mostly extending to 60 ~ 120 mm away from soma whereas CTRL neurons have more longer dendrites extending to 200 ~ 230 mm away from soma (Figure 5.8 C). Together, these results suggest that adult born neurons express defects in dendritic refinement by showing increased number of short dendritic branches, when the primary cilia are ablated even after neuronal maturation.

5.2.3 Direction of early neuronal migration of adult born neurons in GCL is regulated by primary cilia

During early neuronal development, radial stem cells generate new neurons at the SGZ of the DG. Before adult born immature neurons enter GCL and start radial migration, it is unknown whether these neuroblasts undergo tangential migration from their birth site (Gu et al., 2013). Next, I set out to determine whether primary cilia are regulating early migration of adult born neurons in the DG.

To examine the migrating direction of adult born neurons I analyzed the orientation of primary dendrites and categorized the newborn DGCs into three groups; tangential dispersion: 0-30°, intermediate stage: 30-60°, and radial migration: 60-90° (Figure 5.9). I ablated primary cilia from newborn DGCs in *IFT20* fl/fl mice by inducing tamoxifen at 5 days after injecting retrovirus carrying inducible Cre recombinase. Dendritic orientation was analyzed at 7 and 14 dpi (Figure 5.10). At 7dpi, significantly more IFT20 (-/-) neurons showed dendritic orientation between 0 and 30° compared to CTRL (Figure 5.11 left two bars, chi square test: p=4.21E-06). Although majority of newborn neurons were in radial position, significantly more IFT20 (-/-) neurons showed dendritic orientation of 0-30° compared to CTRL at 14dpi (Figure 5.11 right two bars, chi square test: p=0.004).

To confirm this phenotype is due to ciliary function of IFT20, I ablated primary cilia in adult born neurons by injecting retrovirus carrying inducible dnKif3A. Administration of doxycycline blocks assembly of primary cilia starting from 5dpi. Dendritic orientation was analyzed at 7 and 14dpi (Figure 5.12). At 7dpi, significantly more dnKif3A expressing neurons showed dendritic orientation between 0 and 30° compared to CTRL neurons (Figure 5.13 left two bars, chi square test: p=0.015). Furthermore, more dnKif3A expressing neurons still showed dendritic orientation of 0-30° at 14dpi (Figure 5.13 right two bars, chi square test: p=0.002). Together, these results suggest that primary cilia ablation prolongs the tangential dispersion of adult-born DGCs during early neuronal development.

5.2.4 Ablation of primary cilia does not alter early migration of adult born neurons.

Previous results show that radial migration of adult born neurons towards ML was altered by ablation of primary cilia after 21days (Figure 5.3, 5.5, and 5.7). Since ablation of primary cilia prolongs the horizontal phase of adult-born DGCs, next asked whether primary cilia ablation alters early tangential migration of these new neurons. To test this hypothesis, I marked and traced clonal families of adult-born DGCs using viral labeling approach. Briefly, I co-injected lentivirus expressing Cre recombinase under GFAP promoter and retrovirus with double-floxed reversed GFP. GFP expressing neurons within a cluster are considered as lineages from one neural stem cell (Figure 5.14B). Early migration distance was analyzed by measuring neuronal distances within individual clone at 7 and 14dpi. Average of neuronal distance was considered as tangential migration distance from mother stem cell (Figure 5.15 A).

At 7dpi, distance between neurons did not show big difference between CTRL and IFT20 (-/-) neurons (Figure 5.16 A, 56.66±10.71 mm for CTRL and 41.76±5.84 mm for IFT20 (-/-) neurons, two tailed unpaired t-test: $p=0.24$). Distance between neurons was similar between CTRL and IFT20 (-/-) neurons at 14dpi (Figure16 B, 59.67±6.16 mm for CTRL and 56.68±4.22 mm for IFT20 (-/-) neurons, two tailed unpaired t-test: $p=0.69$). These data showed that averaged neuronal distance within a clonal family was similar between 7 and 14dpi, suggesting that adult born neurons finish tangential dispersion by 7 dpi, which corresponds to previous results that adult born neurons re-orient migration direction from tangential migration to radial migration at around day 7 (Figure 5.11 and 5.13). Taken together, these data indicate ablation of primary cilia assembly does not alter early tangential migration of adult born neurons.

5.2.5 Defects in primary cilia assembly alters early dendritic development of adult born neurons

To determine whether primary cilia are also regulating early dendritic development, I injected retrovirus with inducible Cre recombinase into IFT fl/fl mice and induced with tamoxifen from 5dpi. Dendritic arborization was traced at 7dpi by analyzing total dendritic length, dendritic branch number, and the number of crossings from the soma. IFT20 (-/-) neurons showed shorter dendrites (Figure 5.16 A, 148.42±14.82 mm for CTRL and 114.70±8.84 mm for IFT20 (-/-) neurons, two tailed unpaired t-test: p=0.054) and less branches compared to CTRL neurons at 7dpi (Figure 5.16 B, 2.76±1.80 for CTRL and 1.93±1.71 for IFT20 (-/-) neurons, two tailed unpaired t-test: p=0.027). Number of dendritic crossings also supports that IFT20 (-/-) neurons had less dendritic branches compared to CTRL neurons at 7dpi (Figure 5.16 C). Together, these results suggest that during early neuronal development primary cilia depleted adult born neurons express short and simple dendrites at 7dpi.

5.3 Discussion

Primary cilia associate with the centrosome, guides direction of migration in fibroblast and interneurons (Albrecht-Buehler, 1977, Baudoin et al., 2012, Higginbotham et al., 2013). Here I addressed the requirement of primary cilia in termination of radial migration and final positioning of adult born DGCs in hippocampus. Further, the results I obtained from inhibition of primary cilia assembly in neuroblasts and immature neurons imply the role of primary cilia regulating early migration direction. By varying the time

point of primary cilia removal in adult born DGCs, this research allows to find the critical time point for primary cilia regulating neuronal migration during the development.

IFT20 is localized to both the basal body of cilia and the Golgi complex. It is known that not only required for ciliary protein transport within the ciliary membrane, it also transports ciliary protein from the Golgi complex to the basal body (Follit et al., 2006). To exclude this possibility, I stained adult born neurons with a cis-Golgi marker,GM130. The shape and the location of the Golgi complex were not altered by IFT20 removal (data not shown) suggesting the phenotype that I observed from this research is not from the non-ciliary function of IFT20. In addition, I confirmed this phenotype through dominant negative Kif3A expression in DGCs. Yet suppressing Kif3A expression alters endosome and lysosome trafficking and axon targeting (Brown et al., 2005, Gu et al., 2006). The effect on endosome and lysosome trafficking and axon growth needs to be investigated further.

One major finding from this research is that removing primary cilia in migrating adult born neurons exhibits abnormal localization in GCL indicating adult born neurons receive a stop signal under primary cilia expression. The localization of wild-type adult born neurons was similar at 21,28 and 35dpi, suggesting that primary cilia expressing newborn neurons terminate radial migration at day 21. Interestingly, radial migration of adult born neurons towards ML was initiated again when primary cilia were removed after they terminate radial migration (Figure 5.7). These data suggest the function for primary cilia in adult born neurons act as an anchor of cells so that neurons can finalize their position and integrate with other DGCs.

The molecular mechanism underlying the absence of primary cilia leads to mis-localization in GCL is unknown. One promising signaling pathway is through cyclin dependent kinase 5 (CDK5). CDK5 is a serine/threonine kinase protein known to regulate neuronal migration during brain development (Su and Tsai, 2011). Previously, Lagace et al have shown that CDK5 protein is expressed in immature and mature granule neurons in DG but not in the dividing progenitor cells which overlaps with the primary cilia expression in neurons (Lagace et al., 2008). CDK5 interacting with β-catenin, disrupts N-cadherin mediated cell adhesion (Kwon et al., 2000). As primary cilia ablation activates Wnt-β-catenin signaling, leading to an increase in the β-catenin level (Kumamoto et al., 2012), it is likely that primary cilia depleted adult born neurons undergo this signaling pathway and restart or continue neuronal migration within GCL.

Another finding is that primary cilia are also regulating early migration. During the initial development of adult born neurons, neuroblasts or immature neurons experience transition from tangential dispersion to radial migration (Seki et al., 2007). By removal of *IFT20* gene or *dnKif3A* expression, I found that neurons having defective primary cilia fail to enter radial migration and remained in tangential dispersion suggesting primary cilia direct cells to radial migration.

Primary cilia also regulate dendritic development and absence of primary cilia showed different effect on different developmental stage of neurons. When primary cilia were ablated in mature neurons, they have more numbers of short but complicated dendrites (Figure 5.8) whereas immature neurons ablated primary cilia express less numbers of simple dendrites (Figure 5.16). Short and complicated dendrites expressed in primary cilia ablated adult born neurons can be explained with initiation of radial

migration. I speculate that primary cilia removed neurons retract elaborated dendrites to respond to the re-initiation of radial migration. Still cellular mechanism of this retracted dendrite need to be studied.

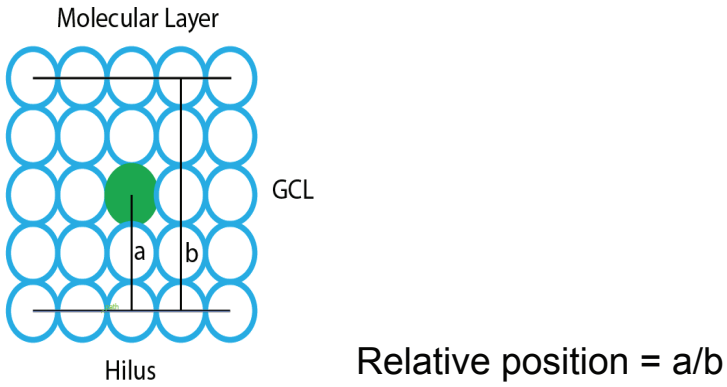

Figure 5.1. Analysis of final position of adult born DGCs
A schematic drawing showing the measurement of final position of adult-born DGCs. A perpendicular distance SGZ to adult born neuron (a), and thickness of GCL (b) was measured. Relative migration distance (a/b) was analyzed for final position of an adult born neuron.

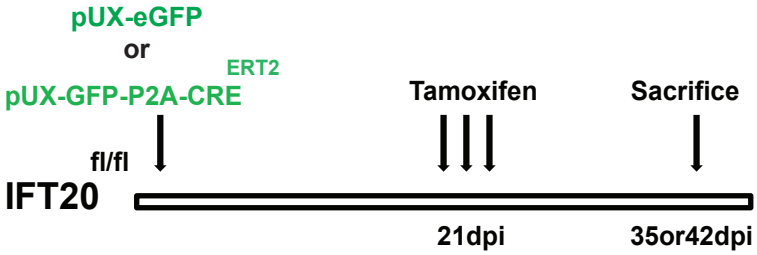

Figure 5.2. Experimental design to ablate primary cilia by IFT20 removal from 21dpi

A scheme of experimental design for testing effect of ablation of primary cilia on final positioning of adult born neurons. Retrovirus expressing inducible Cre was injected into *IFT20* fl/fl mice. Tamoxifen was administered following induction of Cre recombinase to ablate primary cilia at day 21. Final positioning of adult born neurons was analyzed at 35 or 42 dpi.

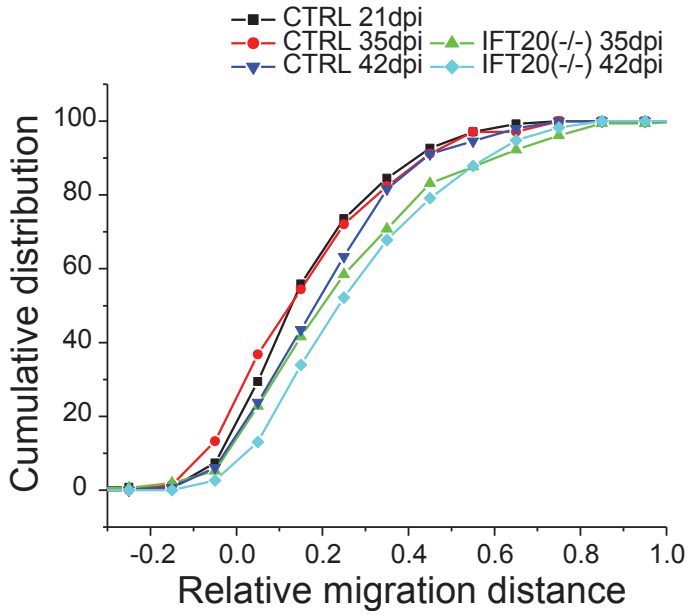

Figure 5.3. Distribution curves of final neuronal positioning of adult born neurons in GCL at 35 and 42 dpi in IFT20 mice

IFT20 (-/-) neurons, in which primary cilia were ablated from day 21, localized closer to ML compared to CTRL neurons at both 35 and 42 dpi (CTRL 35dpi red line n=68 and IFT20 (-/-) 35dpi green line n=154, KS-test: p=0.048, CTRL 42pi blue line n=147 and IFT20 (-/-) sky blue line n= 115, KS-test : p=0.098). Final position of IFT20 (-/-) neurons did not differ between day 35 and 42 (green and sky blue line, KS-test: p=0.268).

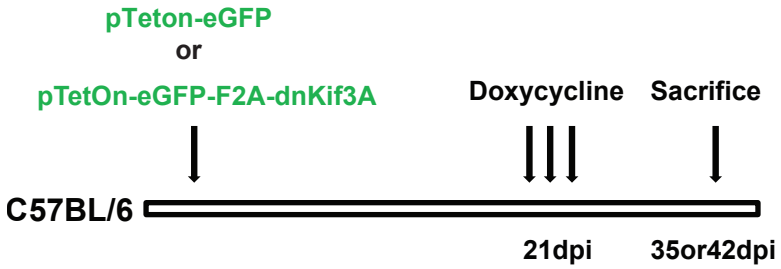

Figure 5.4. Experimental design to ablate primary cilia by dnKif3A expression from 21dpi
Scheme of alternative experimental design to ablate primary cilia from adult born neurons. Retrovirus with inducible expression of dnKif3A was injected into C57BL/6 mice. Doxycycline administration induces dnKif3A expression and ablates primary cilia from day 21. Final positioning of adult born neurons was analyzed at 35 and 42dpi.

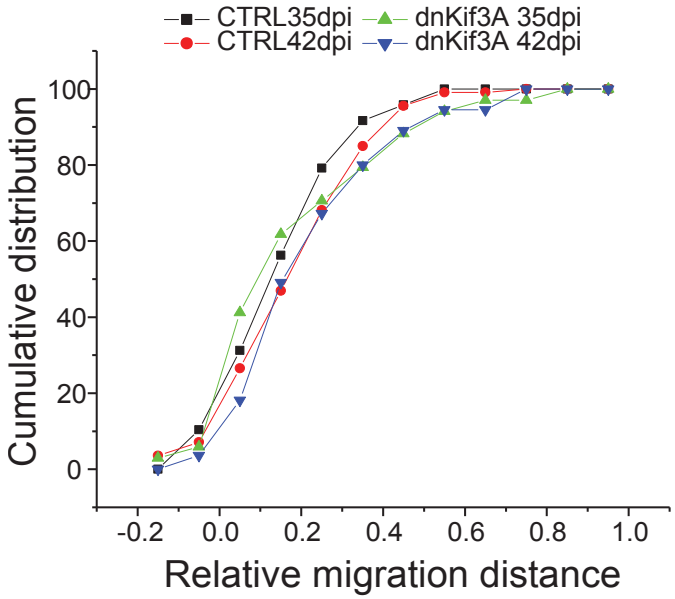

Figure 5.5. Distribution curves of final neuronal positioning of adult born neurons in GCL at 35 and 42 dpi

Neurons without primary cilia under expression of dnKif3A from day 21, tend to localize closer to ML compared to CTRL neurons at 35 and 42 dpi (CTRL 35dpi black line n=48 and dnKif3A 35dpi green line n=34, KS-test: p=0.680, CTRL 42dpi red line n=113 and dnKif3A 42dpi blue line n=55, KS-test: p=0.687).

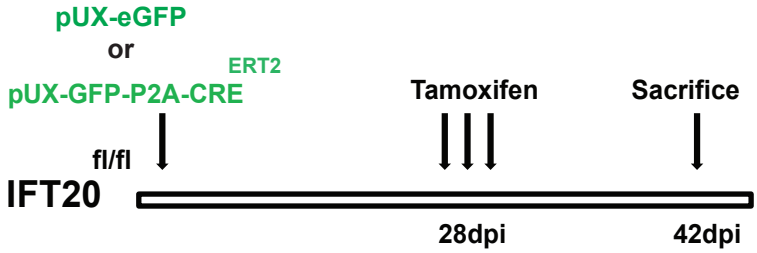

Figure 5.6. Experimental design to ablate primary cilia by IFT20 removal from 28dpi

Scheme of experimental design to ablate primary cilia from day 28 in adult born neurons. Retrovirus with inducible Cre was injected into *IFT20* fl/fl mice. Tamoxifen was administrated following induction of Cre recombinase to ablate primary cilia at day 28. Final poisoning of adult born neurons was analyzed at 42dpi.

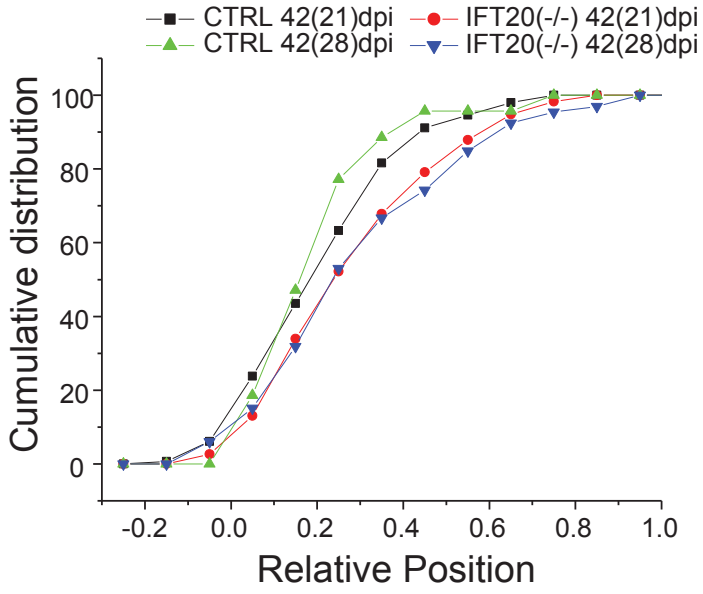

Figure 5.7. Distribution curves of final neuronal positioning of adult born neurons in GCL at 42 dpi

IFT20 (-/-) neurons, primary cilia ablated from day 28, localized closer to ML compared to CTRL neurons at 42 dpi (CTRL 42dpi green line n=70 and IFT20 (-/-) 42dpi blue line n=66, KS-test: p=0.004).

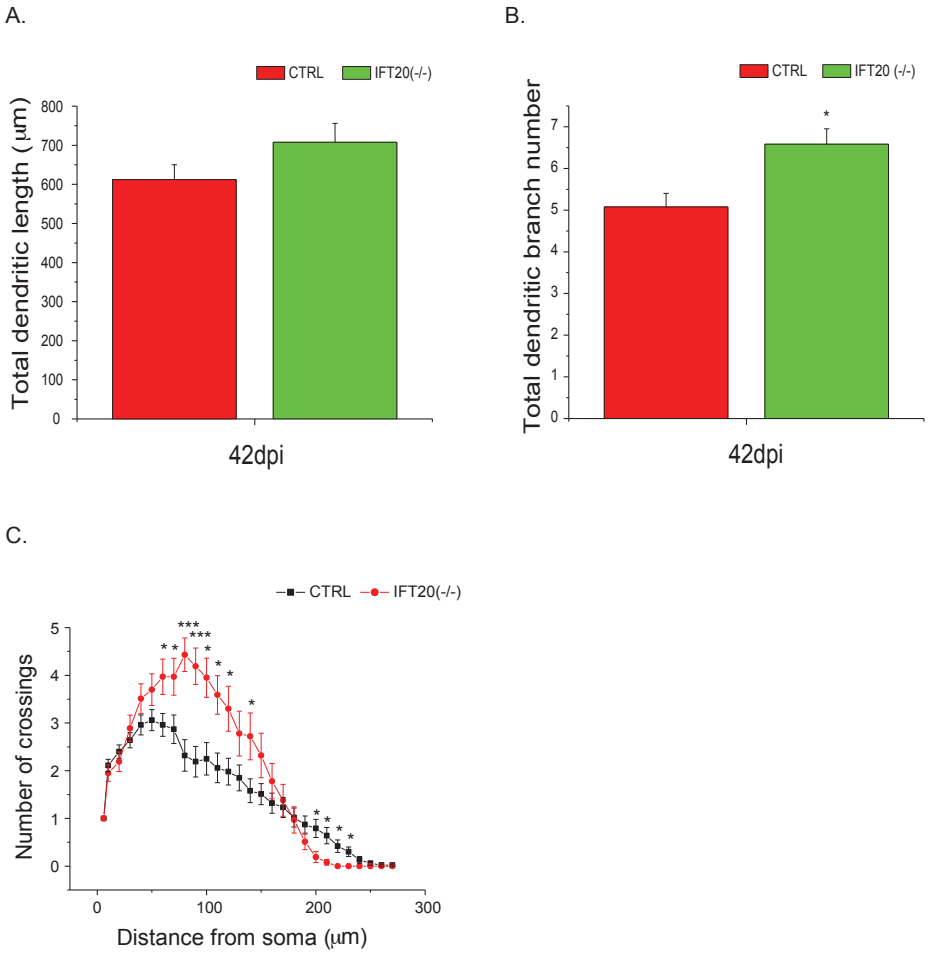

Figure 5.8. Ablation of primary cilia in adult-born neurons alters dendritic refinement

A. Averaged total dendritic length for CTRL (n=46) and IFT20 (-/-) neurons (n=44) at 42dpi. Retrovirus with inducible Cre recombinase was injected into IFT20 (-/-) mice. Tamoxifen was administrated to ablate primary cilia from 28dpi. No significant difference between two groups. $p>0.05$

B. Averaged total dendritic branch number for CTRL and IFT 20(-/-) neurons at 42dpi. IFT20 (-/-) neurons show more dendritic branches than CTRL neurons ($p=0.003$).

C. Sholl analysis of dendritic arborization of CTRL and IFT20 (-/-) neurons at 42dpi. *$p<0.05$, **$p<0.001$, and ***$p<0.0001$ two-tailed unpaired t-test, Data are expressed as mean values ± SEM.

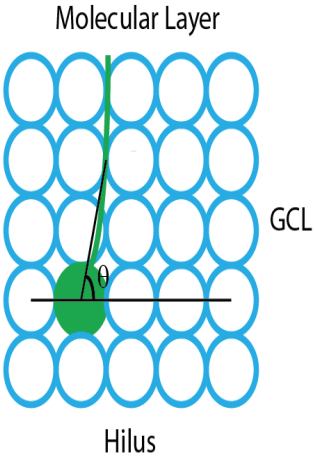

5.9. Analysis of dendritic angle in adult born neurons

Schematic drawing of dendritic angle measurement. Angle between SGZ and dendrite of adult born neurons was measured as shown in the cartoon. Measured angle was categorized into three groups (0-30°, 30-60° and 60-90°) for the analysis.

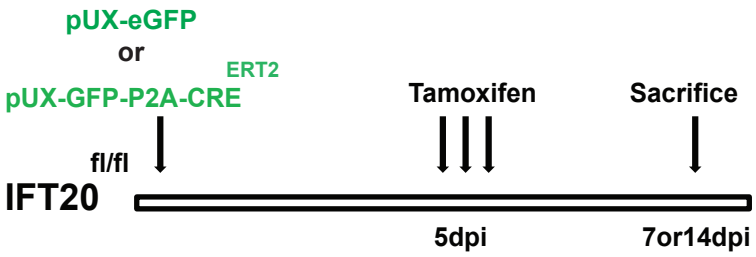

Figure 5.10. Experimental design to test effect of primary cilia ablation on dendritic angle of adult born neurons in IFT20 mice
Retrovirus with inducible Cre was injected into *IFT20* fl/fl mice. Tamoxifen administration following the Cre recombinase induction ablates primary cilia from day 5. Dendritic angle of adult born neurons was analyzed at day 7 and 14.

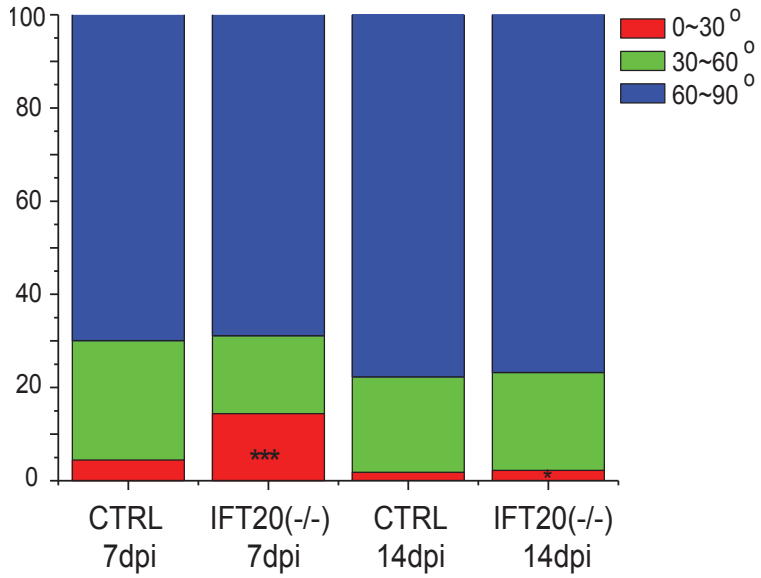

Figure 5.11. Display of dendritic angle at 7 and 14dpi in adult born neurons of IFT20 mice

The bar graph shows distribution of dendritic angle at 7 and 14 dpi. More IFT20 (-/-) neurons, in which primary cilia were ablated from day 5, remained in horizontal position (0 – 30˚) compared to CTRL neurons at both 7 (red box, CTRL n=113 and IFT20 (-/-) n= 167, p=4.21E-06) and 14dpi (red box, CTRL n=112 and IFT20 (-/-) n=224, p=0/004). *p<0.05, ***p<0.001 chi square test, Data are expressed as mean values ± SEM.

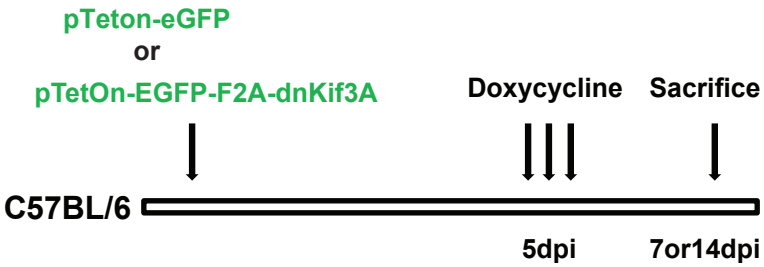

Figure 5.12. Experimental design to test effect of primary cilia ablation on dendritic angle of adult born neurons
Scheme of alternative experimental design to ablate primary cilia with dnKif3A expression from day 5. Retrovirus with inducible dnKif3A was injected into C57BL/6 mice. Doxycycline administration following dnKif3A expression ablates primary cilia from day 5. Dendritic angle of adult born neurons was analyzed at day 7 or 14.

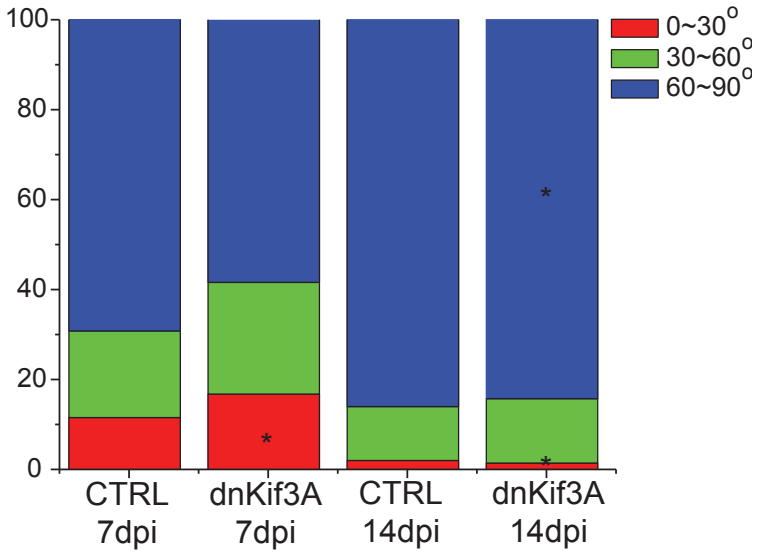

Figure 5.13. Display of dendritic angle at 7 and 14dpi in dnKif3A expressing adult born neurons

The bar graph shows dendritic angle distribution at 7 and 14 dpi. More dnKif3A expressing neurons, in which primary cilia were ablated from day 5, remained in horizontal position (0 - 30˚) compare to CTRL neurons at both 7 (red box, CTRL n=104 and dnKif3A n=346, p=0.015) and 14dpi (red box, CTRL n=100 and dnKif3A n=140, p=0.002).

*p<0.05, ***p<0.001 chi square test, Data are expressed as mean values ± SEM.

A.

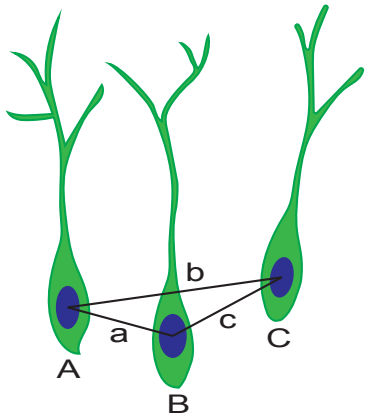

Tangential migration distance =
((a+b)+(b+c)+(c+a))/6

B.

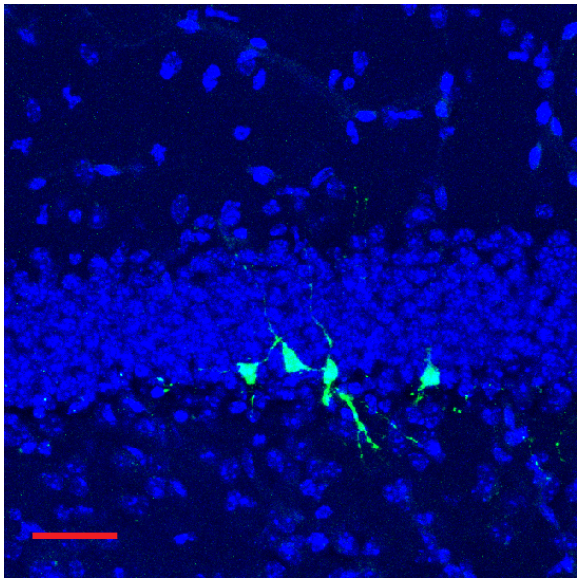

Figure 5.14. Clonal analysis

A. A cartoon showing the measurement of tangential dispersion distance between cells within a clone. Newborn neurons within a same clonal family were labeled by co-injection of pHAGE-GFAP-Cre and pUX-DIO-rEGFP into *IFT20* fl/fl mice. Tangential dispersion distance was analyzed by averaging the distance between cells at 7 and 14dpi.

B. A representative image of newborn DGCs within a clonal family. GFP positive neurons are from the same neural stem cell.

Scale bar: 20 μm.

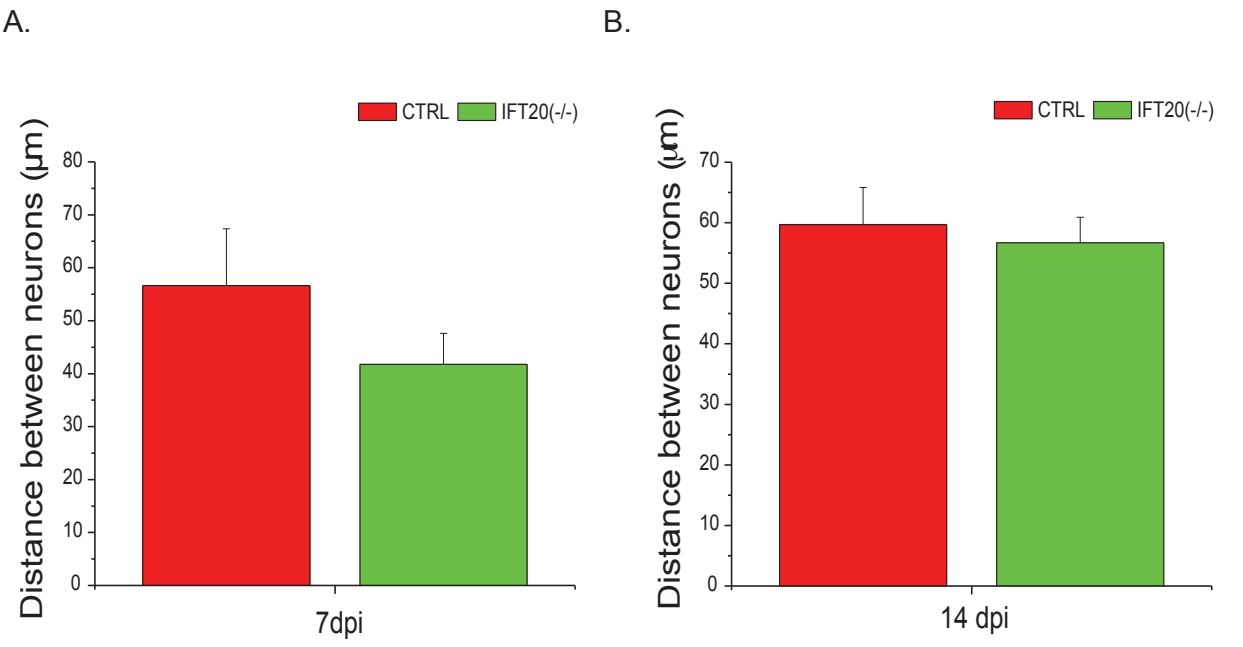

Figure 5.15. Ablation of primary cilia assembly does not alter tangential migration distance of adult born neurons.
A. Averaged distance between neurons within same clonal family at 7dpi. CTRL (n=10) and IFT20 (-/-) neurons (n=20) do not show difference in tangential migration distance at 7dpi.
B. Averaged distance between neurons within same clonal family at 14dpi. CTRL (n=27) and IFT20 (-/-) neurons (n=54) do not show difference in tangential migration distance at 14dpi.
$p>0.05$, two-tailed unpaired t-test, Data are expressed as mean values ± SEM.

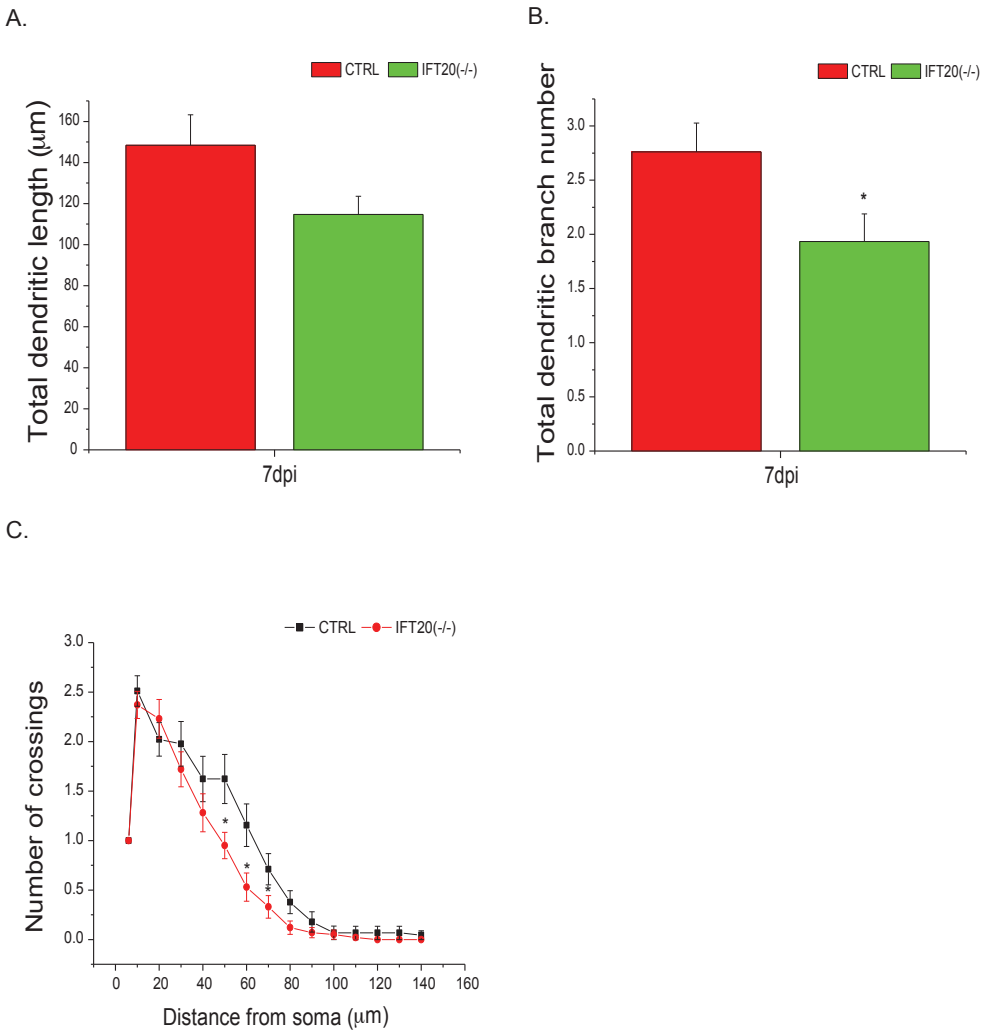

Figure 5.16. Primary cilia regulate early dendrite development of adult born neurons.

A. Averaged total dendritic length of CTRL and IFT20 (-/-) neurons at 7dpi. IFT20 (-/-) neurons showed shorter total dendrite length than CTRL neurons (CTRL red bar n=46 and IFT20 (-/-) green bar n=45, p=0.054).

B. Averaged number of dendritic branches for CTRL and IFT20 (-/-) neurons at 7dpi. IFT20 (-/-) neurons showed significantly less numbers of dendritic branches than CTRL neurons (p=0.027).

C. Sholl analysis of dendritic arborization of CTRL and IFT20 (-/-) neurons at 7dpi. IFT20 (-/-) neurons display simple dendrites compare to CTRL neurons.

*p<0.05, two-tailed unpaired t-test, Data are expressed as mean values ± SEM.

Chapter 6 Conclusion and perspective

Cilium is a microtubule-based structure that is expressed in most human cells. Despite its small structural size, absence or malfunction of cilia causes a broad range of defects in human from mental retardation to polydactyly (Goetz and Anderson, 2010). However, functionality of neuronal primary cilia especially in adult born neurons in the dentate gyrus is unknown. My research is focused on demonstrating the function of neuronal primary cilia expressed in the dentate gyrus of the hippocampus. I investigated the role of primary cilia during different neuronal developmental stages by depleting or reducing *IFT20* gene or *Kif3A* expression so that ablates primary cilia selectively in neuronal populations expressing specific neuronal markers.

The results I have collected through this research showed that mice with ablation of primary cilia in mature DGCs exhibit impaired contextual fear memory, spatial memory and pattern completion. On the other hand, contextual fear discrimination was enhanced when primary cilia were removed in mature DGCs. Based on the related literatures and cognitive impairment result, I speculate that ablation of primary cilia inhibit neuronal activity of mature DGCs. Coincidently, electrophysiological recordings showed that MF-CA3 synaptic plasticity was increased in IFT20 (-/-) mice. When adult neurogenesis in the dentate gyrus was depleted, MF synaptic plasticity was diminished regardless of primary cilia expression in mature DGCs. This implies MF synaptic plasticity is largely dependent on the activity of immature neurons, which are more excitable and plastic than mature neurons. This supports my hypothesis that ablation of primary cilia inhibits activity of mature DGCs shifting the MF-CA3 pathway to a more immature state. Enhanced contextual fear discrimination and increased mossy fiber

synaptic plasticity have been reported to be found in mice with increased adult neurogenesis levels. Therefore, I speculate neuronal primary cilia regulate neuronal activity. The activity balance between immature neurons and mature neurons is a switch between contextual fear discrimination and pattern completion (Sahay et al., 2011b). Therefore, I speculate neuronal cilia regulate neuronal activity. Decreased activity of mature DGCs by primary cilia removal leads to memory encoding failure but enhanced contextual fear discrimination, which suggests neuronal primary cilia are important for physiological functions of DGCs.

Next I speculate primary cilia are regulating adult generated neuronal migration and dendritic development. I selectively removed primary cilia after adult born neurons terminate radial migration and start to integrate into existing circuits. Results revealed that radial migration was re-initiated when primary cilia were removed, implying that primary cilia expression is regulating the final position of adult born DGCs in GCL. This finding is interesting since it shows adult born neurons can migrate even after the synaptic integration when primary cilia are ablated. For instance, DGCs are more dispersed and the GCL is wider in primary cilia ablated brains compared to control brains (data not shown, preliminary study). Moreover, the reorientation of migration direction was also regulated by neuronal primary cilia. Together, my findings speculate neuronal primary cilia, expressed in the base of apical dendrite, regulate both initiation and termination of the radial migration in adult born neurons.

According to observed results, I have demonstrated that primary cilia regulate the activity and the neuronal migration of adult born DGCs. Ciliopathies exhibit mental retardation and other behavioral abnormalities which pathological mechanism is

unknown. These findings may help us understand the role for primary cilia during neuronal development. The next step will be defining signaling pathway of primary cilia regulating the activity and the stop signal to cells. Such information will be important for the defining clinical pathway of ciliopathies.

Chapter 7 Reference

1. Albrecht-Buehler, G. (1977) Phagokinetic tracks of 3T3 cells: parallels between the orientation of track segments and of cellular structures which contain actin or tubulin. *Cell* 12, 333-339.
2. Amador-Arjona, A., Elliott, J., Miller, A., Ginbey, A., Pazour, G.J., Enikolopov, G., . . . Terskikh, A.V. (2011) Primary cilia regulate proliferation of amplifying progenitors in adult hippocampus: implications for learning and memory. *The Journal of neuroscience : the official journal of the Society for Neuroscience* 31, 9933-9944.
3. Arruda-Carvalho, M., Sakaguchi, M., Akers, K.G., Josselyn, S.A., and Frankland, P.W. (2011) Posttraining ablation of adult-generated neurons degrades previously acquired memories. *The Journal of neuroscience : the official journal of the Society for Neuroscience* 31, 15113-15127.
4. Badano, J.L., Mitsuma, N., Beales, P.L., and Katsanis, N. (2006) The ciliopathies: an emerging class of human genetic disorders. *Annual review of genomics and human genetics* 7, 125-148.
5. Bannerman, D.M., Rawlins, J.N., McHugh, S.B., Deacon, R.M., Yee, B.K., Bast, T., . . . Feldon, J. (2004) Regional dissociations within the hippocampus--memory and anxiety. *Neurosci Biobehav Rev* 28, 273-283.
6. Baudoin, J.P., Viou, L., Launay, P.S., Luccardini, C., Espeso Gil, S., Kiyasova, V., . . . Metin, C. (2012) Tangentially migrating neurons assemble a primary cilium that promotes their reorientation to the cortical plate. *Neuron* 76, 1108-1122.
7. Berbari, N.F., Johnson, A.D., Lewis, J.S., Askwith, C.C., and Mykytyn, K. (2008a) Identification of ciliary localization sequences within the third intracellular loop of G protein-coupled receptors. *Molecular biology of the cell* 19, 1540-1547.
8. Berbari, N.F., Lewis, J.S., Bishop, G.A., Askwith, C.C., and Mykytyn, K. (2008b) Bardet-Biedl syndrome proteins are required for the localization of G protein-coupled receptors to primary cilia. *Proc Natl Acad Sci U S A* 105, 4242-4246.
9. Berbari, N.F., Malarkey, E.B., Yazdi, S.M., McNair, A.D., Kippe, J.M., Croyle, M.J., . . . Yoder, B.K. (2014) Hippocampal and cortical primary cilia are required for aversive memory in mice. *PloS one* 9, e106576.
10. Bishop, G.A., Berbari, N.F., Lewis, J., and Mykytyn, K. (2007) Type III adenylyl cyclase localizes to primary cilia throughout the adult mouse brain. *J Comp Neurol* 505, 562-571.
11. Boldrini, M., Underwood, M.D., Hen, R., Rosoklija, G.B., Dwork, A.J., John Mann, J., and Arango, V. (2009) Antidepressants increase neural progenitor cells in the human hippocampus. *Neuropsychopharmacology* 34, 2376-2389.
12. Brailov, I., Bancila, M., Brisorgueil, M.-J., Miquel, M.-C., Hamonb, M., and´, D.V. (2000a) Localization of 5-HT6 receptors at the plasma membrane of neuronal cilia in the rat brain. *Brain research*, 271–275

.
13. Brailov, I., Bancila, M., Brisorgueil, M.J., Miquel, M.C., Hamon, M., and Verge, D. (2000b) Localization of 5-HT(6) receptors at the plasma membrane of neuronal cilia in the rat brain. *Brain research* 872, 271-275.

14. Broadbent, N.J., Squire, L.R., and Clark, R.E. (2004) Spatial memory, recognition memory, and the hippocampus. *Proc Natl Acad Sci U S A* 101, 14515-14520.
15. Brown, C.L., Maier, K.C., Stauber, T., Ginkel, L.M., Wordeman, L., Vernos, I., and Schroer, T.A. (2005) Kinesin-2 is a motor for late endosomes and lysosomes. *Traffic* 6, 1114-1124.
16. Brown, J.P., Couillard-Despres, S., Cooper-Kuhn, C.M., Winkler, J., Aigner, L., and Kuhn, H.G. (2003) Transient expression of doublecortin during adult neurogenesis. *J Comp Neurol* 467, 1-10.
17. Cameron, H.A. and McKay, R.D. (2001) Adult neurogenesis produces a large pool of new granule cells in the dentate gyrus. *J Comp Neurol* 435, 406-417.
18. Carr, G.V., Schechter, L.E., and Lucki, I. (2011) Antidepressant and anxiolytic effects of selective 5-HT6 receptor agonists in rats. *Psychopharmacology (Berl)* 213, 499-507.
19. Clelland, C.D., Choi, M., Romberg, C., Clemenson, G.D., Jr., Fragniere, A., Tyers, P., . . . Bussey, T.J. (2009) A functional role for adult hippocampal neurogenesis in spatial pattern separation. *Science* 325, 210-213.
20. Corbit, K.C., Aanstad, P., Singla, V., Norman, A.R., Stainier, D.Y., and Reiter, J.F. (2005) Vertebrate Smoothened functions at the primary cilium. *Nature* 437, 1018-1021.
21. Corbit, K.C., Shyer, A.E., Dowdle, W.E., Gaulden, J., Singla, V., Chen, M.H., . . . Reiter, J.F. (2008) Kif3a constrains beta-catenin-dependent Wnt signalling through dual ciliary and non-ciliary mechanisms. *Nat Cell Biol* 10, 70-76.
22. Dawe, H.R., Farr, H., and Gull, K. (2007) Centriole/basal body morphogenesis and migration during ciliogenesis in animal cells. *Journal of cell science* 120, 7-15.
23. Defer, N., Best-Belpomme, M., and Hanoune, J. (2000) Tissue specificity and physiological relevance of various isoforms of adenylyl cyclase. *Am J Physiol Renal Physiol* 279, F400-416.
24. Deng, W., Aimone, J.B., and Gage, F.H. (2010) New neurons and new memories: how does adult hippocampal neurogenesis affect learning and memory? *Nat Rev Neurosci* 11, 339-350.
25. Einstein, E.B., Patterson, C.A., Hon, B.J., Regan, K.A., Reddi, J., Melnikoff, D.E., . . . Tallent, M.K. (2010) Somatostatin signaling in neuronal cilia is critical for object recognition memory. *The Journal of neuroscience : the official journal of the Society for Neuroscience* 30, 4306-4314.
26. Eriksson, P.S., Perfilieva, E., Bjork-Eriksson, T., Alborn, A.M., Nordborg, C., Peterson, D.A., and Gage, F.H. (1998) Neurogenesis in the adult human hippocampus. *Nat Med* 4, 1313-1317.
27. Follit, J.A., Tuft, R.A., Fogarty, K.E., and Pazour, G.J. (2006) The intraflagellar transport protein IFT20 is associated with the Golgi complex and is required for cilia assembly. *Molecular biology of the cell* 17, 3781-3792.
28. Ge, S., Goh, E.L., Sailor, K.A., Kitabatake, Y., Ming, G.L., and Song, H. (2006) GABA regulates synaptic integration of newly generated neurons in the adult brain. *Nature* 439, 589-593.
29. Ge, S., Yang, C.H., Hsu, K.S., Ming, G.L., and Song, H. (2007) A critical period for enhanced synaptic plasticity in newly generated neurons of the adult brain. *Neuron* 54, 559-566.
30. Gerdes, J.M., Davis, E.E., and Katsanis, N. (2009) The vertebrate primary cilium in development, homeostasis, and disease. *Cell* 137, 32-45.

31. Ghashghaei, H.T., Lai, C., and Anton, E.S. (2007) Neuronal migration in the adult brain: are we there yet? *Nat Rev Neurosci* 8, 141-151.
32. Goetz, S.C. and Anderson, K.V. (2010) The primary cilium: a signalling centre during vertebrate development. *Nature reviews. Genetics* 11, 331-344.
33. Gold, A.E. and Kesner, R.P. (2005) The role of the CA3 subregion of the dorsal hippocampus in spatial pattern completion in the rat. *Hippocampus* 15, 808-814.
34. Gu, C., Zhou, W., Puthenveedu, M.A., Xu, M., Jan, Y.N., and Jan, L.Y. (2006) The microtubule plus-end tracking protein EB1 is required for Kv1 voltage-gated K+ channel axonal targeting. *Neuron* 52, 803-816.
35. Gu, Y., Arruda-Carvalho, M., Wang, J., Janoschka, S.R., Josselyn, S.A., Frankland, P.W., and Ge, S. (2012) Optical controlling reveals time-dependent roles for adult-born dentate granule cells. *Nature neuroscience* 15, 1700-1706.
36. Gu, Y., Janoschka, S., and Ge, S. (2013) Neurogenesis and hippocampal plasticity in adult brain. *Curr Top Behav Neurosci* 15, 31-48.
37. Hamon, M., Doucet, E., Lefevre, K., Miquel, M.C., Lanfumey, L., Insausti, R., . . . Verge, D. (1999) Antibodies and antisense oligonucleotide for probing the distribution and putative functions of central 5-HT6 receptors. *Neuropsychopharmacology* 21, 68S-76S.
38. Han, Y.G., Spassky, N., Romaguera-Ros, M., Garcia-Verdugo, J.M., Aguilar, A., Schneider-Maunoury, S., and Alvarez-Buylla, A. (2008) Hedgehog signaling and primary cilia are required for the formation of adult neural stem cells. *Nature neuroscience* 11, 277-284.
39. Handel, M., Schulz, S., Stanarius, A., Schreff, M., Erdtmann-Vourliotis, M., Schmidt, H., . . . Hollt, V. (1999) Selective targeting of somatostatin receptor 3 to neuronal cilia. *Neuroscience* 89, 909-926.
40. Hastings, N.B. and Gould, E. (1999) Rapid extension of axons into the CA3 region by adult-generated granule cells. *J Comp Neurol* 413, 146-154.
41. Higginbotham, H., Eom, T.Y., Mariani, L.E., Bachleda, A., Hirt, J., Gukassyan, V., . . . Anton, E.S. (2012) Arl13b in primary cilia regulates the migration and placement of interneurons in the developing cerebral cortex. *Dev Cell* 23, 925-938.
42. Higginbotham, H., Guo, J., Yokota, Y., Umberger, N.L., Su, C.Y., Li, J., . . . Anton, E.S. (2013) Arl13b-regulated cilia activities are essential for polarized radial glial scaffold formation. *Nature neuroscience* 16, 1000-1007.
43. Ho, V.M., Lee, J.A., and Martin, K.C. (2011) The cell biology of synaptic plasticity. *Science* 334, 623-628.
44. Huang, P. and Schier, A.F. (2009) Dampened Hedgehog signaling but normal Wnt signaling in zebrafish without cilia. *Development* 136, 3089-3098.
45. Huangfu, D. and Anderson, K.V. (2006) Signaling from Smo to Ci/Gli: conservation and divergence of Hedgehog pathways from Drosophila to vertebrates. *Development* 133, 3-14.
46. Huangfu, D., Liu, A., Rakeman, A.S., Murcia, N.S., Niswander, L., and Anderson, K.V. (2003) Hedgehog signalling in the mouse requires intraflagellar transport proteins. *Nature* 426, 83-87.
47. Hunsaker, M.R. and Kesner, R.P. (2013) The operation of pattern separation and pattern completion processes associated with different attributes or domains of memory. *Neurosci Biobehav Rev* 37, 36-58.

48. Ishikawa, H. and Marshall, W.F. (2011) Ciliogenesis: building the cell's antenna. *Nature reviews. Molecular cell biology* 12, 222-234.
49. Jonassen, J.A., San Agustin, J., Follit, J.A., and Pazour, G.J. (2008) Deletion of IFT20 in the mouse kidney causes misorientation of the mitotic spindle and cystic kidney disease. *The Journal of cell biology* 183, 377-384.
50. Kempermann, G., Jessberger, S., Steiner, B., and Kronenberg, G. (2004) Milestones of neuronal development in the adult hippocampus. *Trends Neurosci* 27, 447-452.
51. Kempermann, G., Kuhn, H.G., and Gage, F.H. (1997) More hippocampal neurons in adult mice living in an enriched environment. *Nature* 386, 493-495.
52. Kesner, R.P. (2007) Behavioral functions of the CA3 subregion of the hippocampus. *Learning & memory* 14, 771-781.
53. Kheirbek, M.A., Drew, L.J., Burghardt, N.S., Costantini, D.O., Tannenholz, L., Ahmari, S.E., . . . Hen, R. (2013) Differential control of learning and anxiety along the dorsoventral axis of the dentate gyrus. *Neuron* 77, 955-968.
54. Kobayashi, T. and Dynlacht, B.D. (2011) Regulating the transition from centriole to basal body. *The Journal of cell biology* 193, 435-444.
55. Komada, M., Takao, K., and Miyakawa, T. (2008) Elevated plus maze for mice. *J Vis Exp*.
56. Kuhn, H.G., Dickinson-Anson, H., and Gage, F.H. (1996) Neurogenesis in the dentate gyrus of the adult rat: age-related decrease of neuronal progenitor proliferation. *The Journal of neuroscience : the official journal of the Society for Neuroscience* 16, 2027-2033.
57. Kumamoto, N., Gu, Y., Wang, J., Janoschka, S., Takemaru, K., Levine, J., and Ge, S. (2012) A role for primary cilia in glutamatergic synaptic integration of adult-born neurons. *Nature neuroscience* 15, 399-405, S391.
58. Kwon, Y.T., Gupta, A., Zhou, Y., Nikolic, M., and Tsai, L.H. (2000) Regulation of N-cadherin-mediated adhesion by the p35-Cdk5 kinase. *Current biology : CB* 10, 363-372.
59. Lagace, D.C., Benavides, D.R., Kansy, J.W., Mapelli, M., Greengard, P., Bibb, J.A., and Eisch, A.J. (2008) Cdk5 is essential for adult hippocampal neurogenesis. *Proc Natl Acad Sci U S A* 105, 18567-18571.
60. Lancaster, M.A., Schroth, J., and Gleeson, J.G. (2011) Subcellular spatial regulation of canonical Wnt signalling at the primary cilium. *Nat Cell Biol* 13, 700-707.
61. Lee, I. and Kesner, R.P. (2004) Encoding versus retrieval of spatial memory: double dissociation between the dentate gyrus and the perforant path inputs into CA3 in the dorsal hippocampus. *Hippocampus* 14, 66-76.
62. Lee, J.E. and Gleeson, J.G. (2011) Cilia in the nervous system: linking cilia function and neurodevelopmental disorders. *Current opinion in neurology* 24, 98-105.
63. Leutgeb, J.K., Leutgeb, S., Moser, M.B., and Moser, E.I. (2007) Pattern separation in the dentate gyrus and CA3 of the hippocampus. *Science* 315, 961-966.
64. Leutgeb, S. and Leutgeb, J.K. (2007) Pattern separation, pattern completion, and new neuronal codes within a continuous CA3 map. *Learning & memory* 14, 745-757.
65. Ludwig, D.S., Tritos, N.A., Mastaitis, J.W., Kulkarni, R., Kokkotou, E., Elmquist, J., . . . Maratos-Flier, E. (2001) Melanin-concentrating hormone overexpression in transgenic mice leads to obesity and insulin resistance. *J Clin Invest* 107, 379-386.

66. Machold, R., Hayashi, S., Rutlin, M., Muzumdar, M.D., Nery, S., Corbin, J.G., . . . Fishell, G. (2003) Sonic Hedgehog Is Required for Progenitor Cell Maintenance in Telencephalic Stem Cell Niches. *neuron*.
67. Malberg, J.E., Eisch, A.J., Nestler, E.J., and Duman, R.S. (2000) Chronic antidepressant treatment increases neurogenesis in adult rat hippocampus. *The Journal of neuroscience : the official journal of the Society for Neuroscience* 20, 9104-9110.
68. Malenka, R.C. and Bear, M.F. (2004) LTP and LTD: an embarrassment of riches. *Neuron* 44, 5-21.
69. Malenka, R.C. and Nicoll, R.A. (1999) Long-term potentiation--a decade of progress? *Science* 285, 1870-1874.
70. Martin, S.J., Grimwood, P.D., and Morris, R.G. (2000) Synaptic plasticity and memory: an evaluation of the hypothesis. *Annu Rev Neurosci* 23, 649-711.
71. May-Simera, H.L. and Kelley, M.W. (2012) Cilia, Wnt signaling, and the cytoskeleton. *Cilia* 1, 7.
72. Ming, G.-l. and Song, H. (2005) Adult Neurogenesis in the Mammalian Central Nervous System.
73. Mongiat, L.A., Esposito, M.S., Lombardi, G., and Schinder, A.F. (2009) Reliable activation of immature neurons in the adult hippocampus. *PloS one* 4, e5320.
74. Moon, R.T., Bowerman, B., Boutros, M., and Perrimon, N. (2002) The promise and perils of Wnt signaling through beta-catenin. *Science* 296, 1644-1646.
75. Moser, M.B. and Moser, E.I. (1998) Functional differentiation in the hippocampus. *Hippocampus* 8, 608-619.
76. Nakashiba, T., Cushman, J.D., Pelkey, K.A., Renaudineau, S., Buhl, D.L., McHugh, T.J., . . . Tonegawa, S. (2012) Young dentate granule cells mediate pattern separation, whereas old granule cells facilitate pattern completion. *Cell* 149, 188-201.
77. Nakashiba, T., Young, J.Z., McHugh, T.J., Buhl, D.L., and Tonegawa, S. (2008) Transgenic inhibition of synaptic transmission reveals role of CA3 output in hippocampal learning. *Science* 319, 1260-1264.
78. Nakazawa, K., Quirk, M.C., Chitwood, R.A., Watanabe, M., Yeckel, M.F., Sun, L.D., . . . Tonegawa, S. (2002) Requirement for hippocampal CA3 NMDA receptors in associative memory recall. *Science* 297, 211-218.
79. Ocbina, P.J., Tuson, M., and Anderson, K.V. (2009) Primary cilia are not required for normal canonical Wnt signaling in the mouse embryo. *PloS one* 4, e6839.
80. Parent, J.M., Yu, T.W., Leibowitz, R.T., Geschwind, D.H., Sloviter, R.S., and Lowenstein, D.H. (1997) Dentate granule cell neurogenesis is increased by seizures and contributes to aberrant network reorganization in the adult rat hippocampus. *The Journal of neuroscience : the official journal of the Society for Neuroscience* 17, 3727-3738.
81. Pedersen, L.B. and Rosenbaum, J.L. (2008) Intraflagellar transport (IFT) role in ciliary assembly, resorption and signalling. *Current topics in developmental biology* 85, 23-61.
82. Qu, D., Ludwig, D.S., Gammeltoft, S., Piper, M., Pelleymounter, M.A., Cullen, M.J., . . . Maratos-Flier, E. (1996) A role for melanin-concentrating hormone in the central regulation of feeding behaviour. *Nature* 380, 243-247.
83. Revest, J.M., Dupret, D., Koehl, M., Funk-Reiter, C., Grosjean, N., Piazza, P.V., and Abrous, D.N. (2009) Adult hippocampal neurogenesis is involved in anxiety-related behaviors. *Mol Psychiatry* 14, 959-967.

84. Rolls, E.T. (2007) An attractor network in the hippocampus: theory and neurophysiology. *Learning & memory* 14, 714-731.
85. Rolls, E.T. (2013) The mechanisms for pattern completion and pattern separation in the hippocampus. *Front Syst Neurosci* 7, 74.
86. Ruat, M., Traiffort, E., Arrang, J.M., Tardivel-Lacombe, J., Diaz, J., Leurs, R., and Schwartz, J.C. (1993) A novel rat serotonin (5-HT6) receptor: molecular cloning, localization and stimulation of cAMP accumulation. *Biochemical and biophysical research communications* 193, 268-276.
87. Sahay, A. and Hen, R. (2007) Adult hippocampal neurogenesis in depression. *Nature neuroscience* 10, 1110-1115.
88. Sahay, A., Scobie, K.N., Hill, A.S., O'Carroll, C.M., Kheirbek, M.A., Burghardt, N.S., . . . Hen, R. (2011a) Increasing adult hippocampal neurogenesis is sufficient to improve pattern separation. *Nature* 472, 466-470.
89. Sahay, A., Wilson, D.A., and Hen, R. (2011b) Pattern separation: a common function for new neurons in hippocampus and olfactory bulb. *Neuron* 70, 582-588.
90. Santarelli, L., Saxe, M., Gross, C., Surget, A., Battaglia, F., Dulawa, S., . . . Hen, R. (2003) Requirement of hippocampal neurogenesis for the behavioral effects of antidepressants. *Science* 301, 805-809.
91. Saxe, M.D., Battaglia, F., Wang, J.W., Malleret, G., David, D.J., Monckton, J.E., . . . Drew, M.R. (2006) Ablation of hippocampal neurogenesis impairs contextual fear conditioning and synaptic plasticity in the dentate gyrus. *Proc Natl Acad Sci U S A* 103, 17501-17506.
92. Schmidt-Hieber, C., Jonas, P., and Bischofberger, J. (2004) Enhanced synaptic plasticity in newly generated granule cells of the adult hippocampus. *Nature* 429, 184-187.
93. Schneider, L., Clement, C.A., Teilmann, S.C., Pazour, G.J., Hoffmann, E.K., Satir, P., and Christensen, S.T. (2005) PDGFRalphaalpha signaling is regulated through the primary cilium in fibroblasts. *Current biology : CB* 15, 1861-1866.
94. Schneider, L., Stock, C.M., Dieterich, P., Jensen, B.H., Pedersen, L.B., Satir, P., . . . Pedersen, S.F. (2009) The Na+/H+ exchanger NHE1 is required for directional migration stimulated via PDGFR-alpha in the primary cilium. *The Journal of cell biology* 185, 163-176.
95. Seki, T. (2002) Hippocampal adult neurogenesis occurs in a microenvironment provided by PSA-NCAM-expressing immature neurons. *J Neurosci Res* 69, 772-783.
96. Seki, T., Namba, T., Mochizuki, H., and Onodera, M. (2007) Clustering, migration, and neurite formation of neural precursor cells in the adult rat hippocampus. *J Comp Neurol* 502, 275-290.
97. Seri, B., Garcia-Verdugo, J.M., McEwen, B.S., and Alvarez-Buylla, A. (2001) Astrocytes give rise to new neurons in the adult mammalian hippocampus. *The Journal of neuroscience : the official journal of the Society for Neuroscience* 21, 7153-7160.
98. Shimada, M., Tritos, N.A., Lowell, B.B., Flier, J.S., and Maratos-Flier, E. (1998) Mice lacking melanin-concentrating hormone are hypophagic and lean. *Nature* 396, 670-674.
99. Simons, M., Gloy, J., Ganner, A., Bullerkotte, A., Bashkurov, M., Kronig, C., . . . Walz, G. (2005) Inversin, the gene product mutated in nephronophthisis type II, functions as a molecular switch between Wnt signaling pathways. *Nat Genet* 37, 537-543.
100. Singla, V. and Reiter, J.F. (2006) The primary cilium as the cell's antenna: signaling at a sensory organelle. *Science* 313, 629-633.

101. Snyder, J.S., Hong, N.S., McDonald, R.J., and Wojtowicz, J.M. (2005) A role for adult neurogenesis in spatial long-term memory. *Neuroscience* 130, 843-852.
102. Snyder, J.S., Soumier, A., Brewer, M., Pickel, J., and Cameron, H.A. (2011) Adult hippocampal neurogenesis buffers stress responses and depressive behaviour. *Nature* 476, 458-461.
103. Sorokin, S. (1962) Centrioles and the formation of rudimentary cilia by fibroblasts and smooth muscle cells. *The Journal of cell biology* 15, 363-377.
104. Sorokin, S.P. (1968) Centriole formation and ciliogenesis. *Aspen Emphysema Conference* 11, 213-216.
105. Squire, L.R. (1992) Memory and the hippocampus: a synthesis from findings with rats, monkeys, and humans. *Psychol Rev* 99, 195-231.
106. Su, S.C. and Tsai, L.H. (2011) Cyclin-dependent kinases in brain development and disease. *Annu Rev Cell Dev Biol* 27, 465-491.
107. Svenningsson, P., Tzavara, E.T., Qi, H., Carruthers, R., Witkin, J.M., Nomikos, G.G., and Greengard, P. (2007) Biochemical and behavioral evidence for antidepressant-like effects of 5-HT6 receptor stimulation. *The Journal of neuroscience : the official journal of the Society for Neuroscience* 27, 4201-4209.
108. Takeuchi, T., Duszkiewicz, A.J., and Morris, R.G. (2014) The synaptic plasticity and memory hypothesis: encoding, storage and persistence. *Philos Trans R Soc Lond B Biol Sci* 369, 20130288.
109. TJ, M., MW, J., JJ, Q., Balthasar N, C.R., Elmquist JK, L.B., MS, F., . . . S., T. (2007) Dentate gyrus NMDA receptors mediate rapid pattern separation in the hippocampal network. *Science* 317 pp. 94-99
110. Tsai, L.H. and Gleeson, J.G. (2005) Nucleokinesis in neuronal migration. *Neuron* 46, 383-388.
111. Valente, E.M., Rosti, R.O., Gibbs, E., and Gleeson, J.G. (2014) Primary cilia in neurodevelopmental disorders. *Nature reviews. Neurology* 10, 27-36.
112. van Praag, H., Schinder, A.F., Christie, B.R., Toni, N., Palmer, T.D., and Gage, F.H. (2002) Functional neurogenesis in the adult hippocampus. *Nature* 415, 1030-1034.
113. van Praag, H., Shubert, T., Zhao, C., and Gage, F.H. (2005) Exercise enhances learning and hippocampal neurogenesis in aged mice. *The Journal of neuroscience : the official journal of the Society for Neuroscience* 25, 8680-8685.
114. Viollet, C., Videau, C., and Epelbaum, J. (2000) Somatostatin and behaviour: the need for genetically engineered models. *J Physiol Paris* 94, 179-183.
115. Vukovic, J., Borlikova, G.G., Ruitenberg, M.J., Robinson, G.J., Sullivan, R.K., Walker, T.L., and Bartlett, P.F. (2013) Immature doublecortin-positive hippocampal neurons are important for learning but not for remembering. *The Journal of neuroscience : the official journal of the Society for Neuroscience* 33, 6603-6613.
116. Wang, Z., Phan, T., and Storm, D.R. (2011) The type 3 adenylyl cyclase is required for novel object learning and extinction of contextual memory: role of cAMP signaling in primary cilia. *The Journal of neuroscience : the official journal of the Society for Neuroscience* 31, 5557-5561.
117. Watanabe, D., Saijoh, Y., Nonaka, S., Sasaki, G., Ikawa, Y., Yokoyama, T., and Hamada, H. (2003) The left-right determinant Inversin is a component of node monocilia and other 9+0 cilia. *Development* 130, 1725-1734.

118. Wharton, K.A., Jr. (2003) Runnin' with the Dvl: proteins that associate with Dsh/Dvl and their significance to Wnt signal transduction. *Developmental biology* 253, 1-17.
119. Wilson, S.L., Wilson, J.P., Wang, C., Wang, B., and McConnell, S.K. (2012) Primary cilia and Gli3 activity regulate cerebral cortical size. *Dev Neurobiol* 72, 1196-1212.
120. Witter, M.P. (2007) The perforant path: projections from the entorhinal cortex to the dentate gyrus. *Prog Brain Res* 163, 43-61.
121. Yassa, M.A. and Stark, C.E. (2011) Pattern separation in the hippocampus. *Trends Neurosci* 34, 515-525.